Construction and optimization of novel recombinant Adeno-Associated Virus rAAV2/5 for targeting microglia to regulate immune responses during neuroinflammation

BY

Hanane Belhoul-Fakir

A thesis

Submitted to the Victoria University of Wellington

in fulfilment of the requirements for the degree of

Master of Science

Victoria University of Wellington

2014

ABSTRACT

Activated microglia promote central nervous system (CNS) inflammation through antigen presentation and secretion of pro-inflammatory cytokines and chemokines. Although this activation is necessary to protect the brain during infection, aberrant release of pro-inflammatory and/or cytotoxic factors such as tumor necrosis factor-α, interleukin-1β, nitric oxide and reactive oxygen substances may lead to neuronal damage and degeneration.

Targeting microglia during neuroinflammation to regulate the expression of cytokines without affecting other cell types in the CNS is challenging since no specific microglial markers have yet been established that distinguish microglia from infiltrating, peripheral myeloid cells. Therefore, we propose that a viral-based gene delivery system might be a better strategy to regulate gene expression in microglia. Using the recombinant Adeno-associated virus (AAV) vector pseudotype 2/5, which preferentially infects microglia (, we constructed a plasmid backbone which contains GFP under the control of the F4/80 promoter, a macrophage-specific marker. In order to demonstrate the specificity of this promoter for macrophages, we transfected human kidney cells HEK 293 cells, mouse leukemic macrophages RAW 264.7 cells, human hepatocytes cell line (HepG2) and human ovarian carcinoma cell line (1A9) with the AAV-F4/80-eGFP construct or the control plasmid AAV-CAG-eGFP. Our results indicate that the rAAV-F4/80-GFP construct is selective for macrophages.

To begin to assess the usefulness of this system to alter microglia function, we have cloned the Membrane Associated Ring-CH protein (MARCHI) into the rAAV-F4/80-eGFP vector that has been shown earlier to regulate antigen presentation by inducing the intracellular sequestration of MHC class II. We were able to confirm this finding by transfecting interferon gamma stimulated macrophages cell line RAW 264.7 cells via our constructed AAV-F4/80-MARCHI-eGFP vector and demonstrate the ability of our recombinant AAV vector that is driven by specific promoter to deliver and express MARCHI to induce MHC class II sequestration. Together this work will lead to the development of tools that will allow us to dissect the pathways by which microglia promote neuroinflammation.

To my parents

my husband Tarik and my three daughters Aya, Lamis and Yousra

ACKNOWLEDGMENT

First of all, I would like to thank A.Prof Anne LaFlamme for giving me the opportunity to do research in her laboratory, for her excellent support and guidance she gave me throughout my post-graduation studies, and for her valuable advice, she was always encouraging me to pursue my own initiatives.

I would like to thank A.Prof Bronwen Connor for providing me the support I needed in the AAV production experiments.

To Laura ,Jessica, Jenni, Deegy and Arun, my best friends, thank you for your huge support and advice you gave me throughout my thesis and for invaluable help which I couldn't have done without. Thank you for your true amazing friendship.

Thank you to Prof. John millar, Prof. Bill Jordan, Dr Lifeng Peng, A.Prof David Ackerley, A.Prof Paul Teesdale-Spittle, for your excellent advice and support.

Thank you to LAF group and my friends; Lisa, Sarrabeth, Maddie, Marie, Nikki, Pirooz, for your huge support and for helping me understanding ''George" the FACS machine.

Thank you to all people of the SBS school Vichy, Arian, Bhumi, Christina, Sara, Namol, Jonathan, Christine, Yee, Ploi, James, Peter Bosh and Alistaire for your amazing help and for saving my time and my experiments by lending me reagents.

To all the SBS staff and faculty of science staff especially to Patricia, Mark and Shauna Desein, thank you so much for making things easier for me in the administration.

To my parents, who have provided unwavering moral support throughout all my life and who have always encouraged me to pursue my studies. Thank you for your loving support and for giving me a good education.

To my brothers Ferhat, Djafer, Abdellah and sisters Nadjet, Souhila, Meriem and Nadia; Thank you very much for encouraging me and giving me the enthusiasm to continue my studies.

To my dear husband Tarik, thank you so much for making things easier for me by taking care of the girls while I was studying, thank you for encouraging me to pursue my own intrest, without your support this thesis would not have been possible.

Finally to my little princesses Aya, Lamis and Yousra, thank you for being patient and for understanding that mumy is busy and needs to be good in her studies. I am sure one of you will be a scientist in the future.

TABLE OF CONTENTS

TABLE OF FIGURES

LIST OF ABBREVIATIONS

AAV: Adeno-Associated Virus

MARCH-I: membrane-associated RING (CH)

MHC-II: Major histocompatibility complex class II

IFN-γ: Interferon gamma

IL-10, IL-4: Interleukine

CAG: CMV/chicken β-actin hybrid

DMEM: Dulbecco's modified eagle medium

IMDM: Iscove's modified eagle medium

FACS: Fluorescence-activated cell sorting

HEK 293: Human embryonic kideny

RFU: Relative Fluorescence Unit

BDNF: Brain-Derived Neurotrophic Factor

NSE: Neuron-Specific Enolase

CNS: Central Nervous System

GFP: Green Fluorescent Protein

YFP: Yellow Fluorescent Protein

PCR: Polymerase Chain Reaction

FCS: Foetal Calf Serum

SDS-PAGE: Sodium Dodecyl Sulfate Polyacrylamide Gel Electrophoresis

VP: Viral Protein

IRES: Internal ribosome entry

PE: PhycoErythrin

CHAPTER 1

INTRODUCTION

1.1 Biology of AAV

1.1.1 AAV Classification and serotypes

The AAV virus belongs to the *Parvoviridae* family and is categorized in the *Dependovirus* genus, since the virus depends on a helper virus such as adenovirus or herpes simplex virus for efficient replication (Daya and Berns, 2008; Gonclaves, 2005). Indeed, AAV was originally discovered in 1965 as a contaminant in rhesus-monkey-kidney cell cultures infected with simian adenovirus type 15 (SV15) (Atchison, 1965).

An AAV serotype is defined as an inability of an AAV isolate to cross-react with neutralizing antibodies that are reactive to the viral capsid proteins of other isolates (Wu et al., 2006; Choi et al., 2005). As of 2008, 12 AAV human serotypes (AAV1-AAV12) had been discovered for which humans are the primary host and new serotypes are continuing to be discovered. AAV2 was the first serotype identified and the best studied (Cucchiarini et al., 2003; Asokan et al., 2012). Although approximately 80% of the human population is seropositive for AAV2, no pathology has been associated with this virus (Asokan et al., 2012). Most of the serotypes were isolated from adenovirus preparations in the laboratory and have similar structure, genome size and organization but different tissue tropism (Wu et al., 2006). For instance, AAV5 was reported to have a high tropism for liver tissue and all regions of the CNS (Mingozzi et al., 2002; Davidson et al., 2000), while AAV4 was shown to highly transduce ependymal and astrocytes in the CNS (Mingozzi et al., 2002; Davidson et al., 2000). AAV1 and AAV7 were shown to have a tropism for skeletal muscle (Chao et al., 2000; Gao et al., 2002).

New serotypes are defined as newly isolated viruses which do not cross-react efficiently with neutralizing antibodies, which are specific for other characterized serotypes. Based on this definition, Wu et al. suggested that AAV 1-5, 7-9 and 12 are the only types that can be defined as true serotypes (Wu et al., 2006). The remaining types 6, 10 and 11 do not seem to fit into the new serotype definition. As an alternative they are called AAV variants because of their similarities with other serotypes, such as variant 6 with serotype 1, or because they are not well characterized (Wu

et al., 2006; Gao et al., 2004; Schmidt et al., 2008) (Table 1.1). However, it was shown previously in Xiao et al. that previous treatment of murine liver with AAV2 generated a partial neutralization of AAV1 vector. This partial neutralization of AAV1 did not occur in murine skeletal muscle (Xiao et al., 1999), suggesting that cross-reactivity between some AAV serotypes may depend on tissue type or species.

AAV	AAV-1	AAV-2	AAV-3	AAV-4	AAV-5	AAV-6	AAV-7	AAV-8	AAV-9
AAV-1	100								
AAV-2	83	100							
AAV-3	87	88	100						
AAV-4	63	60	63	100					
AAV-5	58	57	58	53	100				
AAV-6	99	83	87	63	58	100			
AAV-7	85	82	85	63	58	85	100		
AAV-8	84	83	86	63	58	84	88	100	
AAV-9	82	82	84	62	57	82	82	85	100

Table 1.1 ***AAV serotypes capsid homology.*** (Adapted from Daya and Berns, 2008)

1.1.2 AAV structure and genome map

AAV is one of the smallest viruses (25 nm) with a non-enveloped icosahedral capsid, packaging a linear single-stranded DNA genome, and varies in length between 4642 bp and 4767 bp according to the AAV serotypes (Srivastava et al., 1983; Grimm and Kay, 2003). The genome organization of serotype 2 was first characterized in 1982 by Srivastava et al. and contains in each termini two inverted terminal repeats (ITRs) of 145 nucleotides (Srivastava et al., 1983). The first 125 nucleotides of the repeat are in the form of a palindromic sequence, folding on itself to maximize

base pairing and forming a T-shape hairpin structure (Figure 1.1 A) (Srivastava et al., 1983). The remaining 20 nucleotides are called the D sequence and are unpaired and present only once at each end of the genome. ITRs also contain two elements that are crucial for AAV replication; Rep binding elements (RBE and RBE') and the terminal resolution site (*trs*) (Ryan et al., 1996). The ITRs flank two open reading frames (*orf*) containing the AAV genes *rep* (replication) and *cap* (capsid) genes encoding non-structural and structural proteins respectively (Figure 1.1 B).

The *rep* genes encode four regulatory proteins indicated by their apparent molecular sizes; Rep78, Rep68, Rep52 and Rep40, expressed from transcripts using two promoters (p5) and (p19), which are located at map positions 5 and 19 respectively. Rep78 and Rep52 are expressed from un-spliced transcripts while Rep68 and Rep40 are produced from spliced transcripts (Figure 1.1 B) (Ryan et al., 1996). The *cap* gene, expressed under p40 promoter, encodes for three proteins composing the AAV capsid: VP1, VP2 and VP3, and these proteins are produced from two transcripts. The biggest capsid protein VP1 is 87 kDa and is produced from un-spliced transcript while VP2 (72 kDa) and VP3 (62 kDa) are spliced from a single transcript (A. Srivastava et al., 1983). The three capsid proteins of AAV2 differ from each other by their N terminus and they assemble into an icosahedral protein shell of 60 subunits (93). The three capsid proteins are present at a molecular ratio of 1:1:10 (VP1: VP2: VP3) (Daya and Berns, 2008).

Similar genome organization and capsid morphologies were also found in the other serotypes with small differences in genome length (Grimm and Kay, 2003).

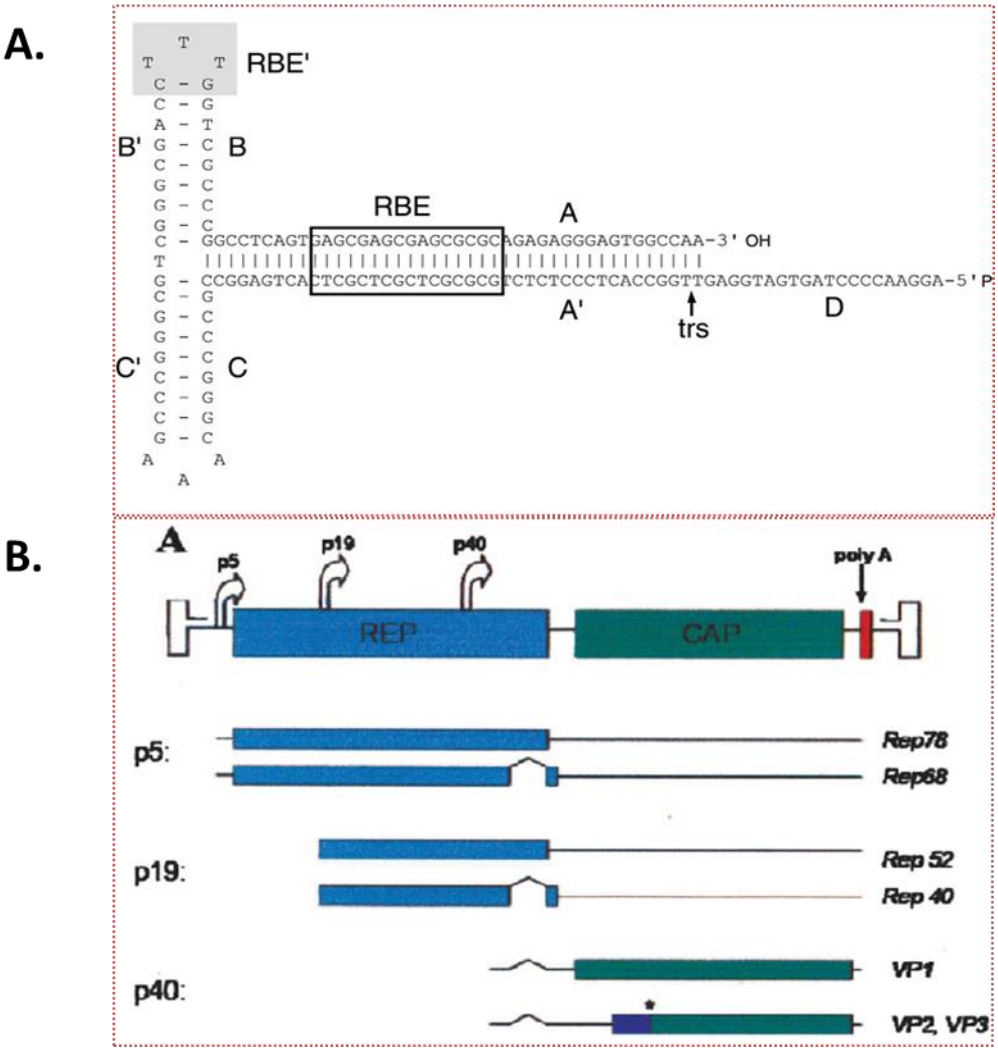

Figure 1.1 The wild type AAV genome organization. A) ITRs secondary structure containing RBE', RBE, trs and the sequence D, which are involved in AAV replication. **B)** Map of AAV genome showing ITRs at the two ends of the genome flanking *rep* and *cap* genes and their promoters' p5, p19 and p40. An alternative ACG codon used for VP3 production is indicated by a star (Daya and Berns, 2008).

1.1.3 AAV infection and replication process

AAV infection starts by AAV attachment to the host cell membrane initiated by the interaction of the capsid with cell surface glycosaminoglycan. This attachment is followed by a secondary interaction of the viral capsid with a co-receptor inducing AAV internalization and trafficking to the nucleus (Wu et al., 2006; Weitzman and Linden, 2011). For AAV2 for instance, the membrane-associated heparan sulfate proteoglycan was shown to be a receptor for this serotype

(Summerford and Samulski, 1998), and this binding was reported to be enhanced by interaction with fibroblast growth factor receptor 1 (FGFR1) (Qing et al., 1999), αVβ5 integrin and hepatocyte growth factor co-receptors (Summerford et al., 1999; Kashiwakura et al., 2005). The rapid internalization of AAV2 was induced by clathrin-mediated endocytosis (Bartlett et al., 2000). On the other hand, AAV5 binding and uptake was shown to be enhanced via sialic acid and platelet-derived growth factor receptor (PDGF-R) respectively (Di Pasquale et al., 2003).

The signalling pathway involved in AAV trafficking and entry into the host nucleus remains unclear; Bartlett et al. for instance have demonstrated by the use of the lysosomotropic drug ammonium chloride and the proton pump inhibitor bafilomycin A1 that, once the virus is internalized into an early endosome, its release into the cytosol requires the endosomal lumen acidification to induce conformational changes to key capsid subunits that are involved in priming virus endosomal escape (Bartlett et al., 2000). Furthermore, it has been suggested that the AAV virus traverses to the nucleus, accumulates in the nuclear envelop and slowly penetrates through the nuclear pore complex (NPC) into the nucleus (Bartlett et al., 2000). Nevertheless, the AAV nucleus entry through NPC hypothesis has been ruled out in Hansen et al. study, as they have shown that blocking active NPC-mediated transport did not inhibit the viral entry into the nucleus (Hansen et al., 2001).

Although it is not clear whether AAV uncoating happens before or after nuclear entry, once the uncoating process occurs, the single stranded viral genome is converted into a double stranded form required for gene expression (Weitzman and Linden, 2011). Rep78/68 proteins were shown to interact with RBE and *trs* sequences to activate the replication process of the viral DNA, and regulate gene expression of AAV (Pareira et al., 1997). The small Rep proteins, Rep52 and Rep 40 are involved in the generation and accumulation of single-stranded AAV genome generated from double-stranded templates intermediates and, the helicase activity of these small Rep proteins was shown to improve genome encapsidation (Merten et al., 2005; King et al., 2001). VP proteins form empty capsids in a rapid reaction in the nucleus and slowly package the single stranded DNA (Myers and Carter, 1980).

1.1.4 AAV life cycle

AAV life cycle contains two cycles; a replication productive cycle, known as *lytic stage* and a latent cycle named *lysogenic stage* (Figure 1.2). The lytic stage takes place in the presence of a helper virus that aids in AAV gene expression and alters the cellular environment to induce an AAV productive life cycle. The typical helper virus is adenovirus (Daya and Berns, 2008); however others such as herpes simplex virus (HSV), vaccinia virus and cytomegalovirus (CMV) were also shown to exert helper function for AAV (Hansen et al., 2001; Schlehofer et al, 1986).

The helper genes that adenovirus provides for AAV gene expression include E1a, E1b, E2a, E4 and the virus associated RNA (VA RNA). It was reported in Shi et al. that the E1a protein stimulates YY1-binding site that is involved in transcriptional repression for the p5 promoter of AAV (Shi et al., 1991). Furthermore, E2a gene that encodes a single-strand DNA binding protein DBP was shown to be necessary for the progressive replication of AAV genome in vitro (Ward et al., 1998). The E1b and E4 gene products function as ubiquitin ligases and were shown in Schwartz et al. to enhance AAV transduction and replication by inducing degradation of the cellular Mre11 repair complex (MRN). This complex was suggested to be critical in DNA damage sensing and repair and interferes with AAV replication (Schwartz et al.,2007). In addition, the VA RNA, a small RNA that is highly produced during adenovirus infection, was suggested to have a role in stimulating AAV proteins expression by preventing eIF2α translation factor phosphorylation, as it was reported previously that eIF2α phosphorylation by the serine-threonine kinase protein kinase (PKR), blocks translation and expression of viral proteins (Nayak and Pintel, 2007; Mathews and Shenk, 1991).

The lysogenic stage occurs in the absence of helper virus, in which expression of Rep68/78 is limited. In this stage AAV gene expression is repressed leading to AAV genome integration into a specific region of the host genome located on chromosome 19 (q13.4) and known as AAVS1 (Daya and Berns, 2008; Kotin et al., 1990). This genome integration results in a latent replication that is tightly coordinated with that of the host. Nevertheless, once the AAV-infected cell is super-infected with a helper virus, integrated AAV genome is rescued from the host genome and viral genes expression is activated leading to a productive replication (Weitzman and Linden, 2011).

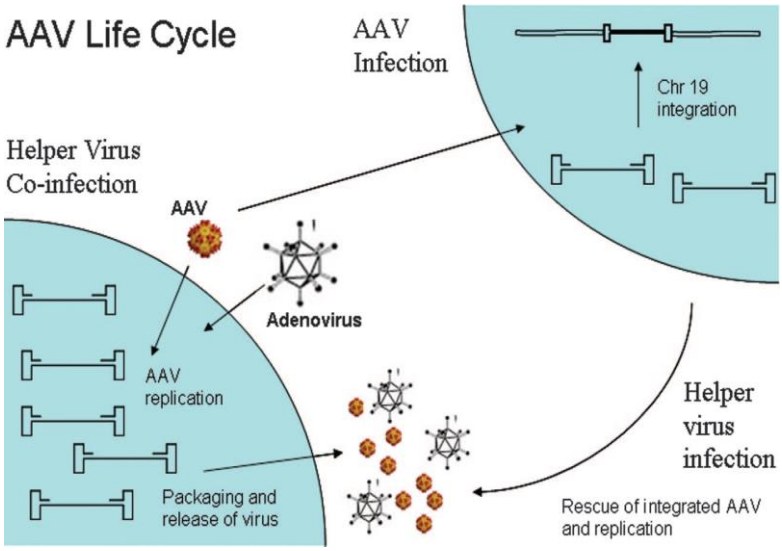

Figure 1.2 ***Wild type AAV virus life cycle.*** (Daya and Berns, 2008)

1.2 Recombinant AAV vector

1.2.1 AAV vector design

Since the first use of recombinant AAV vectors to transduce foreign DNA into human and murine culture cells in 1984 (Hermonat and Muzyczka, 1984), the vector underwent several modifications to improve its efficacy. Current AAV vectors do not encode *Rep* and *Cap* genes and they lack the cis-active IEE, a sequence that is required for site specific integration during lysogenic stage. Because of these deficiencies, AAV vectors persist primarily in the cytoplasm as double-stranded circular or linear episomes (Nakai et al., 2000; Grose et al., 2012). The ITRs are the only part of the virus that is kept in cis in the genome as they are required for replication and packaging (Figure 1.3) (Daya and Berns, 2008). *Rep* and *Cap* ORFs are replaced with a gene expression cassette of interest, whereas for vector production, *Rep* and *Cap* genes are supplied in *trans* with helper virus auxiliary genes which can be from the same serotype or from different serotypes (*Cap* genes are from another serotype). When *Rep* and *Cap* genes are from different serotypes, the AAV produced is called pseudotype or hybrid serotype (Choi et al., 2005).

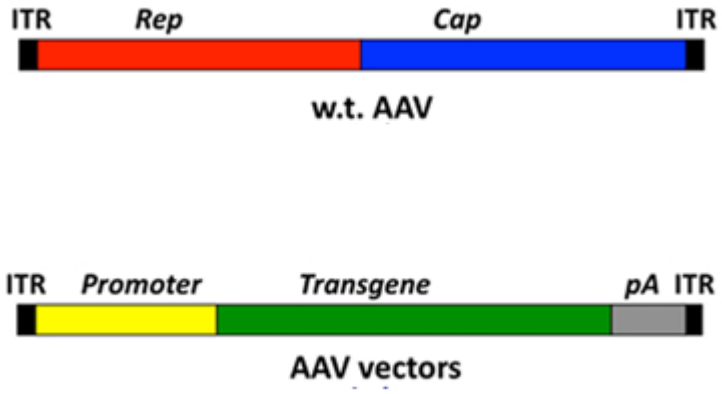

Figure 1.3. ***Comparison between wild type AAV and recombinant AAV vector***. (Masat et al., 2013)

1.2.2 Recombinant AAV production strategies

1.2.2.1 Packaging methods

To ensure high purity, safety and potency of the AAV products, different approaches have been used to package AAV vectors. The classical approach used in laboratories for AAV packaging for pre-clinical studies is transient transfection of adherent HEK 293 (Fraser Wright, 2009).

The very first method was based on a two plasmid transfection of packaging cells with AAV vector backbone and Rep/Cap plasmid (Fraser Wright, 2009). Like wild type AAV, cells were infected with wild type adenovirus few hours later at low multiplicity of infection in order to replicate efficiently (Samulski et al., 1989). The drawback of this method was the use of wild type adenovirus which is produced as well, resulting in contamination of the purified AAV vector preparations and rendering the AAV preparations unsuitable for *in vivo* studies (Matsushita et al., 1998).

In order to overcome this challenge, an alternative approach was developed by Matsushita et al. in 1998, called ‘’a triple transfection method’’, in which AAV vectors were packaged without helper virus infection (Matsushita et al., 1998). In this approach, the adenovirus subset genes that are necessary for AAV replication including E4, E2A, VA RNA were cloned into a separate plasmid and co-transfected into HEK 293 cells along with pRep/Cap and AAV vector plasmids. The E1 gene is another necessary adenovirus helper gene and it is supplied by HEK 293 cells. AAV titer obtained from the helper-free method was equal to that achieved by adenovirus infection with same potency (Matsushita et al., 1998). Consequently, this method generated AAV preparations free of

detectable adenoviral particles (Matsushita et al., 1998). The advantage of this approach is the simultaneous production of AAV serotypes and hybrids, which is convenient for preclinical studies in which AAV vectors characteristic need to be tested. On the other hand, transient transfection of adherent HEK 293 method is difficult to scale up and a number of studies are focusing on improving this technology to make it more efficient for clinical purposes (Liu et al., 2003; Asokan et al. 2011).

The most relevant methods used for DNA plasmid transfer into the packaging cell for AAV production include calcium phosphate precipitation, polyethylenimine (PEI) precipitation and cationic lipids (Fraser Wright, 2009). Of these methods, calcium phosphate-mediated transfection has been extensively used to produce AAV vectors for preclinical studies (Chen et al., 1998; Grose et al., 2013; Klein et al., 1998).

Stable producer cell line is another method used to package the viral vector (Merten et al., 2005). This approach is based on production of AAV in HeLa cells, the chosen producer cell line in this method due to their ability in rescuing integrated copies of AAV very efficiently compared with HEK293 (Blouin et al., 2004). In this method, AAV *Rep* and *Cap* genes and ITR-AAV sequence are integrated in the producer cell line genome requiring only adenovirus infection to produce the virions, thus eliminating the need of transfection (Nakamura et al., 2004). However, while in preclinical studies AAV serotype and genome need to be selected and optimized, AAV production system needs more versatility than this method allows. Moreover, the presence of the human papilloma virus (HPV 18) sequence in these cells makes them potentially dangerous to use for AAV preparations destined to human clinical trials (Schwarz et al., 1985).

The Baculovirus-insect cells method is another strategy used for AAV vectors production. This approach was established in 2004 by Urabe et al. and is based on infection of invertebrate cells *Spodoptera frugiperda* (Sf9) cells that are cultured in suspension, with three recombinant baculoviruses: a Rep-baculovirus containing Rep78 and Rep52 genes, a VP-baculovirus expressing AAV capsid proteins and an ITR-AAV-baculovirus (Urabe et al., 2004). Although this strategy was shown to generate equivalent amounts of AAV particles as in HEK cell transient transfection (Urabe et al., 2004; Viraq et al., 2009), the instability of the baculovirus is very challenging as it depends on the passage number of the insect cell (Virag et al., 2009). Another disadvantage of using this technique is the contamination of the AAV stocks with the recombinant baculoviruses.

1.2.2.2 Purification methods

A variety of purification strategies are used in laboratories. Some labs favour a combination of density gradient ultracentrifugation and chromatography while others chose to perform one-step purification using a density gradient or chromatography (Zolotukhin et al., 1999; Schmidt et al., 2008). The conventional density gradient method for AAV purification is caesium chloride (CsCl), which is still used in many studies (Zolotukhin et al., 1999; Iwata et al., 2013; Xiao et al., 1998). However, the challenge in using this reagent is the large amount of time spent in performing multiple rounds of CsCl gradients to decontaminate AAV stocks from aggregates leading to poor AAV recovery and affecting AAV infectivity when the stocks are not properly purified (Zolotukhin et al., 1999; Auricchio et al., 2001). Furthermore, precautions must be taken when handling the reagent as it is a chemical hazard. In particular, before transduction of cells, the AAV vectors stock must be cesium chloride-free due to the reagent toxicity to cells.

Since discontinuous iodixanol density gradient was adapted by Zolotukhin et al, it became the preferred method in many laboratories to purify AAV vectors, due to its iso-osmotic and inertness properties at all densities (Zolotukhin et al., 1999). Additionally, its non-toxicity to cells makes AAV purification steps quicker when AAV infectivity assays need to be performed directly on AAV-iodixanol gradient fractions without further purification (Iwata et al., 2013; Li et al., 2006). In addition, in terms of AAV vector infectivity, iodixanol gradients were shown to generate the most infective AAV vectors over CsCl (Zolotukhin et al., 1999). The common drawback of both gradients is the limited loading capacity for AAV samples which can impede large scale production of AAV vectors.

Chromatographic methods used for AAV purification were first established when AAV2 interaction with the HSPG receptor was observed. The subsequent identification of the host receptors used by other AAV serotypes facilitated the development of this approach. The most extensively used chromatographic methods include affinity chromatography and ion-exchange chromatography (Smith et al., 2008). Affinity chromatography is used to purify AAV serotypes and variants that have the ability to bind to heparan sulfate including AAV2, AAV6 and AAV3a/3b clone (Kaludov et al., 2002) but since AAV serotypes display different capsids proteins, the use of this method is restricted to few serotypes only. Ion exchange chromatography on the other hand, is more versatile since this method is based on the ionic charge properties of the AAV vectors in solution, permitting the purification of the serotypes with known glycan receptors such as AAV4, AAV5,

AAV2, AAV1, AAV8 (Davidoff et al., 2004; Brument et al., 2002). Although chromatographic approach has been shown to achieve higher yields and purity of AAV stocks compared to density gradient ultracentrifugation methods, this method requires careful optimization at each step. Furthermore, empty capsids are not excluded from the purified AAV stocks comparing with iodixanol gradient density approach. To circumvent this issue, many studies have combined density gradient ultracentrifugation and chromatography to improve the yield and purity of the AAV products. In addition, others have implemented new strategies such as the two-step purification method involving a strong cation exchange chromatography resin (SP sepharose HP) coupled with a strong anion exchange chromatography resin (source 15Q) (Brument et al., 2002), or an anion chromatography using a strong anion exchange resin followed by gel filtration chromatography (Smith et al., 2003).

1.2.3 Recombinant AAV vectors and gene therapy

Gene therapy consists of delivering therapeutic DNA into a target cell to replace a mutated or translocated gene or to regulate a gene expression in order to repair the cell dysfunction. This new approach is very promising vis-a-vis traditional therapies and has been evolving since the first gene therapy trials (phase 1) for adenosine deaminase (ADA) deficiency and malignant melanoma in 1990 (Walther and Stein, 2000). Two methods are used to facilitate the transfer of gene of interest into the target cell; the viral vectors method and the non-viral vectors method. The non-viral approach uses chemical based vectors including cationic lipids, cationic polymers and inorganic nanoparticles or physical forces such as electroporation, sonoporation and hydrodynamic gene transfer (Al-Dosari and Gao, 2009).

The viral vectors-based approach, the most extensively used method in gene delivery, employs a genetically modified virus or *''recombinant virus''.* This method more efficiently transfers the desired gene into the target cell compared with non-viral methods in which transgene expression is at lower level (Al-Dosari and Gao, 2009). A number of DNA and RNA viruses have been widely utilized to generate these viral vectors such as adenovirus, herpes simplex virus (HSV), retrovirus and AAV. The difference between these vectors includes the size of the gene insert, the duration of expression, target cell infectivity and integration of the vector genome into the host genome (Table 1.2).

Viral vector	Genome type	Maximum size of transgene	Ability to infect Non-dividing cells	Stability of expression	Associated pathologies to wt-virus
Adenovirus	ds DNA	8kb for E1/E3 deleted vectors; 35kb for 'gutless 'vectors	yes	Unstable expression (episome)	Conjunctivitis, cold, gastroenteritis
HSV-1	ds DNA	> 25kb	yes	Stable (episome)	Encephalitis, mouth ulcers and genital warts
Retroviruses	ss RNA	≤8kb	Lentivirus only	Stable (integration into host genome)	Acquired immuno-deficiency syndrome (AIDS), tumors induction
AAV	ss DNA	<4kb	yes	Stable (episome)	No known disease
Vaccinia virus	ds DNA	>25kb	yes	Unstable (cytoplasm replication)	Smallpox

Table 1.2 ***Characteristics of the most employed viral vectors in gene therapy*****.** (Adapted from Kathy Ponder, 2001)

The desired features of a viral vector in clinical applications include 1) stable and efficient gene expression to accomplish therapeutic effects, 2) a capacity to harbour a large therapeutic gene, and 3) high infectivity. Retroviruses and HSV vectors for instance, possess these features as they both maintain therapeutic genes permanently in the host cell, have a large genome (>8kb and > 25kb respectively) and very infective (Kathy Ponder, 2001). Nevertheless, although these vectors have shown to achieve promising outcomes in human gene therapy clinical trials (Kathy Ponder, 2001; Walther and Stein, 2000), these vectors do not satisfy safety requirements. The risk of insertional mutagenesis is higher when using retroviruses (Yi et al., 2011); for example, it was reported in a human clinical trial where an *ex-vivo* gene transfer by retrovirus was performed on nine infants with X-linked severe combined immunodeficiency (X-SCID), that leukemia developed in four of them despite the success of the therapy (Yi et al., 2011). Furthermore, vectors based

upon HSV-1 were reported to be challenging due to their toxicity to cells and development of wild-type HSV-1 which can cause encephalitis (Walther and Stein, 2000; Manservigi et al., 2010). In addition, adenovirus, HSV and retrovirus vectors are immunogenic and thus, they are not suitable for sustained gene therapy (Wu and Ertl, 2009).

AAV vector in the other hand, has become very popular in preclinical and clinical trials due to it very attractive features including, its ability to stably express transgenes in the target cell in episomes, ability to infect dividing and non-dividing cells and the lack of pathology linked to AAV compared with other viral vectors (Kay et al., 2001). Furthermore, no adverse effects have been reported so far in clinical trials, in particular in brain disorders such as Parkinson's disease and retinal diseases (Mueller and Flotte, 2008). For instance, in Jacobson et al. study on human retinal disorder RPE65-deficient Leber congenital amaurosis (LCA), AAV2 delivery of the RPE65 gene (retinal pigment epithelium-specific protein 65 kDa) to the retina of blind RPE65-deficient dogs restored their vision with no systemic toxicity and only a mild inflammation that was localised at the site of injection and which resolved over 3 months (Jacobson et al., 2006). In addition, to assess the safety of the retinal administration of AAV2-RPE56, a phase I clinical trial has been conducted on three patients having LCA, and no side effects have been reported (Jacobson et al., 2006). In another study, a unilateral stereotaxic infusion of 12 patients with advanced Parkinson's disease (PD) was carried to transfer the glutamic acid decarboxylase (GAD) gene via AAV vector directly into the subthalamic nucleus (STN), in attempt to alter STN activity that is increased in PD patients. The treatment was restricted to only one hemisphere of the brain to reduce the risks of any side effect that might occur. A significant improvement was observed in PD patients with no detectable toxicity or any side effects observed for more than 3 years after surgery (Kay et al., 2001; Kaplitt et al., 2007).

Although AAV vector is poorly immunogenic, a low immune response to the AAV capsid proteins has been observed in some clinical trials (McPhee et al., 2006; Mano et al., 2006), but several strategies have been considered to evade the host immune response such as transient immunosuppression (Mingozzi et al., 2007), in which AAV vector delivery is coupled with an immunosuppressive agent. Another approach involves reengineering of AAV capsid and generation of serotype mutants (e.g AAV2.15, AAV2.4) containing mutations at key antigenic sites (Maheshri et al., 2006).

1.3 Microglia

Microglia are resident macrophage-like cells of the central nervous system (CNS). They perform similar functions as other macrophages in the body while protecting and supporting CNS functions (Ulvestad et al., 1994). These cells belong to the glial system and are located throughout the brain parenchyma (E. Ulvestad et al., 1994), representing around 10% of the non-neuronal cells in adult mouse brain (Pintado et al., 2011) and up to 13% in human CNS (Ulvestad et al., 1994). The origin of microglia has been controversial since their first description by Franz Nissl in 1880 (Pintado et al., 2011); however, evidence has accumulated for cells of hematopoietic origin entering the CNS during foetal life (Frederic Vilhardt, 2004; Kettenmann et al., 2011). Microglia density varies between brain regions, but the most populated areas include the hippocampus, substantia nigra, olfactory telencephalon and basal ganglia (Pintado et al., 2011; Lawson et al., 1990), and they are closely connected to both neurons and astrocytes (Trembley and Majewska, 2011).

1.3.1 Microglia in the healthy brain

In the healthy mature brain, microglia exhibit morphological and functional plasticity and can be found in a highly ramified or ameboid macrophage-like morphology (Kettenmann et al., 2011). The ramified microglia differ from classical macrophages as they possess a dendritic-like phenotype with small rod-shape somata and numerous branching processes (Napoli and Neumann, 2009). This phenotype has long been referred to as ''resting microglia'' due to their immobile morphology and low activity. Additionally, they express surface receptors at low levels including CD45, CD14 and CD11b/CD18 (Francesca Aloisi, 2001; Georg W Kreutzberg, 1996; Glenn et al., 1992). However Nimmerjahn et al. provided evidence that in fact, these cells are not in a ''dormant state'' but instead they are highly dynamic in the resting state *in vivo* as they constantly changing their morphology by extending and retracting highly motile processes in a time scale of minutes (Nimmerjahn et al., 2005). Indeed, Ramified microglia were shown to display protrusions of variable shapes appearing transiently at the main processes and at their terminal endings, with spontaneous swallowing of tissue components that were transported towards the soma, suggesting a role in collecting tissue debris and metabolic products (Nimmerjahn et al., 2005). Thus ramified microglia were suggested to have a role in a constant surveillance of their own microenvironment in order to maintain CNS homeostasis (Nimmerjahn et al., 2005; Perry and

Teeling, 2013). Furthermore, Vinet et al. have reported in their recent *in vitro* study, that ramified microglia possess neuroprotective properties as well. By implementing an *in vitro* system comparable to the *in vivo* conditions, they were able to demonstrate the essential role of ramified microglia in protecting dentate gyrus and CA3 neurons N methyl-D-aspartic acid (NMDA)-induced excitotoxicity (Vinet et al., 2012).

During infection, injury or ischemia in the CNS, signals from stressed or damaged cells, immune cells or pathogens activate microglia, which are rapidly transformed into an ameboid macrophage-like shape. These activated microglia actively move to the site of injury or infection following a chemotactic gradient and proliferate (Kettenmann et al., 2011; Georg W Kreutzberg, 1996; Rogove et al., 2002). The early sign of activated microglia in response to CNS inflammation is the up-regulation of MHC class II and adhesion molecules (Francesca Aloisi, 2001; Georg W Kreutzberg, 1996). MHC molecules presenting antigenic peptides on the surface of microglia play a crucial role in stimulating protective T-cell responses against infection, tumoral cells and certain inflammatory conditions. Adhesion molecules CD58, CD54 and CD11b as well as co-stimulatory molecules CD40, CD80 and CD86 are also involved in this interaction for an optimal antigen presentation function (Francesca Aloisi, 2001).

These resident macrophages secrete pro-inflammatory cytokines, reactive oxygen species (ROS), nitrogen intermediates to destroy invading agents, but these factors can also act as neurotoxins and damaged tissue. However, microglia also produce neuroprotective factors to repair damaged neurons and restore CNS homeostasis (Frederik Vilhardt, 2004). The proinflammatory cytokines induced by activated microglia include pleiotropic cytokines, which have a role in humoral and cellular immune responses induction, such as IL-6, IL-12, IL-18 and IL-15 (Francesca Aloisi, 2001), and TNF-α and IL-1β. TNF-α and IL-1β are the two major proinflammatory cytokines produced by activated microglia and macrophages. TNF-α has been shown to have a critical role in promoting microglia phagocytosis and inducing inflammatory cytokines production that may have a role in protecting the CNS against LPS and bacteria (Francesca Aloisi, 2001). In addition, TNF-α was reported to have a neurotoxic effect as it inhibits the re-uptake of the primary excitatory neurotransmitter glutamate by astrocytes inducing an accumulation of extracellular glutamate generating higher and toxic concentrations of this neurotransmitter (Rogove and Tsirka, 1997).

IL-1β is another critical proinflammatory cytokine that is suggested to be a major activator of astrocytes (Paul Moynagh, 2005). It was shown to be the key cytokine to induce the expression of

type II inducible nitric oxide synthase (iNOS) in astrocytes, which have a role in vasodilatation (Liu et al., 1996). IL-1β was also shown to stimulate the transcription factor NF-κB that induces adhesion molecules and chemokines expression such as IL-8, VCAM-1 and ICAM-1 in astrocytes (Paul Moynagh, 2005).

Rogove and Tsirka have demonstrated in their study that inhibition of activated microglia by macrophage migration inhibitory factor (MIF) in an excitotoxin-mediated brain injury model system resulted in resistance in neuronal death and attenuation of microglia activity (Rogove and Tsirka, 1997). Furthermore, in the same study, the amount of microglia-derived tissue plasminogen activator (tPA), a serine protease that is produced from both microglia and neurons, was found reduced (Rogove and Tsirka, 1997). The same investigators showed previously that tPA is rapidly produced from microglia upon an excitotoxic insult to induce neuronal cell destruction (Rogove and Tsirka. 1996). In addition, it was reported that the major source of tPA at the site of injury is microglia (Rogove and Tsirka. 1997; Rogove et al., 2002). These findings suggest that microglia have a toxic effect on affected neurons while non-affected neurons are not destroyed by activated microglia (Rogove and Tsirka, 1997; Gehrmann et al., 1995).

Other neurotoxic products generated from activated microglia include reactive oxygen species which are superoxide (O_2^-) and reactive nitrogen species such as nitric oxide (NO). Moss and Bates demonstrated that following LPS and IFN-γ stimulation of murine microglial cell lines, an inducible form of nitric oxide synthase NOS is induced and NO is released into the medium. These products were shown to have deleterious effects on brain energy metabolism including inhibition in mitochondrial oxidative phosphorylation and a decrease in mitochondrial ATP production as well as inhibition of mitochondrial respiratory chain enzyme activities (Moss and Bates, 2001; Brookes et al., 1999).

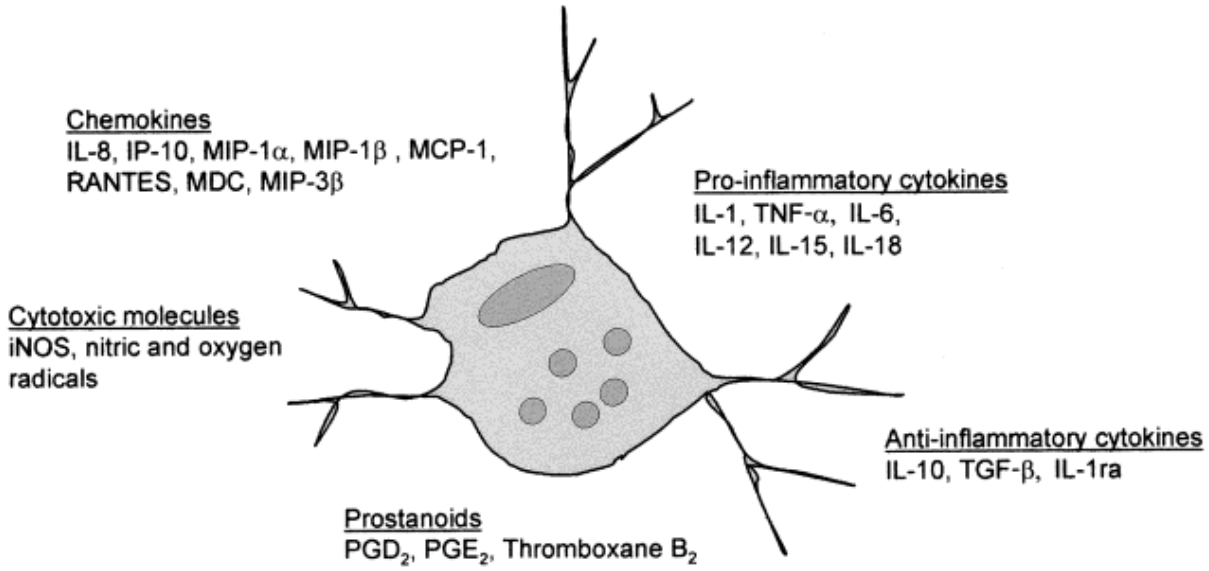

Figure 1.4. Inflammatory factors expressed from activated microglia. (Francesca Aloisi, 2001)

Down regulation of immune responses at site of inflammation in the CNS is necessary to allow healing and reduce secretion of pro-inflammatory cytokines, chemokines and infiltration of T lymphocytes. The neuronal survival can be compromised when this pro-inflammatory response lasts for a long period of time. The down-regulation process involves the production of anti-inflammatory cytokines including IL-10, TGF-β and IL-4 and IL-1ra (IL-1 receptor antagonist) (Tremblay et al., 2011). Cell death by apoptosis is mediated by receptors of TNF-R super-family and is also crucial in terminating immune responses in the inflamed CNS (Pender and Rist, 2001).

1.3.2 Microglia in neurodegenerative diseases

Although the exact mechanism by which innate inflammation contributes to neurodegenerative diseases is still unclear, it is now well accepted that microglia are involved in neuroinflammatory and neurodegenerative disorders including multiple sclerosis (MS), Alzheimer's disease (AD) and Parkinson's disease (PD). In response to the insult generated from these disorders, microglia become reactive and induce an innate immune response in an attempt to restore CNS homeostasis (Napoli and Neumann, 2009). Nevertheless, the repeated stimulation of these local macrophages induces a chronic inflammation in which infiltration of other immune cells through

the blood brain barrier (BBB) into the parenchyma is increased along with MHC-II expression, inflammatory cytokines, oxidative and nitrosative stress, which in fact harms the CNS (Vinet et al., 2012; Luo and Chen, 2012).

In MS for instance, the most common chronic inflammatory demyelinating disease of the CNS, microglia was reported to have a key role (Ulvestad et al., 1994; Becher et al., 2001). MS is characterised by demyelination of axons resulting in neurodegeneration (Wolfgang Bruck, 2005). During MS, demyelination is observed in the white matter as focal lesions as well as in the cortical and subcortical grey matter (Wolfgang Bruck, 2005). These lesions contain various infiltrating immune cells including T-cells, peripheral macrophages and B cells and local immune cells such as microglia (Hansen Lassmann, 1999). Remyelination is also observed in MS lesions following the resolution of acute inflammatory episodes in up to 40% of MS lesions (Wolfgang Bruck, 2005).

Numerous studies have shown the direct contribution of activated microglia in myelin sheath destruction and induction of chronic inflammation. It was reported by Lucchienetti et al. that the loss of oligodendrocytes (OG) in MS lesions correlated with an increased number of microglia and infiltrating macrophages secreting excitotoxic factors such as TNF-α, IL-1β and reactive antigen intermediates (Lucchinetti et al., 1999). The persistent release of these neurotoxins can be detrimental to myelin and oligodendrocytes (Lucchinetti et al., 1999; Diemel et al., 1998). Furthermore, it was reported that in early MS lesions, microglia are the major phagocytes that contain myelin debris and peripheral macrophages are recruited as the lesions develop (Diemel et al., 1998).

In addition, these cells may participate in the remyelination of demyelinated MS lesions (Wolfgang Bruck, 2005; Graca and Blakemore, 1986). Indeed, it was previously demonstrated that in induced demyelination of areas in the white matter of the lumbar rat spinal cord by ethidium bromide, remyelination was delayed in the glia free regions where few macrophages were observed (Graca and Blakemore, 1986). In addition, *in vitro* studies showed that microglia produced growth factors including fibroblast growth factor-2 (FGF-2), transforming growth factor-β1 (TGFβ1), nerve growth factor (NGF), and neurotrophins. Neutrophins are produced from both microglia and macrophages which may be released during remyelination mechanism to induce myelinogenesis and oligodendrocytes proliferation and survival (Diemel et al., 1998).

Microglia involvement in Parkinson's disease has also been studied extensively. This neurodegenerative disorder is characterized by a progressive degeneration of dopaminergic cells

in the substancia nigra, a region that has a crucial role in the body movements (Hamani and Lozano, 2003). This region is highly populated with microglia and the intensity of the LPS-induced inflammation (TNF-α, IL-1, ROS) was reported to be positively correlated with microglial cell density *in vivo* (Pintado et al., 2011). Another feature of the substancia nigra which makes it highly susceptible to inflammation is, the higher blood brain barrier permeability (BBB) suggesting that plasma cytokines released from systemic inflammation or infectious agents, could penetrate the BBB and activate microglia in this region (Pintado et al., 2011). In fact, it was reported that an infection with a certain type of viruses or a previous traumatic brain injury may induce later in life a post-encephalitic Parkinsonism (Liu and Hong, 2003). In Alzheimer's disease in the other hand, in which β-Amyloid (Aβ) proteins are aggregated both within neurons and the extracellular space, microglia were found surrounding Aβ plaques in both humans and animal models of AD (Prokop et al., 2013). *in vivo* studies have reported an increase in IL-1, IL-12, IL-23 and complement proteins in the amyloid plaques, and in *in vitro* numerous inflammatory cytokines were expressed following stimulation of microglia with the Aβ peptides derived from the amyloid precursor protein (APP), suggesting the reactivity of microglia in AD (Prokop et al., 2013; Ransohoff and Perry, 2009). All these findings are consistent with the involvement of microglia in neurodegenerative disorders; however, more studies are needed to identify the key pathways to chronic inflammation in order to establish the right treatments for these disorders.

1.4 MARCH-I

Ubiquitination is an essential control mechanism in cell growth and proliferation by causing the down-regulation of receptors and transporters by rapid endocytosis and degradation of ubiquitinated substrate proteins (Ohmura-Hoshino et al., 2006). Three enzymes are required for this role including ubiquitin-activating enzyme *E1* which activates ubiquitin and transfers it to the ubiquitin-carrier enzyme *E2* and ubiquitin-ligase *E3* catalyses activated ubiquitin (Hershko and Ciechanover, 1998). Nine human membrane-associated RING-CH (MARCH) proteins have been identified belonging to the E3 ubiquitin ligases family (Bartee et al., 2004). These proteins were found structurally and functionally related to the viral E3-ubiquitin ligases such as K3, K5 and mK3 (Ohmura-Hoshino et al., 2006; Bartee et al., 2004), and these viral ubiquitin ligases were shown to induce ubiquitination of MHC-I molecules and other co-stimulatory molecules such as ICAM-1, CD86 (B7.2) and CD1d (Lehner et al., 2005).

MARCH-I is one of the ubiquitin ligase E3 family members and is homologous to MARCH-VIII. Both proteins were shown to induce ubiquitination and downregulation of MHC-I, MHC-II, CD86 (B7.2), CD95 (Fas) and transferrin receptor (Tfr) surface expression (E. Bartee et al., 2004). While MARCH-VIII is broadly expressed (Bartee et al., 2004), MARCH-I is highly expressed in secondary lymphoid tissues particularly in resting APCs including B cells, dendritic cells (DCs) and monocytes (Cho and Roch, 2013). MARCH-I was shown to be the only ubiquitin ligase to down-regulate MHC-II surface expression in B cells (Matsuki et al., 2007), and in DCs, MARCH-I is the major regulator of MHC-II ubiquitination (De Gassart et al., 2008). In mouse macrophages, human monocytes and B cells, IL-10 was shown to up-regulate MARCH-I expression which induced MHC-II ubiquitination (Thibodeau et al., 2008; Cho and Roch, 2013). MARCH-I expression is down-regulated in mature APCs (Lai et al., 2010), and was reported to be significantly reduced in APCS stimulated with toll-like receptor (TLR) signals (Walseng et al., 2010; Cho and Roch, 2013). The exact mechanism by which MHC-II is ubiquitinated by MARCH-II is still not fully understood. Data obtained from Walseng et al. showed that MARCH-I induced MHC-II degradation following ubiquitination in immature DCs and this degradation was blocked at 40% only in MARCH-I knockout DCs within 6h compared with wild type control, in which the MHC-II degradation was at 70 % (Walsenga et al., 2010). These findings suggest that another pathway may be involved in the MHC-II degradation in immature DCs.

When expressed, MARCH-I is rapidly degraded with an estimated half-life of <30 min in primary APCs and their cell lines. This decrease in stability may be regulated by auto-ubiquitination and other factors that have not been identified yet (Jabbour et al., 2009), and the mechanism by which MARCH-I is degraded is still not fully elucidated. However, it was demonstrated by Jabbour et al. that a portion of MARCH-I was degraded by the proteasome since this ubiquitin ligase was partially stabilized by treatment of DCs with a proteasome inhibitor (MG132) (Jabbour et al., 2009). Furthermore, the same study showed that inhibition of lysosomal peptidases led to a stable expression of MARCH-I in immature bone marrow DCs, and therefore both proteasome and lysosome pathways are involved in the degradation of MARCH-I proteins (Jabbour et al., 2009). In addition, the N-terminus domain was shown to be directly involved in the stability of MARCH-I in the cytoplasm (Jabbour et al., 2009).

1.5 F4/80

F4/80 is a mouse antigen marker that its expression is restricted to macrophages (Gordon et al., 2011). Three decades ago, the F4/80 monoclonal antibody was described by Austyn and Gordon that was found to react specifically against a 160 kDa antigen on mouse macrophages after the immunization of rats with thioglycollate-elicited mouse peritoneal macrophages (Austyn and Gordon, 1981). No reactivity was observed for other hematopoietic cells of myeloid lineage (Austyn and Gordon, 1981). the antibody was found to react against macrophages from different sites such as blood monocytes, spleen and peritoneal cavity (Austyn and Gordon, 1981).

F4/80 is a 160 kDa glycoprotein, belongs to the EGF-TM7 family and represents the longer form of this family along with EMR1 (EGF module-containing, mucin-like hormone receptor 1) the human ortholog of F4/80 and CD97. F4/80 protein comprises seven extracellular EGF-like domains at the N-terminus followed by a Ser/Thr-rich spacer region linked to the C-terminal of the GPCR-related MT7 domain (G-protein-coupled seven-transmembrane-spanning hormone receptor) (McKnight and Gordon, 1998; Lin et al., 2010) (Figure 1.5).

F4/80 is expressed during the foetal life and throughout the adult life and its presence is strictly correlated with the distribution of macrophages. It was demonstrated previously that macrophages cell lineage appears in the mouse embryo around day 10 of gestation in the yolk sac, liver followed by spleen and surrounding mesenchymal tissues (De Felici et al., 1986; Takahashi et al., 1989; Morris et al., 1991). Indeed, in Hopkinson et al., study on the limb embryo, F4/80 antigens were detected in aorta-gonad-mesonephros (AGM) region and yolk sac at day 8 and 9; the expression of the antigen has increased with the development of the embryo and before birth in foetal liver, splenic red pulp and bone marrow macrophages (Hopkinson et al., 1994). In the adult, F4/80 is highly expressed in the phagocytic cells including Kuppfer cells in the liver, red pulp in the spleen, thymic cortex, bone marrow, and adrenal glands as well as in the microglia in the CNS and Langerhans cells in the skin (Gordon et al., 2011). However, in monocytes, this expression is very low. Therefore, since the identification of this macrophages marker, F4/80 became widely used as a marker in macrophages studies (Levin et al., 2012; Imtiyaz et al., 2010; Bilyk et al., 1988).

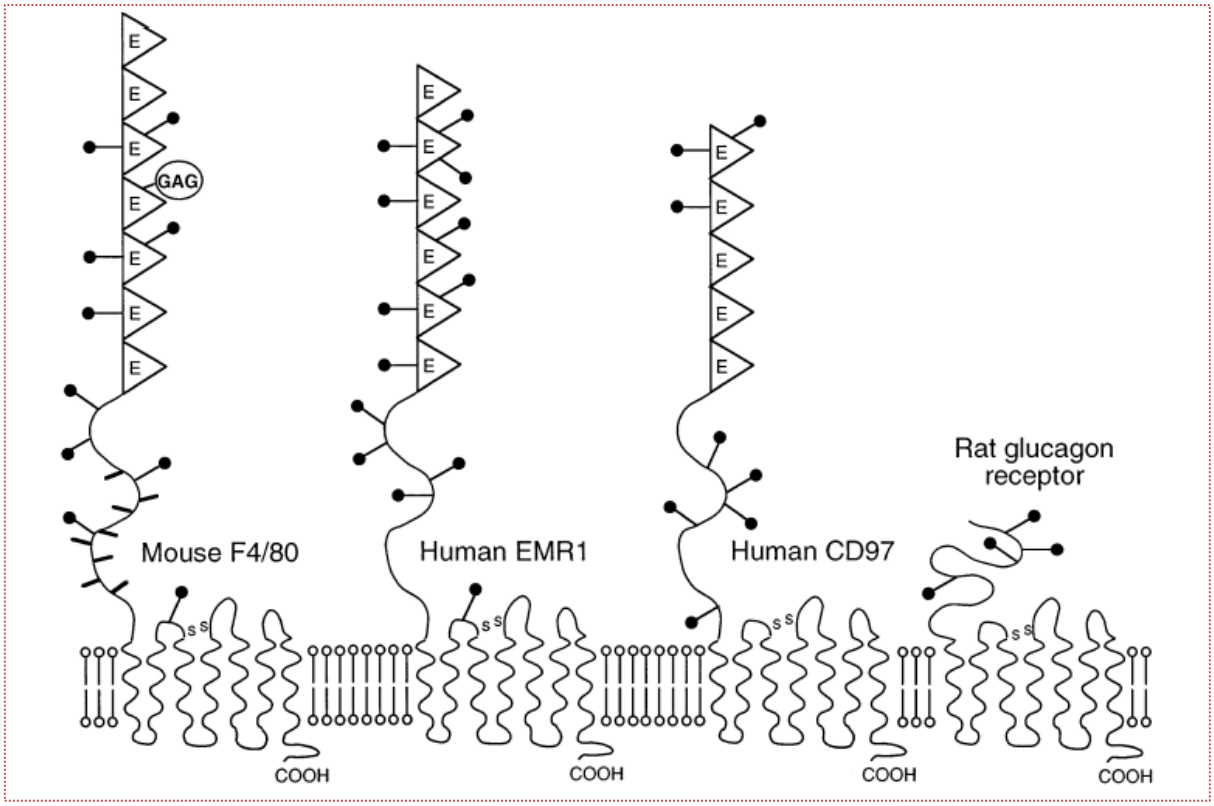

Figure 1.5. structure of the longer forms of the EGF-TM7 family members (F4/80, EMR1 and CD97). This image illustrates the structure of the Three longer forms of the EGF-TM7 family which are the mouse F4/80, the human EMR1 and CD97. The rat glucagon receptor that is the shorter form and lacking the EGF domain is shown for comparison. EGF domain is represented by triangles and the N-linked glycosylation sites are shown in black circles. The ss are disulphide bonds between the first and the extracellular loops. F4/80 contains O-linked sugars shown as short black bars and the GAG represents the glycosaminoglycan modification (McKnight and Gordon, 1998).

1.6 Thesis objectives

This thesis aims to construct and optimize an AAV tool that can be used to investigate the role of microglia in neuroinflammatory disorders such as multiple sclerosis. The first aim of this thesis is to construct a macrophage/microglia-specific adeno-associated virus (AAV) vector by inserting the F4/80 promoter sequence into the ITR-plasmid backbone. Our hypothesis is that this AAV vector driven by the F4/80 promoter will be expressed exclusively in macrophages and CNS-resident microglia. By achieving this, the expression of the gene of interest in microglia could be controlled and the risk of off-target expression reduced.

After testing the specificity of the viral vector, the second aim is to optimize the production of the AAV vector based on pseudotype 2/5 using the most commonly employed production strategy calcium-phosphate mediated triple transfection for AAV2/5 packaging followed by a discontinuous iodixanol density gradient ultracentrifugation. By producing these AAV particles, we could test their tropism for microglia and potency in infecting the cells by monitoring its pathway in vitro or in vivo via enhanced green fluorescent protein (eGFP).

The final aim is to investigate the role of MARCH-I molecule, an E3 ubiquitin ligase shown to have a crucial role in regulating MHC-II expression. MARCH-I will be inserted into the AAV-F4/80-eGFP vector and its function tested on IFN-γ-stimulated macrophages-like cells (RAW 264.7). Our hypothesis is that IFN-γ-primed MHC-II surface expression will be inhibited following the forced expression of MARCH-I in RAW 264.7 cells. The ability to down-regulate MHC-II expression on activated microglia using this viral tool could provide a better understanding of the role of these cells in neuroinflammation.

CHAPTER 2

GENERAL METHODS

2.1 Molecular biology techniques

2.1.1 Escherichia coli DH5alpha chemically competent cells

E.coli DH5α λpir (Invitrogen, Carlsbad, CA, USA) was cultured for 16 h on agar without antibiotics at 37°C. Five to ten mL of TYM broth culture were inoculated with a single colony and incubated for 16 h at 37°C on a shaker (Bioline, London, UK) at 200 rpm. Once the optic density (OD_{600}) reached 3.0 – 4.0, 100 µL of overnight culture was added to 40 mL TYM broth media. Cells were grown to an OD_{600} of 0.35-0.40, were immediately chilled on ice for 20 min and spun at 3000 g for 10 min at 4°C. Three mL of cold TFB I was added to the pellet and resuspended by pipetting. Then the volume was bought to 40 mL using same solution, and it was incubated on ice for 2 - 3 h. Cells were centrifuged at 3000 g for 10 min at 4°C, resuspended in 4 mL ice cold TFB II (Appendix), and stored in 100 µL aliquots at -80°C until use.

2.1.2 Chemically competent cells transformation

To transform competent DH5α cells, 5 µL of plasmid DNA (Table 2.1) was added to 100 µL of competent cells in a 1.7 mL eppendorf tube and mixed gently. A Puc19 plasmid control (Invitrogen) was used to monitor transformation efficiency. Tubes were incubated on ice for 30 min followed by a heat shock for 45 seconds to 2 min in a 42°C water bath or heat block, and placed again on ice for further 2 - 15 min. 600 µL of pre-warmed LB medium (Appendix 4) was added to each tube and incubated at 37°C on the shaker at 225 rpm for 1 h. 100 µL of each transformation mixture was plated onto antibiotic-containing agar plates and incubated overnight at 37°C (Table 2.1).

Plasmid name	Plasmid construct	Supplier	Antibiotic resistance
Empty AAV backbone	pFBAAVmcsIRESeGFPBgHpA	Gene transfer vector core	Gentamicin/Ampicillin
AAV-CAG	pFBAAVCAGmcsIRESeGFPBgHpA	Gene transfer vector core	Gentamicin/Ampicillin
pHelper	pSR449B	Robert Kotin Lab	Ampicillin
pRep/Cap	pAAVRep2/Cap5	Colleen Stein-Davidson Lab	Ampicillin
AAV-yfp	pAMCAG-dYFP-WPRE-BgHpA	Bronwen Connor Lab	Ampicillin
MARCHI cDNA donor	pCMV6-AC-GFP	Origen	Ampicillin/Neomycin
F4/80 promoter donor	pEZX-PG02	GeneCopoeia™	Kanamycin
AAV-F4/80	pFBAAVF4/80mcsIRESeGFPBgHpA		Gentamicin/Ampicillin
AAV-F4/80-MARCHI	pFBAAVF4/80MARCHImcsIRESeGFPBgHpA		Gentamicin/Ampicillin

Table 2.1 Source of Plasmids

2.1.3 Plasmid preparation

2.1.3.1 Plasmid Miniprep

Small-scale plasmid purifications were undertaken using a High-speed plasmid mini kit (Geneaid, New Taipei, Taiwan). A pellet of 3-4 mL of cultured bacterial cells containing the plasmid of interest was obtained by centrifugation at 14-16,000 x g for 1 min. Cells were resuspended in 200 µL RNase suspension buffer and lysed by adding 200 µL lysis buffer. In order to separate plasmid

DNA and cellular debris, 300 µL of chilled binding buffer was added to the tube and centrifuged at 14-16,000 x g for 3 min. Plasmid DNA-containing supernatant was transferred to a column and centrifuged at 14-16,000 x g for 30 sec. The column containing bound plasmids was washed with 600 µL of ethanol containing wash buffer and centrifuged twice at 14-16,000 x g for 30 sec and then for 3 min to dry the column matrix. To elute plasmid DNA, 50 µL of TE buffer was added to the matrix column and the latter was centrifuged at 14-16,000 x g after letting it standing for 2 min.

2.1.3.2 Plasmid Maxiprep

Large-scale DNA plasmids purification was performed using PureLink Maxiprep kit (Invitrogen). 250 mL of DNA plasmid-containing bacterial cell culture was centrifuged at 4000 x g for 10 min. The pellet was resuspended in 10 mL of resuspension buffer containing RNase and lysed with 10 mL lysis buffer. 10 mL of precipitation buffer was added to the mixture and precipitated lysate was transferred into the HiPure filter maxi column and was run through the filter by gravity flow. After the lysates stopped dripping, the column was washed with 50 mL of wash buffer and the solution was allowed to drain by gravity flow. DNA plasmid was eluted by adding 15 mL of elution buffer to the maxi column and precipitated by adding 10.5 mL isopropanol and centrifuged at >12,000 x g for 30 min at 4°C. To resuspend the DNA plasmid pellet, 5 mL of 70% ethanol was added to the tube and centrifuged at > 12,000 x g for 5 min at 4°C. After leaving the pellet to air-dry for 10 min, DNA plasmid pellet was resuspended with 500 µL TE buffer and stored at -20°C.

2.1.3.3 Restriction enzyme digestion reaction

Restriction digests were performed to prepare plasmids to confirm their identities for use in further experiments (Table 2.2) or for cloning (Table 2.3). In a 25 µL reaction, 15 µL of plasmid DNA was added to 5.5 µL of nuclease-free sterile ddH_2O, 2.5 µL of 10x NEB buffer 4 (New England Biolabs, MA, USA) and 20 U of each restriction enzyme. The reaction was incubated at 37°C for 3 h to overnight.

Plasmids	RE	Expected fragment sizes
AAV-CAG	EcoRI/NotI	6960/1404
pHelper	NcoI	4277/4238/1722/1398
pRep/Cap	SalI	5089/1541
Empty AAV backbone	NcoI/NotI	5798/723
MARCHI donor plasmid	NcoI	3876/1215/1166/735/423
F4/80 donor plasmid	EcoRI	4788/875

Table 2.2 Restriction enzymes used for plasmids identification

AAV plasmids	cDNA insert	RE
AAV backbone	F4/80	SalI/NheI
AAV-F4/80	MARCHI	SpeI/ClaI

Table 2.3 Restriction enzymes used for cloning

2.1.3.4 DNA electrophoresis

Following restriction enzyme digest, 5 µL of digested DNA fragments from desired plasmid were loaded onto 0.9 % low melting point agarose gel in TAE buffer (Appendix 4). DNA fragment size was estimated using a 1 kb plus DNA ladder (Invitrogen) suitable for sizing linear double-stranded DNA fragments from 100 bp to 12 kb. Electrophoresis was run at 90 V for 120 min, stained for 20

min with ethidium bromide (Sigma Aldrich, MO, USA), at 0.5 µg/mL and washed with sterile ddH_2O. To visualize the bands, AlphaImager® Mini UV System (ProteinSimple, Santa Clara, CA, USA) was used.

2.1.4 AAV shuttle construction

2.1.4.1 PCR primers design

To isolate the cDNA of interest from its source plasmid, primers shown in Table 2.2 were customized, and in order to allow insertion of the PCR-amplified cDNA fragment, unique restriction enzymes sites were incorporated that complemented the restriction sites at the multiple cloning site of the AAV backbone plasmid. After adding the desired restriction site to the 5' end of both forward and reverse primers, a string of four Cs preceding the restriction site was added in order to form a G:C clamp at the end of the amplified PCR product allowing an efficient enzyme cut. NEB cutter V2.0 software was used to map restriction sites that are present in the desired plasmid, and ClustalW and Oligo Analizer 3.1 (IDT Sci Tools, Coralville, IA,USA) were used to check and analyse primers sequences respectively. Primers were manufactured by Integrated DNA Technologies (IDT).

cDNA	Forward	Reverse
MARCHI	**5'**CCCCACTAGTATGCCCCTCCACCAGATTTC**3'** ***SalI***	**5'**CCCCATCGATGACTGGTATAACCTCAGGTG**3'** ***NheI***
F4/80	**5'**CCCCGTCGACATTACAGGTGCCTAACACCA**3'** ***SpeI***	**5'**CCCCGCTAGCTATGCTGTAGTTCTGTCATT**3'** ***ClaI***

Table 2.4 PCR primers sequences

2.1.4.2 Standard PCR

The gene of interest sequence was isolated from its plasmid source via PCR. In a 50 µL reaction, 25 µL of MyTaq™ Mix (Bioline) was mixed with 20 µM final concentration of each desired cDNA forward (IDT) and reverse primers (IDT) and 200 ng of the plasmid source. The PCR reaction was set up on ice and the amplification reaction was run on Techne Tc-5000 PCR thermal cycler (GMI, Ramsay, MN, USA) under the following conditions: 1 cycle of initial denaturation at 94°C for 3 min, 35 cycles of: denaturation at 94°C (30 sec), annealing at 57°C (30 sec) and extension at 68°C (30 sec per kb). The final extension was at 68°C for 10 min.

2.1.4.3 DNA fragment purification from agarose gel

To extract PCR or restriction digestion cDNA products from agarose gel for ligation, gel/PCR DNA fragments extraction kit (Geneaid) was used following the manufacturer instructions. After running the products in an agarose gel electrophoresis (see section 2.1.3.4 for protocol), the agarose gel portion containing the relevant DNA fragment was excised and transferred to a 1.5 mL microcentrifuge tube. 500 µL of DF buffer containing chaotropic salt was added to the tube and the sample was incubated at 55-60°C for 10-15 min to dissolve agarose gel. The dissolved sample (800 µL) was transferred to a column after letting it to cool to room temperature, and centrifuged at 14-16,000 x g for 30 sec. After binding DNA fragments in chaotropic salt by the glass fibre matrix of the spin column, the latter was washed twice with 400 µL W1 buffer and 600 µL ethanol-containing wash buffer and spun for 30 sec and 3 min respectively at 14-16,000 x g. The purified DNA fragments were eluted by adding 50 µL of TE buffer to the column and spinning it for 2 min at 14-16,000 x g. Purified DNA stocks were stored at -20°C.

2.1.4.4 DNA fragment ligation to the AAV vector backbone

The empty AAV vector backbone (Figure 2.1) used to construct the AAV-F4/80-eGFP and AA-F4/80-MARCHI-eGFP vectors was an Invitrogen pFastBac™ plasmid (Gene transfer core, Iowa, USA) containing enhanced green fluorescent protein eGFP. The expression of eGFP was further enhanced by a Internal Ribosome Entry site element (IRES), and this element is useful in gene delivery to coordinate and efficiently express two genes that are under control of same promoter

in a single vector. Both eGFP and IRES were flanked by the AAV two inverted terminal repeats (ITR) from serotype 2.

F4/80 promoter ortholog EMR1 “Homo sapiens EGF-like module containing, mucin-like, hormone receptor-like 1”, was PCR amplified from pEZX-PG02 plasmid (GeneCopoeia, Rockville, USA) and the mouse membrane-associated ring finger (C3HC4) 1 (MARCH1) cDNA was derived from pCMV6-AC-GFP vector (Origen, Rockville, USA), using the primers described in Table 2.4 (see Appendix 1 for the plasmid maps).

Inserts were cloned into the empty AAV backbone at their corresponding restriction sites (Table 2.3) using T4 DNA Ligase (Invitrogen) following the manufacturer’s instructions. Ligation was setup with 4 µL of ligase reaction buffer, 0.1 U T4 DNA ligase (5 U/µL), 50 ng AAV vector and 150 ng insert (1:3 ratio of vector: insert). The reaction was made up to 20 µL with sterile ddH2O.

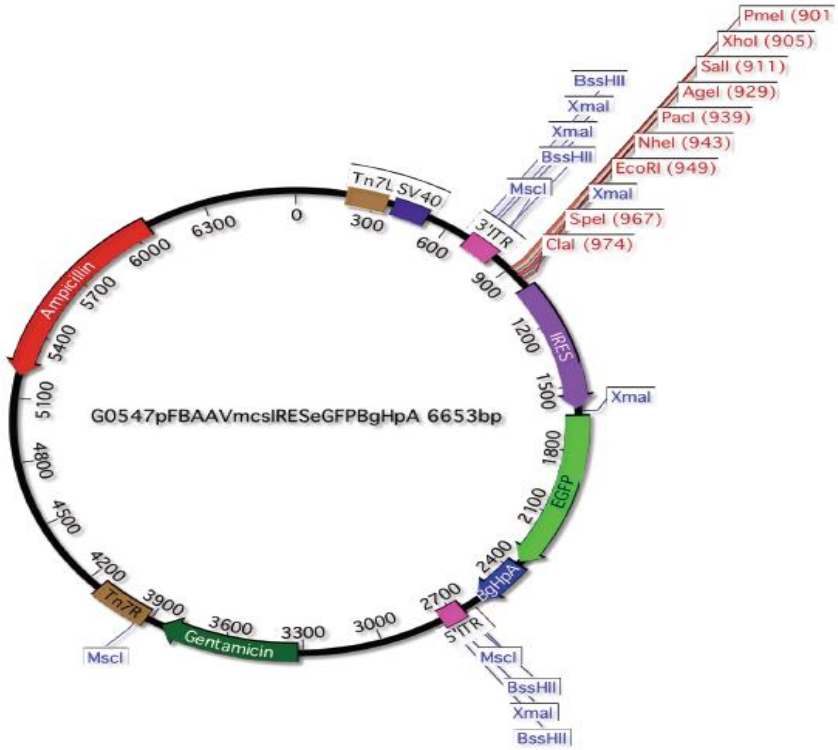

Figure 2.1 Empty AAV plasmid backbone map

2.1.4.5 Colony PCR

Following transformation of *E.coli* with ligation products, a colony PCR was performed to screen *E.coli* colonies for the presence of the cDNA sequence of interest in the AAV plasmid. The reaction was set up by transferring single colonies to each PCR tube and adding 25 µL of MyTaq™ Mix (Bioline) and 20 µM final concentration of each forward and reverse primer that amplified the relevant cDNA sequence. PCR reaction was performed as described in section 2.1.4.2. To confirm clone identity, agarose gel electrophoresis was performed as described in section 2.1.3.4.

2.1.4.6 ITRs integrity analysis

As recombination at both the transposable elements (Tn7L and Tn7R) and the ITRs is possible in the pFBAAV plasmid throughout cloning process and amplification to midi or maxi preps, Integrity of ITRs in constructed AAV vectors were checked by performing a single digest each of *MscI* and *XmaI* (New England Biolabs) following the protocol described in section 2.1.3.3.

2.2 Mammalian Cell lines culture and assays

2.2.1 Mammalian cell lines culture

Human embryonic kidney 293 cells (HEK), packaging-type, were used to package AAV-F4/80 vector because they have the adenovirus gene, early region 1 (E1) containing two transcription units E1a and E1b, which is required for AAV packaging. This human cell line was first described in Graham et al. and was created by the transformation and culturing of normal human embryonic kidney cells with fragment of mechanically sheared DNA of adenovirus serotype 5 (Graham et al., 1977). This resulted in the incorporation of approximately 4.5 kilobases from the viral genome into the human chromosome 19 of HEK cells (Louis et al., 1997). Human ovarian carcinoma cell lines 1A9 and human hepatocellular carcinoma HePG02 were a kind gift from Professor John Miller (VUW) and Dr Lifeng Peng (VUW) respectively.

The murine macrophage-like cell line RAW 264.7 has been shown to express the same key surface markers (CD11 and F4/80) and to have similar responses to three microbial ligands LPS, Pam_3CSK_4 and Poly I:C as bone marrow macrophages (Hartley et al., 2008). RAW cells were established from

an Abelson murine leukemia virus (MuLV)-induced tumor developing in a BAB/14 mouse, a congenic strain of BALB/c IgH (Hartley et al., 2008).

All mammalian cell lines were maintained in Dulbecco's Modified Eagle Medium (DMEM) supplemented with 10% foetal calf serum (FCS), 100 units/mL Penicillin/streptomycin, 2mM L-Glutamine, 2% HEPES and 1% non-essential amino-acids (all reagents from Invitrogen). Cultures were incubated at 37°C/5% CO_2, and cells were passaged twice weekly to maintain them at their exponential growth phase. All cell processing was performed in biosafety cabinets (LABCONCO, Kansas, MO, USA).

2.2.2 Mammalian Cell lines transfection and use of fluorescence microscope

A day before transfection, cells were cultured in a 24 well plate at 0.5 x 10^6 cells/well in 500 µL complete DMEM (see section 2.2.1 for recipe). All cell lines were used at low passage number (< 20). Once cells were 70-80% confluent, media was changed and replaced with complete DMEM with or without antibiotics. Cells were transfected via DNA plasmid using Lipofectamine® LTX and PLUS Reagent (Invitrogen). Transfection was performed as per manufacturer instructions. Briefly, plasmid DNA was added to 250 µL of Opti-MEM reduced serum medium (Invitrogen). "PLUS" reagent was added to the DNA mix at 1:1 ratio ("PLUS" reagent: DNA) and tubes were incubated 15 min at room temperature before adding 4 µL of Lipofectamine® LTX reagent. The mixture was incubated 30 min at room temperature and 50 µL DNA-Lipofectamine was added to each culture well. Non-transfected cells were used as a negative control. Plates were incubated at 37°C/5% CO_2 for 16-24 h then analysed under an Olympus fluorescent microscope (Olympus 1x 51, magnification 10x, 4x).

2.2.3 IA/IE surface expression assay

RAW cells were cultured in 24-well plates at 4 x 10^5 cells/ well in complete DMEM at 2% FCS with antibiotics. To induce IA/IE surface expression, RAW cells were treated with interferon gamma (IFN-γ) at 20 U/mL or left untreated as a control. Cells were incubated at 37°C/5% CO_2 and harvested at 1-3 days later for FACS analysis. At each time point, cells were washed and collected with warm dPBS (Gibco™), and cell pellets were obtained by centrifugation at 300 g for 5 min.

RAW cells were collected in 300 µL ice-cold FACS buffer containing dPBS supplemented with 2% FCS and 0.1% sodium azide (1M). 1 x 10^6 cells from each sample were transferred to each well in a U-bottom 96-well plate, and cell pellets were obtained by centrifugation at 400 g for 5 min. Cells were incubated on ice for 10 min with 50 µL of rat anti-CD16/32 at 1:300 (BD Pharmingen, USA) in order to block non-specific IgG Fc receptors prior to staining with the antibody. Cells were washed with 200 µL FACS buffer and the plate was spun for 5 min at 400 g. Cells were stained with PE-conjugated rat anti-mouse MHC-II (IA/IE) antibodies (1:200; eBioscience, San Diego, CA, USA) and incubated on ice in the dark for 30 min. Each sample was washed with 200 µL of FACS buffer, re-suspended and filtered through a 70 µm mesh in 300 µL FACS buffer and analysed immediately using a BD FACSCanto II (BD Biosciences, USA) flow cytometer. PE-conjugated rat IgG2b, κ isotype control antibody (1:200; eBioscience, San Diego, CA, USA) was used as a negative control.

2.3 Flow cytometry

Samples were acquired on a FACScanto II flow cytometer (BD Bioscience) with FACSDiva 6.1.2 software. The gated live cell population of interest was determined using the forward scatter (FSC-A) and side scatter (SSC-A) data of non-stained cells. 5000-10,000 live events were recorded per assay. All analyses were carried out using FlowJo software (Tree Star Inc. Ashland, OR, USA).

2.4 Statistics

To analyse results and generate graphs, GraphPad, Prism v. 4.0 (GraphPad Software, San Diego California USA, www.graphpad.com) was used. Tests for significance were performed using one-way ANOVA with Sidak's multiple comparison test, comparing multiple treatments with vehicle control. P-values under 0.05 were considered significant.

2.5 $AAV_{2/5}$-F4/80 virus production

2.5.1 HEK 293 cells triple transfection

All procedures involving AAV virus were performed exclusively in biosafety cabinets. Prior to transfection, HEK 293 cells were maintained in complete DMEM (Section 2.2.1). Three 150 cm^2 flasks of HEK 293 cells were plated at 5 x 10^6 cells/flask for each vector type. Once cells reached 80% confluency, the complete DMEM was removed and replaced by Iscove's modified Dulbecco's media IMDM (high glucose) (Gibco®, USA) 3 h prior to transfection. HEK cells were transfected with three plasmids for each AAV virus type to be packaged (Table 2.5). Helper plasmid contained necessary adenovirus genes required for an efficient AAV replication which are E2A, VA, and E4. E1 adenovirus gene that is also necessary for AAV replication is supplied in HEK 293 cells genome (Section 2.2.1). Replication and capsid genes were supplied in *trans* via pRep/Cap plasmid and were from the same or different serotypes.

Packaged AAV	***Plasmids***
AAV2/5-F4/80 virus	AAV-F4/80-eGFP pAd helper plasmid pRep2/Cap5 plasmid
AAV2/5-CAG-GFP	AAV-CAG-eGFP pAd helper plasmid pRep2/Cap5 plasmid
AAV2-CAG-yfp	AAV-CAG-yfp pAd helper pRV1 (encodes for Rep2/Cap2 genes)

Table 2.5. Plasmids required for triple transfections

The triple-transfection of HEK 293 cells was set up as follow: for each confluent T150 flask, 12.5 µg of AAV backbone plasmid, 25 µg pAd helper plasmid and 12 µg pRep2/Cap5 plasmid or pRV1 (35) were added to 2.4 mL of sterile water in a 15 mL Falcon tube, then 330 µL of 2.5 M $CaCl_2$ was added to the mixture. The transfection mixture was filtered through a 0.2 µm syringe filter into another 15 mL Falcon tube and whilst vortexing the solution vigorously, 2.5 mL of 2x HeBs buffer (280 mM NaCl, 1.5 mM Na2HPO4, 50 mM HEPES, PH 7.05) was added quickly. The mixture was incubated 2 min at room temperature and 5 mL was applied to the corresponding T150 flask. Transfected cells were incubated at 37°C/5% CO_2. 16 h post-transfection, media was removed and replaced with fresh complete DMDM.

2.5.2 AAV purification

2.5.2.1 HEK 293 cells harvesting

96 h post-transfection, HEK 293 cells from AAV2/5-F4/80-eGFP and AAV2-CAG-yfp control flasks were washed with warm dPBS and harvested with warm 5 mM EDTA in dPBS. Cell were after centrifuged at 600 g for 35 min at 4°C, and the pellets resuspended in Tris-NaCl lysis buffer (50 mM Tris, 150 mM NaCl at pH 8.4) with vigorous pipetting to release the AAV virions. In order to release as many virions as possible from the cells, the samples underwent three freeze and thaw cycles by alternating tubes between dry-ice ethanol and 37°C water bath. To determine isolate AAV2/5 virions released into medium (Vandenberghe et al., 2010), the AAV2/5-F4/80 supernatant was centrifuged at 600 g for 35 min at 4°C to remove cell debris. AAV2-CAG-yfp vector control was purified from cell lysates only (Vandenberghe et al., 2010).

Benzonase endonuclease was added to the cell lysates and AAV2/5-F4/80-eGFP culture medium at a final concentration of 50U/mL in order to dissociate aggregated AAV particles and digest any extraneous DNA before the Iodixanol gradient step. Lysates and culture medium samples were incubated at 37°C for 30 min in water bath, and cell debris were removed by centrifugation at 3000 g for 15 min at 4°C. Samples were stored at -20°C until Iodixanol gradient step.

2.5.2.2 Iodixanol gradient

Four Iodixanol step gradients were used to purify AAV virus from cell lysate or culture medium samples. The 15% interface contained 1 M NaCl to destabilize ionic interactions between macromolecules. 40% and 25% steps were used to remove contaminants with lower densities including empty capsids. 60% interface was used to gather genome containing AAV Virions. Phenol red (Sigma-Aldrich, St Louis, MO, USA), was added in the upper 25% and lower 60% steps to clearly see the steps. Iodixanol solutions were prepared as described in Table 2.5.

Density gradient %	*Density gradient composition (for 2 gradients)*
15%	4.5 mL of 60% + 13.5 mL of 1 M NaCl/PBS-MK buffer
25%	5 mL of 60% + 7 mL of PBS-MK buffer + 30 µl of phenol red
40%	6.7 mL of 60% + 3.3 mL of PBS-MK buffer
60%	10 mL of 60% + 45 µl of phenol red

Table 2.5 Iodixanol density gradient steps composition

The solutions were overlaid in a Beckman ultracentrifuge tube as follows: 60% Iodixanol step (5 mL), 40% Iodixanol step (5 mL), 25% Iodixanol step(6 mL) and 15% Iodixanol step (9 mL) using 18 gauge needle (BD, Franklin lakes, NJ, USA) (Figure 2.2). The AAV containing sample was divided between four Iodixanol gradients, and cell lysis buffer (50 mM Tris, 150mM NaCl, PH 8.4) was added on the top of the sample. Tubes were centrifuged at 48,000 g for 2 h 10 min at 18°C with maximum acceleration and deceleration in a Beckman Ti70 rotor on a Beckman ultracentrifuge (Beckman Coulter, Indianapolis, USA). Approximately 3 mL of virus were collected from each tube using 18 gauge needle attached to a 5 mL syringe (BD, Franklin lakes, NJ, USA) below (3-5 mm) the 60% and 40% interface (Figure 2.3). At this stage the collected virus was stored at 4°C prior to concentration.

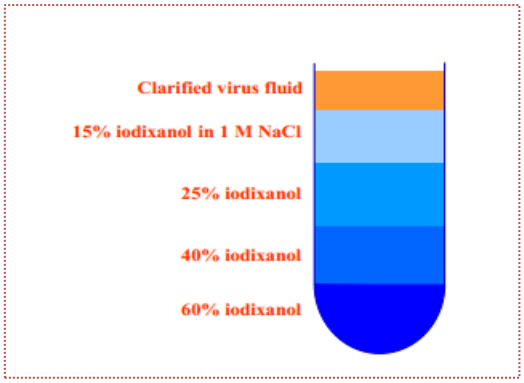

Figure 2.2 Iodixanol density gradient steps

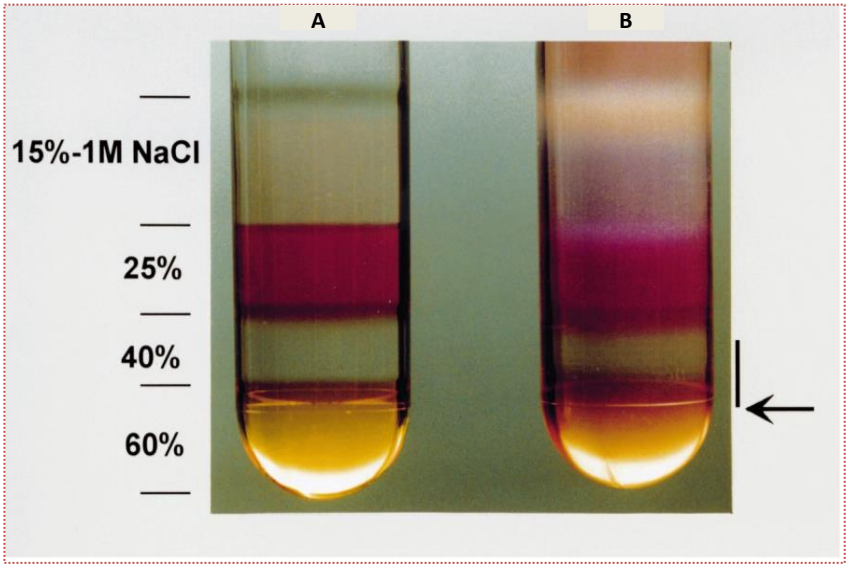

Figure 2.3. Iodixanol density gradient for the purification of AAV. Gradient steps before ultracentrifugation (A). The gradient was established from four different densities in Beckman ultracentrifuge tubes, using an 18-gauge needle. The gradient included a 15% step containing 1 M NaCl to destabilize ionic interactions between macromolecules, 40% and 25% layers allowing the removal of contaminants with lower densities including empty capsids and 60% interface gathers genome containing AAV Virions. To distinguish between the steps, phenol red was added to the 25% and 60% steps. After centrifugation (tube B), the AAVs were collected from each tube 3-5mm below the 60% and 40% interface (see arrow in tube B) using an 18-gauge needle and syringe (Zolotukhin et al., 1999).

2.5.2.3 Purified AAV samples concentration

Samples were concentrated at 3000 g at 4°C for 30-45 min using Vivaspin® 4 centrifugal concentrator (Vivaproducts, MA, USA). Three cycles of centrifugation have been performed for each sample; in the first cycle the sample was spun down to 250 µl-500 µl, resuspended with 4 mL of 1x dPBS+ 1 mM $MgCl_2$ to prevent virus from aggregation and spun again to as small volume as possible. Samples were removed from the concentrator to a sterile microcentrifuge tube and the concentrator was rinsed with 250 µl of dPBS+ 1 mM $MgCl_2$ and transferred to the same centrifuge tube. Concentrated samples were passed through a 13 mm 0.2 µm syringe filter (JetBioFil, Guangzhou, China) and stored at 4°C for short term storage (less than a month) or at -80°C for long term storage.

2.5.3 AAV stocks Titering

2.5.3.1 Total genome copies quantification

Genome copies of the purified $AAV_{2/5}$-F4/80 and AAV_2 control stocks were titered using QuickTiter AAV quantification kit (Cell Biolabs- INC, Israel). Eleven AAV DNA standards were used in the assay: 10 µg/mL, 5 µg/mL, 2.5 µg/mL, 1.25 µg/mL, 0.625 µg/mL, 0.313 µg/mL, 0.156 µg/mL, 0.078 µg/mL, 0.039 µg/mL, 0.020 µg/mL, 0.010 µg/mL and 0 µg/mL as the blank. 13.5 µL of each purified AAV sample was added to 1.5 µL of 10X QuickTiter™ Solution C containing beads that capture the virus capsid and incubated 1 h at 75°C to denature the capsid and release viral DNA. A non-heated reaction of each sample was used as a control. Standards, samples and controls were transferred to a 96-well plate in duplicates. 90 µL of freshly prepared 1X CyQuant® GR Dye which labels viral nucleic acid was added to each well. The relative fluorescence unit (RFU) was calculated for each sample using Enspire 2300 fluorescence at 480/520 nm. To calculate the Net RFU we used the following formula:

Net RFU = RFU (viral sample) – RFU (non-heated) control sample

2.5.3.2 Single-Cell Fluorescent Assay

In addition to the total genome copies quantification assay, a single-cell fluorescent assay was performed to titer infectious AAV2/5-F4/80 and AAV2 control vectors that express GFP and YFP respectively. RAW cells and HEK 293 cells were transduced each in triplicates in a 24-well plate with serial volumes (5 µl, 10 µl, 15 µl, 20 µl, 40 µl) of AAV2/5-F4/80 virus or AAV2 control respectively. On day 5, fluorescent cells were visually scored and number of infectious units was calculated for each AAV serotype following the formula below:

$$\text{X (Infectious units/mL)} = \frac{\text{number of transduced cells x 1000 µL}}{\text{Volume of AAV vector (µL)}}$$

2.5.3.3 AAV capsid protein detection

To detect the encapsulated AAV2/5-F4/80-GFP and AAV2-CAG-YFP virions in the purified samples, SDS-PAGE electrophoresis was performed to identify the three capsid proteins of the virus VP1, VP2 and VP3. Protein concentrations were determined by Bradford assay (Biorad®) and 5 µg of each sample was mixed to 2.5 µl of NuPAGE LDS sample buffer (x4) and 1 µl of NuPAGE sample reducing agent (x10). Samples were heated for 10 min at 70°C. The gel chamber was loaded with 800 mL of MOPS buffer and 500 µl of NuPAGE antioxidant. 1.5 µL of protein size marker was loaded onto the first well and 10 µl of AAV_2 vector control (cell lysate), $AAV_{2/5}$ (cell lysates and culture medium) were loaded onto well 2, 3 and 4 respectively. SDS-PAGE gel was run for 45 min at 200 V (400mA).

CHAPTER 3

REPROGRAMMING OF RECOMBINANT AAV INTO A MICROGLIA SPECIFIC VECTOR

3.1 Introduction

Using recombinant AAV-gene delivery based technology to target a specific mammalian cell without affecting other neighbouring cells can be very challenging if the transgene is under control of a non-discriminatory promoter such as CMV. Additionally, CMV and other non-specific promoters can be silenced in the mammalian host cell *in vivo,* and silencing is believed to occur by methylation resulting in instable transgene expression (Prosch et al, 1996). This issue has been overcome through the use of CMV hybrid promoters such as CMV/chicken β-actin hybrid (CAG) in Niwa at al. study, in which CAG promoter achieved a long-term expression of GFP in the hippocampal pyramidal neurones lasting for at least 7 months (Niwa et al., 1991). However, the AAV expression driven by CAG was not exclusive to hippocampal pyramidal neurones since GFP fluorescence was detected also in the areas that innervate hippocampus (i.e. the medial septum and the entorhinal cortex neurones) (Peel and Klein, 2000).

Since the first use of a cell-specific promoter in the Klein et al. study, where the brain-derived neurotrophic factor (BDNF) was controlled and stabilised in the hippocampus by using the Neuron-Specific Enolase (NSE) promoter (Klein et al., 1998), the hurdle of delivering a transgene of interest to the target cell and affecting neighbouring cells in the CNS has been surmounted. In addition, it was suggested that promoters that are derived from elements of the target cell can induce synthesis of transgene proteins that result in concentrations closer to physiological levels (Peel and Klein, 2000).

Therefore, the aim of this research was to construct a recombinant AAV vector that targets resident macrophage cells in the brain (i.e. microglia). To achieve this aim, the F4/80 promoter was inserted into an AAV-eGFP vector backbone, and the specificity of this recombinant AAV vector for macrophages was investigated.

3.2 Results

3.2.1 Construction of AAV-F4/80-eGFP

F4/80 promoter sequence was amplified from the pEZX-PG02 plasmid (see map in appendix 1B) by polymerase chain reaction (PCR) using customized primers containing restriction sites *SalI* and *NheI* (Table 2.4). After cleaving the PCR product with *SalI* and *NheI* to create complementary ends, the F4/80 promoter was ligated to the AAV-eGFP shuttle vector using T4 DNA Ligase at 0.1 units at 1:3 ratio of vector: insert. Following the transformation of DH5α competent cells with the ligation product and culture overnight, a colony PCR was carried out using F4/80 primers to check that the promoter was successfully ligated to the AAV-eGFP backbone. PCR screening of thirty colonies of transformed E.coli with ligation products (Figure 3.1A) confirmed insertion of F4/80 promoter into the AAV-GFP vector in eleven colonies. However, since the negative control C2, which contained PCR reagent and F4/80 promoter insert primers only, showed a contamination with F4/80 insert sequence, another colony PCR was performed to double check the insertion of the promoter into the vector, using different stocks of MyTaq™ Mix and primers, which showed no contamination and confirmed the result (Figure 3.1B).

A double digestion of the newly constructed AAV-F4/80-eGFP clone was performed using *SalI* (cuts at 911 bp) and *NheI* (cuts at 2279 bp) generated a 6653 bp band and 1368 bp band, corresponding to the vector AAV-GFP backbone and the F4/80 promoter sequence respectively (Figure 3.2A). Once the positive clone was identified, the integrity of the inverted terminal repeats (ITRs), which can recombine during amplification process, was checked by performing a restriction digestion at the ITRs sites. *XmaI* and *MscI* enzymes cut at both ITRs regions (see chapter 2, figure 2.1 for restriction sites); therefore to verify if these viral sequences were still intact, a single restriction digest of the plasmid was performed using these enzymes. The band sizes that were expected to be generated from each restriction enzyme were present (Figure 3.2B) confirming the integrity of both ITRs in the newly constructed AAV-F4/80-GFP vector.

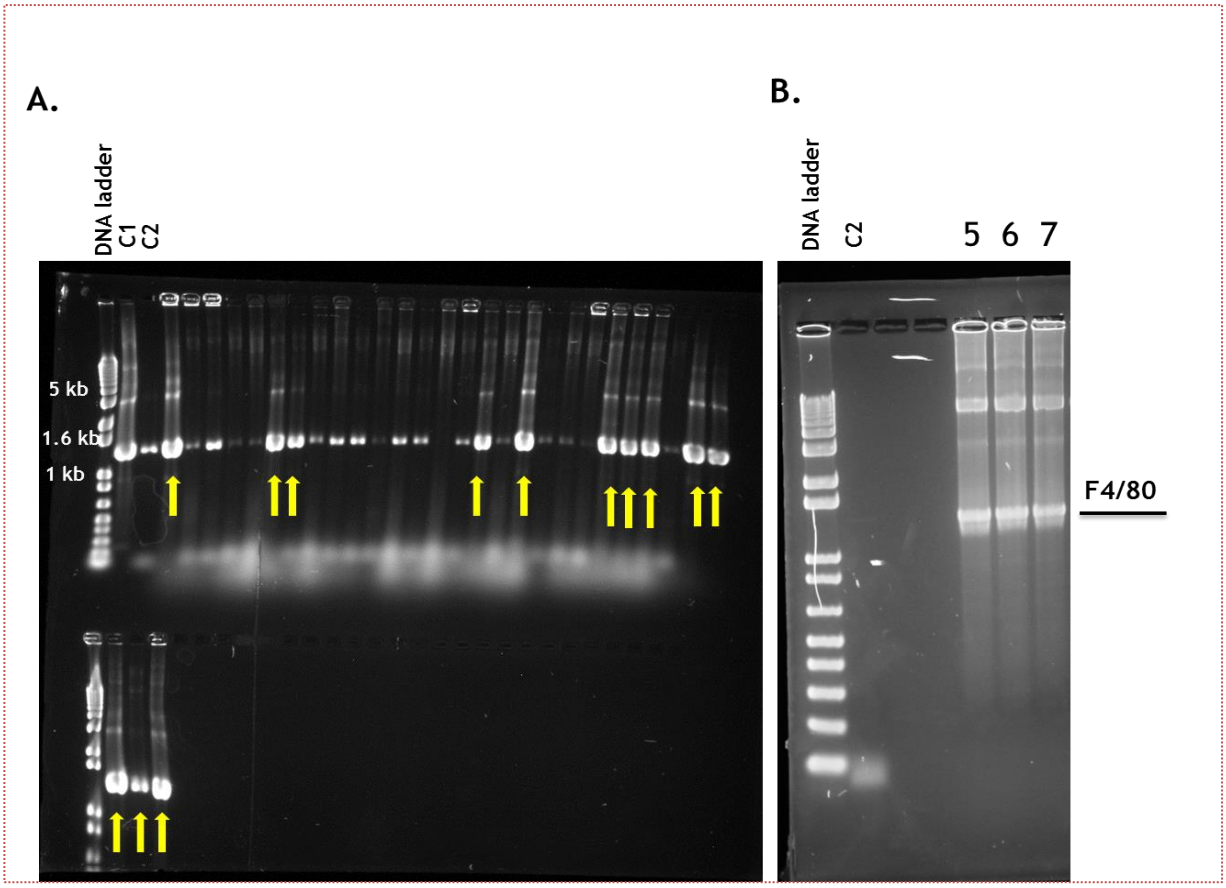

Figure 3.1 ***PCR screening of transformed E.coli colonies.*** **A)** Thirty colonies of *E. coli* transformed with the ligation were added each to a PCR tube with MyTaq™ Mix and the following customized F4/80 promoter primers : Forward **5'**CCCCGTCGACATTACAGGTGCCTAACACCA**3'**and Reverse **5'**CCCCGCTAGCTATGCTGTAGTTCTGTCATT**3'** (20µM final concentration each). The PCR reaction was run as described in Chapter 2, Section 2.1.4.5. The inserted F4/80 promoter has been identified in 13 out of 30 colonies (highlighted by yellow arrows). C1 was a positive control containing the MyTaq™ Mix, primers and the F4/80 promoter plasmid source pEZX-PG02 to monitor the primers' efficacy. C2 was a negative control containing the MyTaq™ Mix and insert primers only in order to check for reagents contamination with F4/80 insert sequence. The presence of a thin band corresponding to F4/80 insert size in the C2 control was related to the reagents contamination. **B)** Another colony PCR was performed with MyTaq™ Mix reagent and insert primers obtained from different stocks to verify the result obtained in gel A. Three colonies from the 13 colonies identified to have F4/80 promoter inserted in gel A, were chosen to run in lanes 5,6 and 7. The C2 negative control contained PCR reagents from different stocks showed no contamination and the bands obtained in Lines 5, 6 and 7 represented amplified F4/80 insert.

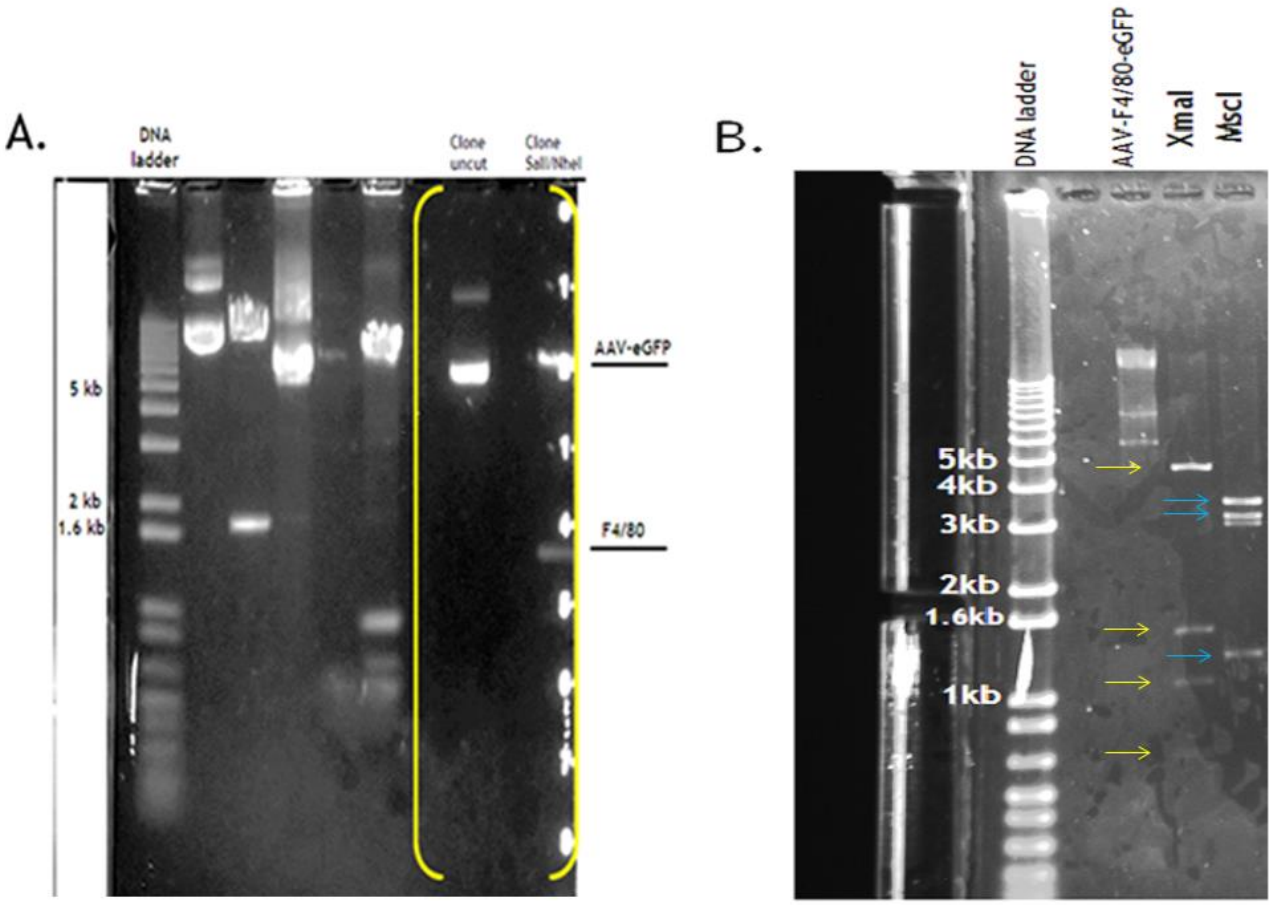

Figure 3.2 ***AAV-F4/80-eGFP clone confirmation*****. A)** The constructed AAV-F4/80-eGFP clone digested with SalI (at 911) and NheI (at 2279) restriction enzymes and the uncut clone were run in a 0.9% low melting point agarose gel in TAE buffer (shown between yellow brackets). **B)** A single digestion of AAV-F4/80-GFP plasmid was performed to check ITRs integrity. Following XmaI digestion four bands were generated including: 4686 bp, 1578 bp, 1104 bp and 659 bp (shown with yellow arrows).Three bands were generated following MscI digestion: a 3503 bp, a 3230 bp and a 1288 bp band (shown with blue arrows). The band shadow under the 3230 bp band is an artefact.

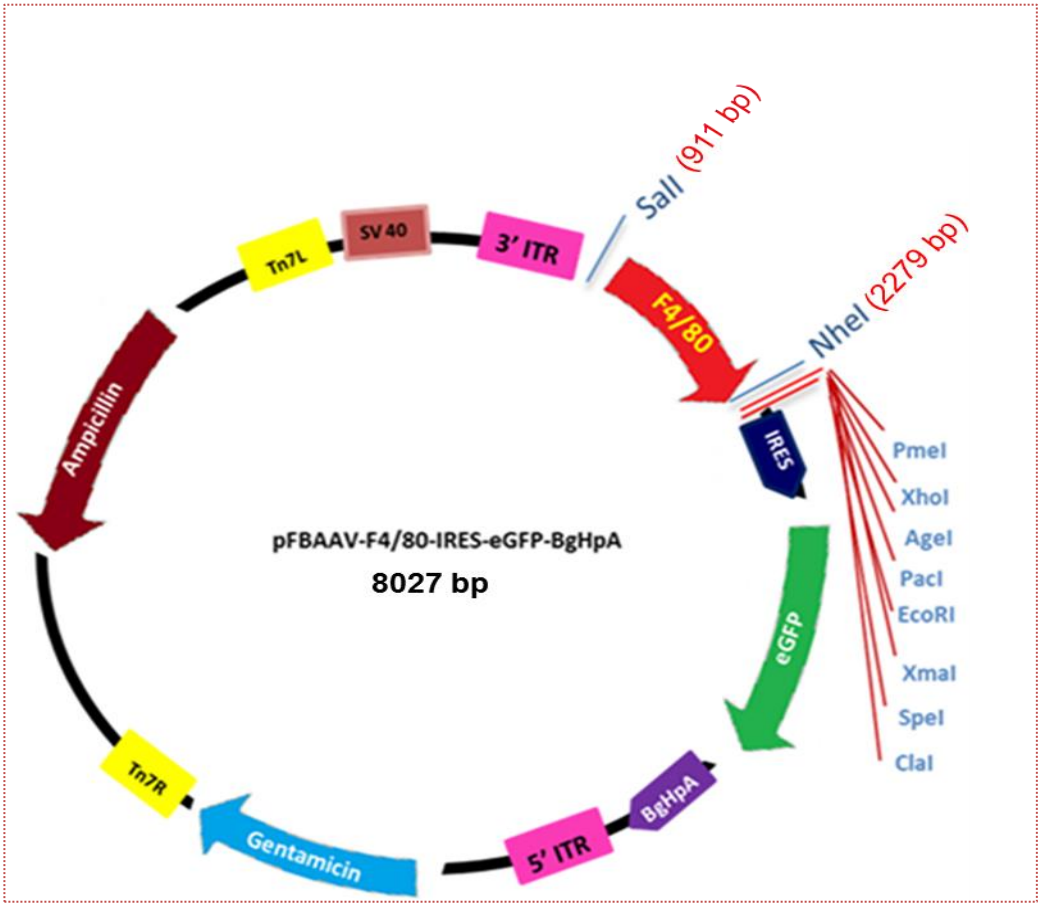

Figure 3.3 ***AAV-F4/80-eGFP vector plasmid map.*** The newly constructed AAV-F4/80-eGFP plasmid contained the F4/80 promoter inserted at *SalI* (911 bp) and *NheI* (943 bp) restriction sites, driving the expression of enhanced green fluorescent protein eGFP. eGFP expression was further enhanced by Internal Ribosome Entry site element (IRES), this element is useful in gene delivery to coordinate and efficiently express two genes that are under control of same promoter in a single vector. All plasmid genes were flanked by the AAV two ITRs from serotype 2. The vector backbone is an Invitrogen pFastBac ™ plasmid.

3.2.2 The F4/80 promoter drove eGFP expression in RAW 264.7 cells but not in HEK 293 cells

Once the AAV-F4/80-eGFP vector was constructed, we tested whether the F4/80 promoter would regulate the expression of eGFP in a macrophage-specific manner compared to the CAG promoter. This promoter is a non-discriminatory promoter which is a combination of the cytomegalovirus (CMV) early enhancer element and chicken β-actin promoter, and is widely expressed in eukaryotic cells. Thus, we compared the expression of eGFP by the HEK 293 (human embryonic kidney) and RAW 264.7 (macrophage) cell lines transfected with AAV-F4/80-eGFP or AAV-CAG-eGFP.

To optimize the transfection efficiency, RAW 264.7 and HEK 293 cells were serially transfected with increasing concentrations of AAV-CAG-eGFP plasmid in a 24-well plate to determine the lowest amount of the plasmid that would transfect the cells efficiently. Cells treated with Lipofectamine only were used as a negative control to assess background fluorescence. Cells were analysed 16-24 h post-transfection, using a fluorescence microscope to visualize GFP expression before being harvested for flow cytometry analysis. In RAW 264.7 cells, eGFP expression was observed by fluorescent microscope under the control of both F4/80 and CAG promoters (Figure 3.4). When the level of eGFP expression was measured by flow cytometry, the mean fluorescence intensity obtained from 1 μg or 2 μg of AAV-F4/80-eGFP plasmid DNA was similar to that of AAV-CAG-eGFP and was higher than the Lipofectamine only control (Figure 3.5B). Furthermore, a similar percentage of cells were eGFP positive with both F4/80 and CAG promoters in RAW 264.7 cells (Figure 3.6). Thus, although the level of expression was modest, this finding confirms the ability of the F4/80 promoter to drive gene expression in macrophages.

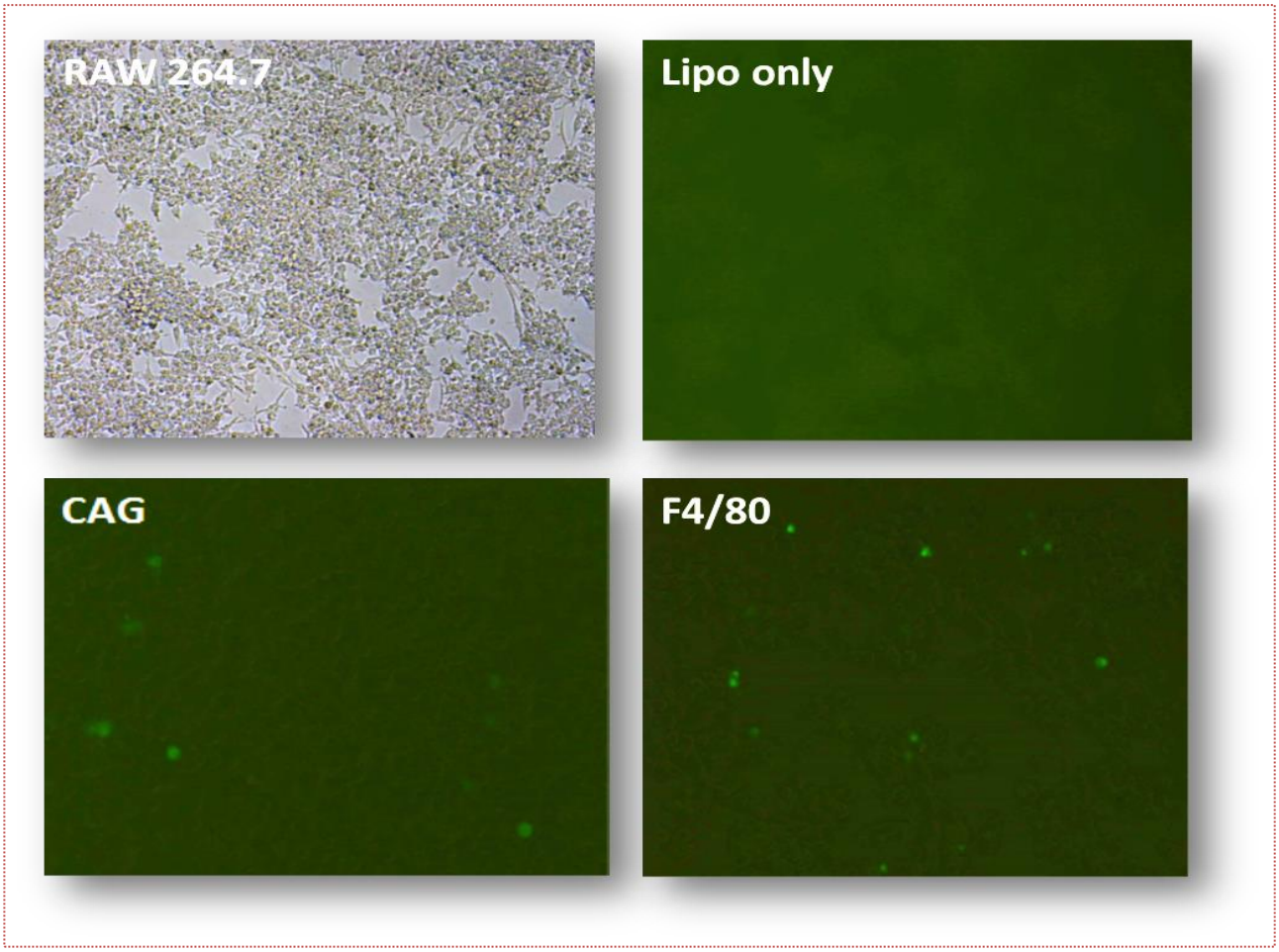

Figure 3.4 ***eGFP was expressed under both F4/80 and CAG promoters in RAW 264.7 cells***. On approaching confluence, plated RAW 264.7 Cells in complete DMEM media in a 24-well plate, were transfected with 1 µg or 2 µg of AAV-CAG-eGFP or AAV-F4/80-eGFP plasmids using 4ul of Lipofectamine LTX plus reagent (Invitrogen,) according to the protocol described in chapter 2, section 2.2.2 and incubated overnight at 37°C in 5% CO_2. Cells containing lipofectamine only were used as a control to check fluorescence background. After 24h, cells were analysed under fluorescent microscope (Olympus 1x 51) to visualize eGFP expression from each vector plasmid. The up left image shows the RAW cells confluency at the time of transfection. EGFP fluorescence was seen in RAW cells transfected with AAV-F4/80 (bottom right image) or AAV-CAG plasmids (bottom left image). Scale bar: 200 µM, magnification = 10 x.

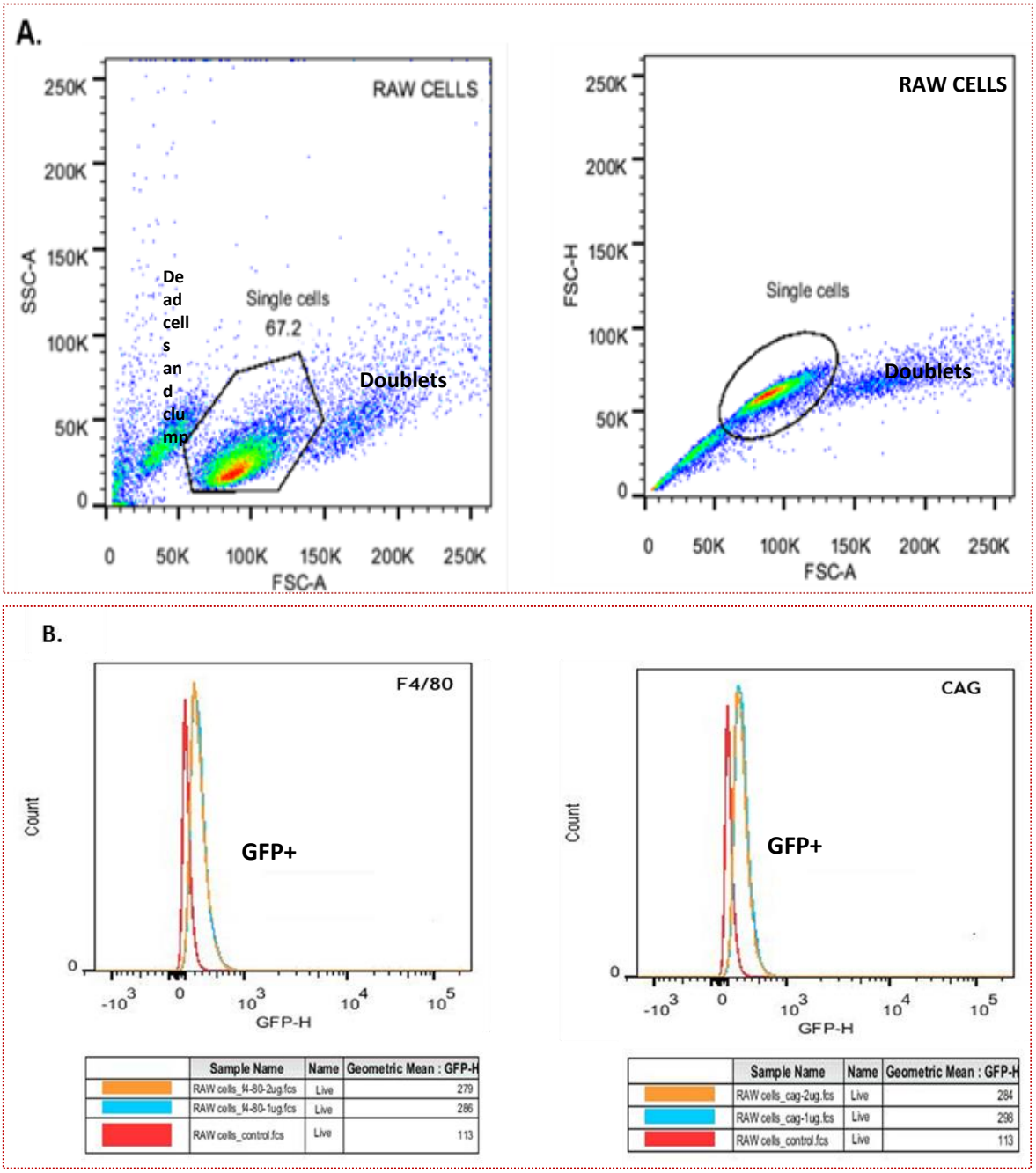

Figure 3.5 ***Similar eGFP expression was found with the AAV-CAG-eGFP or AAV-F4/80-eGFP plasmids.*** RAW 264.7 cells were washed and harvested at 24 h post-transfection with warm dPBS. After centrifugation at 300 g for 5 min, the cell pellets were resuspended with ice-cold FACS buffer, and samples were transferred to FACS tubes for analysis. Live cells were gated based on forward scatter (FSC-A) and side scatter (SSC-A) of untransfected RAW cells. All single cells have been clustered diagonally to exclude dead cells, doublets and clumps (A). GFP expression in RAW cells was determined by flow cytometry and shown as the geometric mean fluorescence (B).

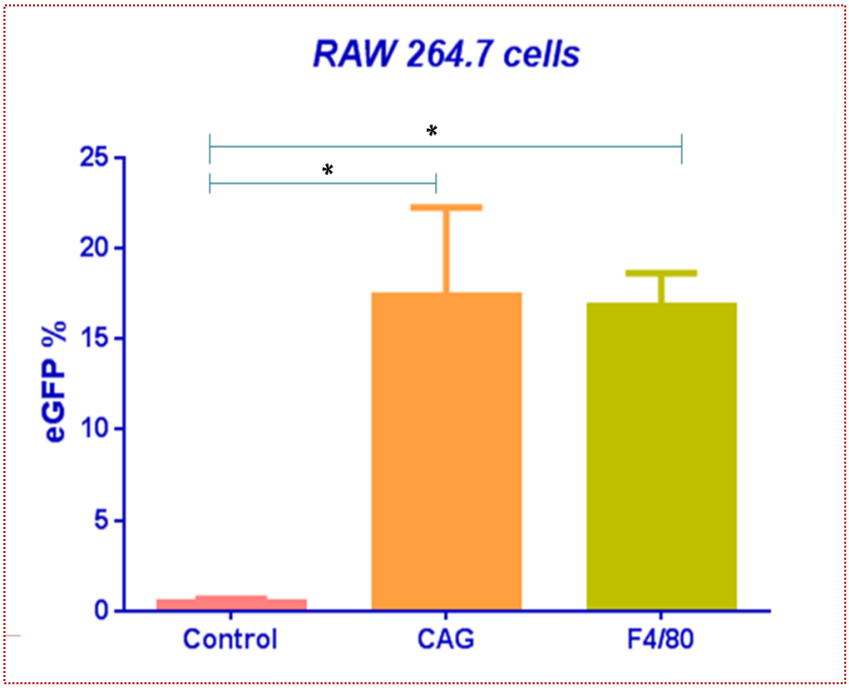

Figure 3.6 ***eGFP expression percentage was equivalent under control of both promoters.***

RAW cells were washed and harvested at 24 h post-transfection with warm dPBS. After centrifugation at 300 g for 5 min, the cell pellets were resuspended with ice-cold FACS buffer, and samples were transferred to FACS tubes for analysis. Live cells were gated as shown in Figure 3.5 and the % of eGFP positive cells determined. EGFP expression in transfected RAW cells with AAV-F4/80-eGFP or AAV-CAG-eGFP promoters were compared each against Lipo only control using one way ANOVA with Sidak's post hoc test. Shown are the means and SD of duplicates wells from one representative experiment of 3 replicates. * $P < 0.05$.

In HEK 293 cells, fluorescence microscopy indicated a high expression of eGFP under control of CAG promoter while only a few cells expressed eGFP under control of the F4/80 promoter (Figure 3.7). Flow cytometric analysis of live HEK 293 cells was consistent with the fluorescence microscopy findings (Figure 3.8) and the reporter gene expression was not detected in HEK cells despite the high amount of AAV-F4/80 plasmid used (Figure 3.9). Comparing the F4/80 promoter activity with both cell lines, we can see a shift in eGFP expression in RAW 264.7 cells which indicates that the promoter is active only in macrophages cell line and not in HEK cells (Figure 3.10).

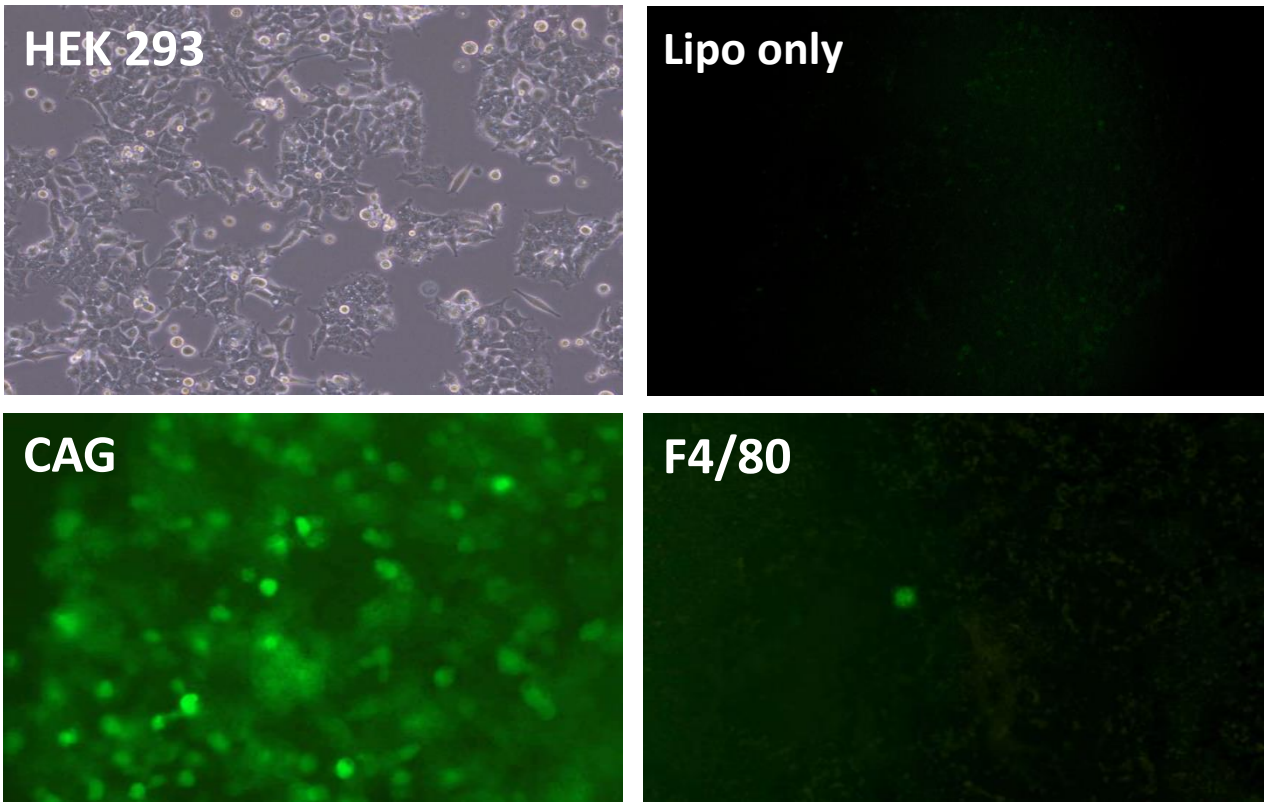

Figure 3.7 ***EGFP expression was extremely low under F4/80 promoter control in HEK 293.*** Twenty-four hours prior to transfection, HEK 293 cells were plated out in a 24-well plate at 0.4 x 10^6 cells/well in complete DMEM. Cells were transfected at 70% confluency (upper left) with 1 µg or 2 µg of AAV-F4/80-eGFP shuttle plasmid or AAV-CAG-eGFP. Transfected cells were incubated for 16-24 h at 37°C in 5% CO_2, and eGFP fluorescence in transfected cells was evaluated under fluorescence microscopy (magnification = 10x) and was compared against untransfected cells (Lipo only).

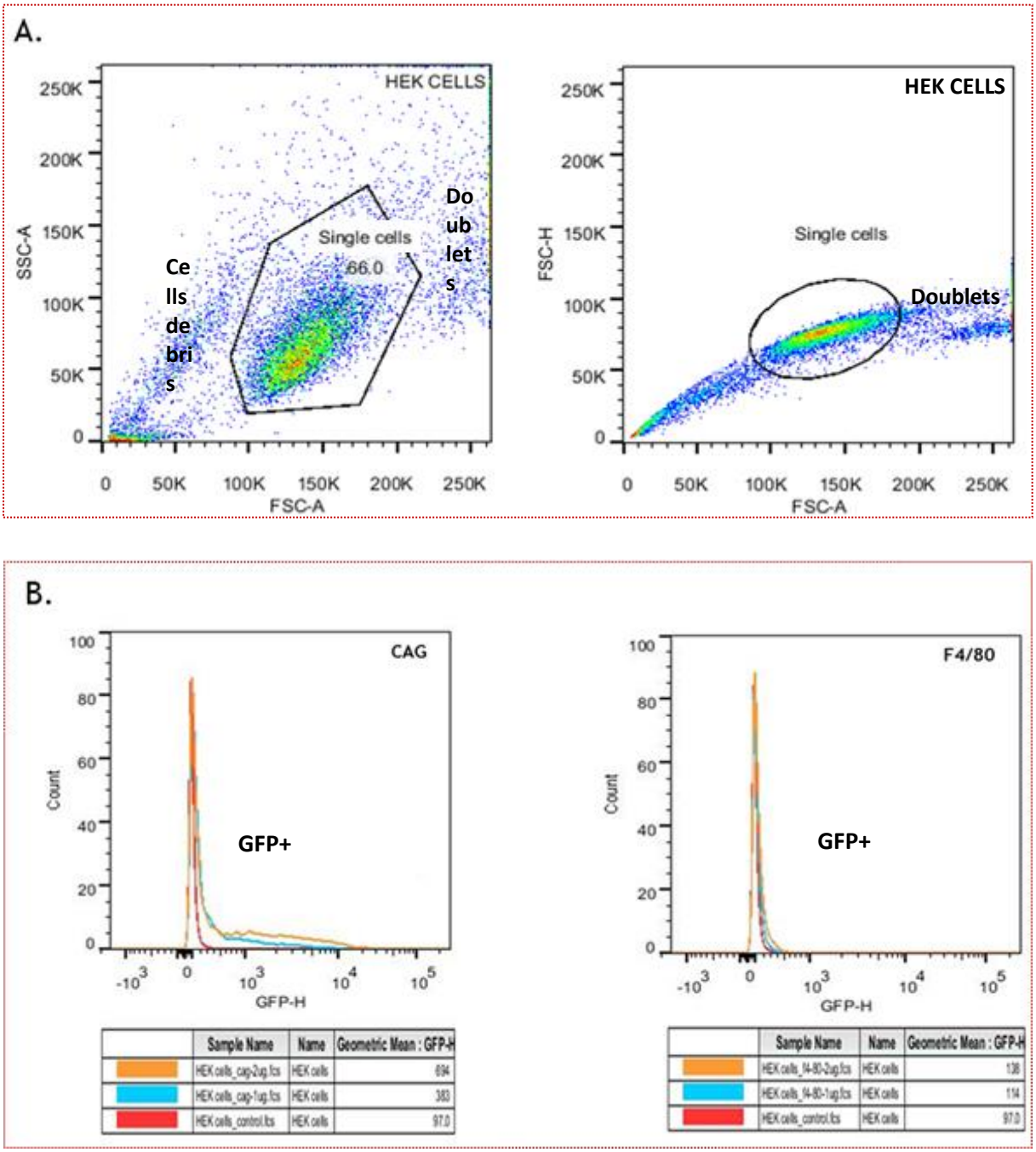

Figure 3.8 ***Increasing the amount of AAV-F4/80-eGFP plasmid did not boost GFP expression in HEK 293.*** HEK 293 cells were harvested 24 h post-transfection to quantify eGFP fluorescence via FACS analysis using same protocol described previously (Figure 3.5). All single cells have been clustered diagonally to exclude dead cells, doublets and clumps (A).

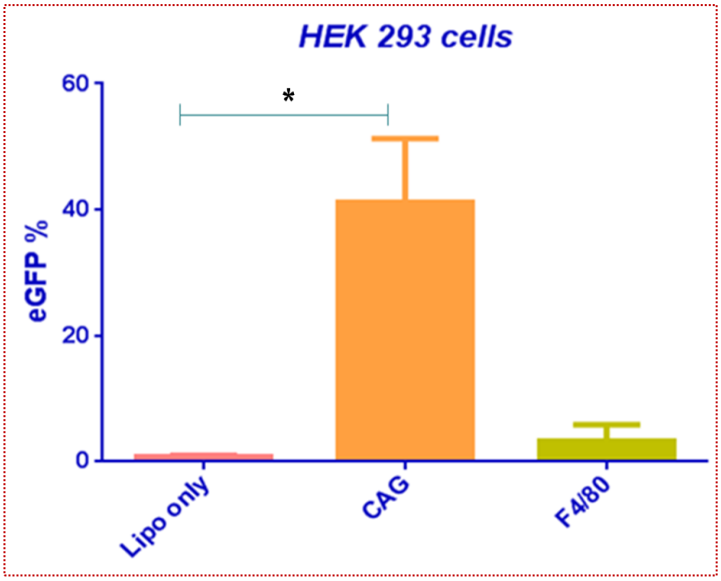

Figure 3.9 ***EGFP expression was not induced under F4/80 promoter control in HEK 293.*** EGFP expression was compared in HEK 293 cells transfected with AAV-CAG-eGFP, AAV-F4.80-eGFP, or Lipo only control using one way ANOVA with Sidak's post hoc test. Shown are the means and SD of duplicate wells from one representative experiment of three replicates. * $P < 0.05$.

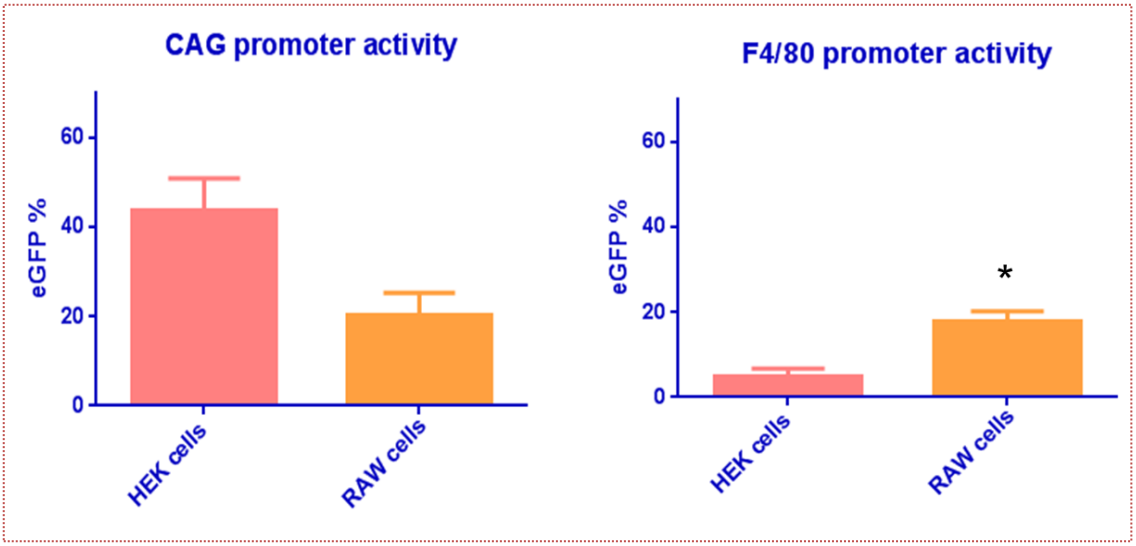

Figure 3.10 ***F4/80 Vs CAG in HEK and RAW cells***. The significance of GFP expression was compared under each promoter in both cell lines using unpaired t test with Welch's correction of one-way ANOVA test. * $P < 0.05$.

3.2.3 The F4/80 promoter did not drive eGFP expression in HepG2 and 1A9 cell lines

To confirm this finding, we transfected other human cell lines including the human hepatocytes cell line (HepG2), and human ovarian carcinoma cell line (1A9). The transfection protocol used was the same as described previously, and eGFP expression was assessed using fluorescence microscopy 16-24 h post-transfection. Fluorescence microscopy indicated the CAG promoter was active in both HepG02 (Figure 3.11) and IA9 cell lines (Figure 3.12); however, no GFP expression was observed when the AAV-F4/80-eGFP plasmid was used in either cell line. This result further suggests that the F4/80 promoter is selective for macrophages.

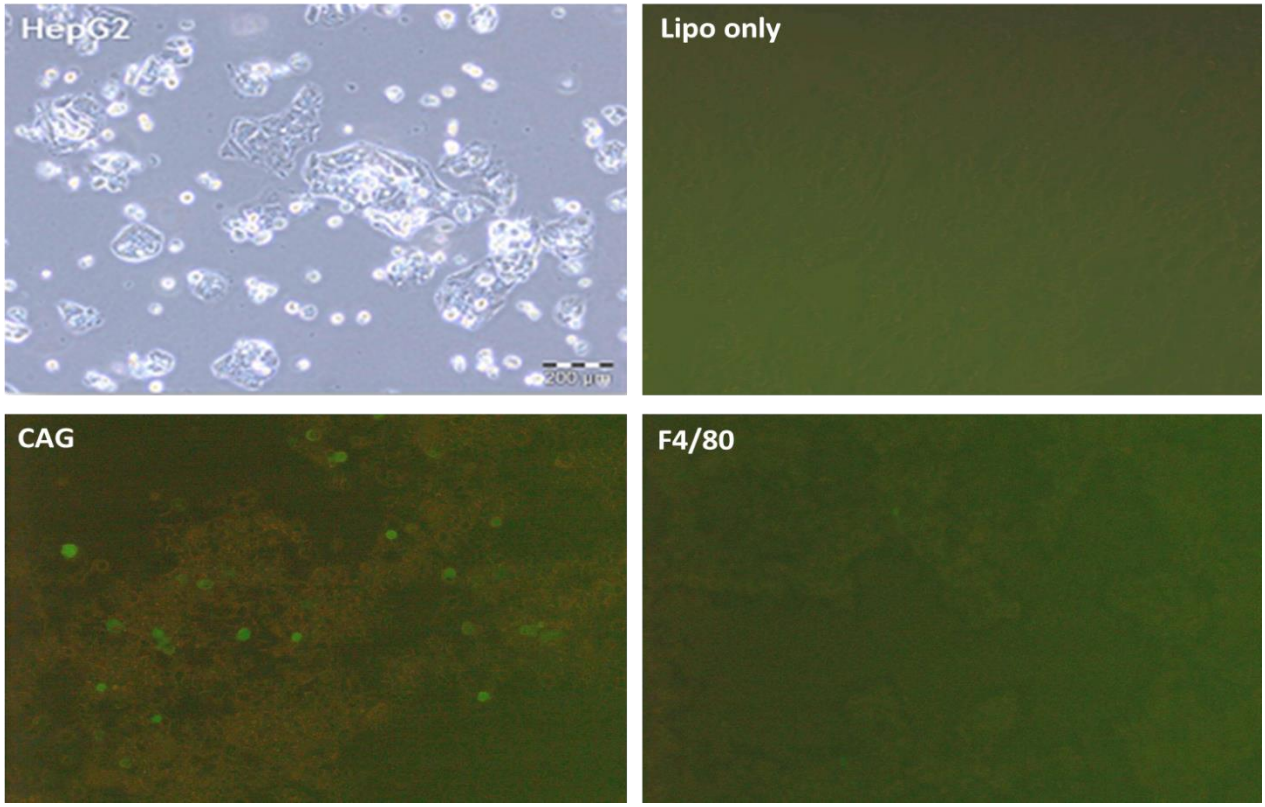

Figure 3.11 ***F4/80 promoter did not induce eGFP expression in HepG2 cells.***

HepG2 cells were plated out in a 24-well plate at 0.4 x 10^6 cells/well and maintained in complete DMEM media prior to transfection. Once confluency reached 70%, cells were transfected with 1 µg or 2 µg of AAV-F4/80-eGFP or AAV-CAG-eGFP plasmid. eGFP was expressed under CAG control (bottom left image) and no expression was detected under control of F4/80 promoter (bottom right image). Scale bar: 200 µm, magnification = 10x.

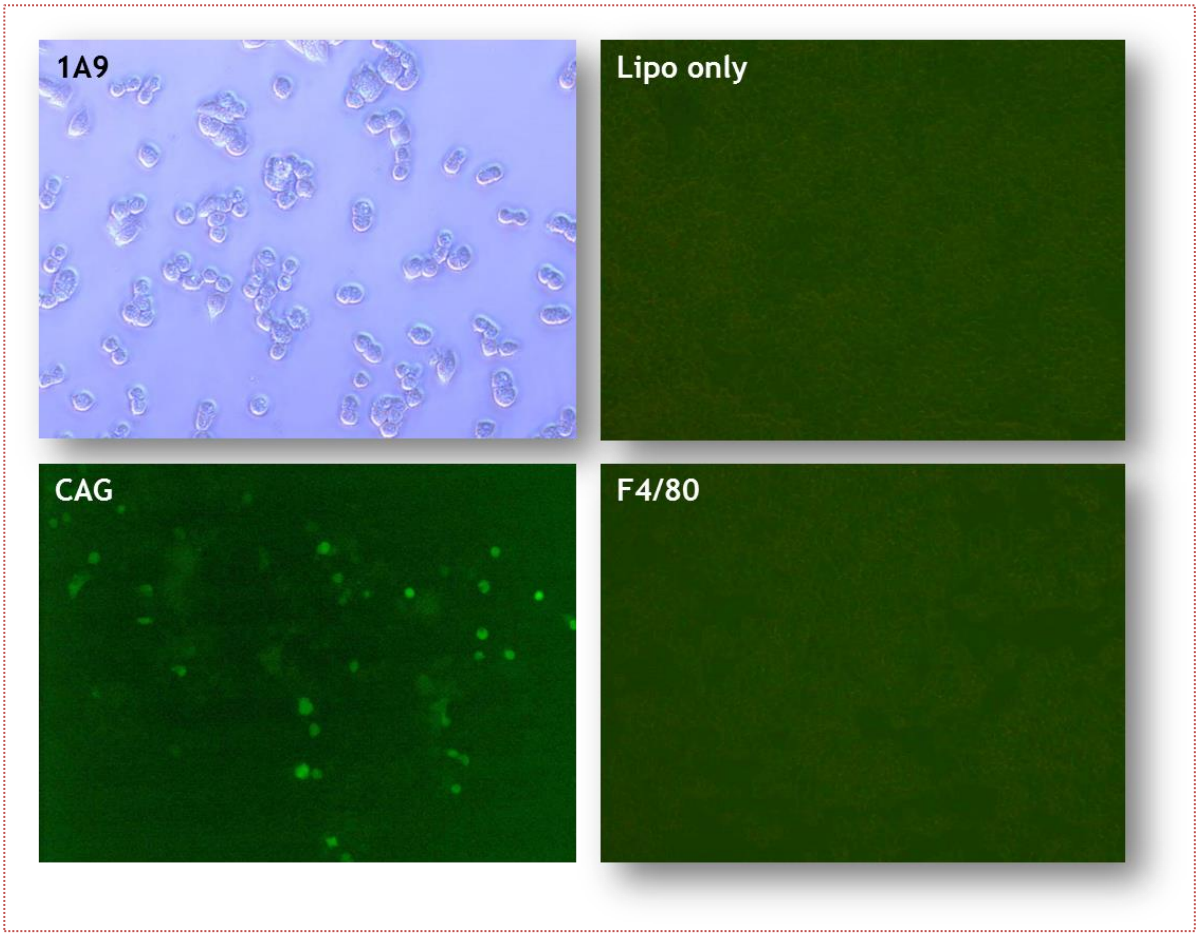

Figure 3.12 ***F4/80 promoter did not induce eGFP expression in 1A9 cells.***

1A9 cells were maintained in complete DMEM and transfected using the same protocol as described in Figure 3.11. After 16-24h, eGFP fluorescence was visualized by fluorescent microscopy. eGFP was not expressed in cells transfected with AAV-F4/80-eGFP plasmid (bottom right image) compared with AAV-CAG-eGFP (bottom left image) where eGFP was expressed. Scale bar: 200 µm, magnification = 10x.

3.3 Discussion

3.3.1 AAV-F4/80 shuttle vector construction

Prior to investigating the role of microglia in neurodegeneration, we first aimed to create a microglia-specific recombinant AAV vector. We constructed our AAV vector by inserting the F4/80 promoter into an empty AAV shuttle vector containing the reporter gene eGFP, which would help monitor the promoter activity as well as identifying transfected cells. An IRES sequence was located between the F4/80 promoter and eGFP gene. This sequence has a role in coordinating both the expression of a transgene of interest and reporter gene. Both the F4/80 promoter and eGFP gene were flanked by two ITRs sequences derived from AAV serotype 2. These viral sequences are required for AAV vector replication and packaging (Frase Wright, 2009), and represent the only viral-derived DNA present in the packaged recombinant AAV virus. The maximal length of inserted DNA that the two ITRs can hold is 4-6kb (Lai et al, 2010). Our newly constructed AAV expression cassette contained ~3.4 kb of ITR flanked DNA. A single restriction enzyme digestion with *MscI* and *XmaI* was performed to check the integrity of both AAV-F4/80 ITRs sequences that can recombine during cloning process and amplification. This is an alternative method to sequencing as ITRs contain a heparin secondary structure (Chapter 1, figure 1.1A), rendering their sequencing very difficult.

3.3.2 F4/80 promoter specificity investigation

Since no microglia-specific marker has been established yet, we chose to use the macrophage F4/80 element as a promoter, which would drive AAV expression exclusively in microglia when the AAV particles are injected into the brain. Although F4/80 is expressed on tissue macrophages (including peritoneal, liver, splenic, kidney, epidermal, thymis and bone marrow macrophages), within the central nervous system in a healthy mouse, F4/80 is expressed specifically on microglial cells (Cucchiarini et al, 2003, McKnight and Gordon, 1998). In addition, it was demonstrated by Cucchiarini et al. that F4/80 promoter has a restricted activity to microglia (McKnight, Gordon, 1998). Their group have evaluated AAV vector expression under control of the three myeloid-specific elements: CD11, CD68 and murine F4/80 in primary rat microglia and other brain cell populations as well as a different lineage of macrophages (mature human lung alveolar macrophages). Their results showed a restricted expression of transgene in microglia under F4/80

promoter control *vis-à-vis* other promoters and other cell types. Prior to packaging our constructed recombinant AAV-F4/80-eGFP, we wanted to confirm this finding by testing the vector *in vitro* on human cell lines that have not been investigated, including HEK 293, HepG2 and 1A9 cell lines. Promoter activity was compared in these cell lines against the commonly used macrophages cell line RAW 264.7 cells (Hartley et al, 2008).

We elected to use HEK 293 cells as they are very easy to transfect and are commonly used for packaging AAV vectors. Thus we were able to optimize the mammalian cell transfection protocol as well as investigate F4/80 promoter specificity. The specificity of our vector was compared against an AAV-CAG-eGFP vector control driven by a widely employed non-discriminatory CAG promoter (Balakrishnan et al., 2013, 28). The AAV-CAG-eGFP plasmid size was approximately the same as the AAV-F4/80-eGFP plasmid (8.3 kb, ~8 kb respectively), and cells were transfected with serial amounts of AAV-CAG plasmid in order to ascertain the lowest amount of DNA plasmid that would transfect the cells efficiently. We found 0.25 µg of AAV-CAG DNA plasmid was sufficient to efficiently transfect HEK 293 cells (Appendix 3, figure 3A); however, this amount was not enough to achieve a good transfection of RAW 264.7 cells. Instead, 1 µg was required to see a reasonable level of eGFP fluorescence in RAW 264.7 cells (Appendix 3, figure 3B).

In this study we demonstrated that the human F4/80 (EMR1) promoter worked well in the mouse macrophages cell line, which was demonstrated by clear expression of eGFP comparable to the one obtained under CAG promoter control. The promoter was tested in non-macrophage human cell lines including HEK 293, HepG2 and 1A9 and did not show any activity. This result was consistent with and complementary to Cucchiarini et al. providing strong evidence that our viral tool has a restricted activity to microglia and can be used to investigate the role microglia in neuro-inflammatory conditions (Cucchiarini et al ,2003).

CHAPTER 4

RECOMBINANT AAV2/5 PRODUCTION

4.1 Introduction

After construction of the recombinant AAV (AAV) vector and verification of its specificity for macrophages, we aimed to further confirm its exclusive gene delivery to macrophages *in vitro* by transducing splenocytes, which is a mixed leukocyte population containing macrophages, as well as *in vivo* via a systemic injection. Once confirmed, we could then deliver the AAV2/5 to microglia *in vivo* via a stereotactic injection into mice brain. The most extensively studied AAV serotype and the most used in CNS gene delivery is AAV2 (Choi et al., 2005). However, because the capsid of the serotype 2 was shown to primarily transduce neurons (Davidson et al., 2000), we replaced the AAV capsid 2 with the serotype 5 capsid. This capsid has been shown to have a much broader tropism and is capable of selectively infecting microglia when driven by a specific promoter (Cucchiarini et al., 2003). In addition, the use of the pseudotype 2/5 will reduce the host immune response and stabilize transgene expression compared with AAV2, which is prone to induce local inflammatory reactions since 80% of human population is AAV2 seropositive (Choi et al., 2005; Vasileva and Jessberger, 2005).

In order to test the infectivity and specificity of our AAV2/5 virus, the latter needs to be produced. The major steps of AAV production include: 1) packaging of the virus in a transitory producer cell, 2) purifying the AAV particles, and 3) titering the AAV stock.

For the AAV vector packaging, transient transfection of HEK 293 or HeLa is the most commonly used method because it is a flexible and convenient method for pre-clinical studies when a specific transgene construct and serotype may need to be tested prior to use in clinical studies (Fraser Wright, 2009). In comparison, the baculovirus system, in which recombinant AAV is packaged in insect cells, is time consuming and may be suited only to large-scale clinical studies (Virag et al., 2009; Urabe et al., 2006). We therefore selected the former method to produce our AAV vector of interest using HEK 293 cells given that HeLa cells are considered hazarduous to use due to the presence of the Human Papilloma Virus 18 sequence (HPV18) (Schwarz et al. 1985).

In order to achieve an efficient transient transfection of adherent HEK 293 cells, calcium phosphate (CaPO4) precipitation prepared in-house is currently the method of choice in many laboratories due to its simplicity (McClure et al., 2011;, Li et al., 2006; Iwata et al., 2013). This method is also cost effective compared with commercial cationic lipids reagents such as Lipofectamine LTX plus reagent, and although these reagents are very efficient, cost is a limiting factor considering the large volume of cultured HEK 293 cells required to produce a scalable amount of AAV. Therefore, calcium phosphate method was chosen to transfect our packaging plasmids in HEK 293 cells.

We selected the simplest and most extensively used method in preclinical studies - the triple transfection approach (Xiao et al., 1999; McClure et al., 2011). This versatile method requires co-transfection of three plasmids permitting simultaneous manufacture of different AAV vectors. These plasmids are: 1) the expression cassette, 2) Rep/Cap plasmid, and 3) the helper plasmid. The expression cassette contains the AAV 145bp inverted terminal repeats (ITRs) flanking the transgenes of choice as well as a fluorescent probe such as YFP or GFP to monitor the vector pathway and investigate its characteristics. The Rep/Cap plasmid contains replication and capsid genes of AAV that are supplied in trans and are necessary to package recombinant AAV. These genes could be from the same or different serotype. Finally, the helper plasmid carrys the necessary adenovirus genes required for an efficient AAV replication, since the wild type AAV needs co-infection with another virus such as adenovirus or Vaccinia virus for an efficient production in the host cell (Daya and Berns, 2008). There are four adenovirus helper genes required for the AAV production; E2A, VA, E4 which are delivered in trans in a plasmid and E1 is supplied in HEK 293 cells. These cells have been transformed with an adenovirus serotype five to express the E1 (E1A and E1B) gene (Merten et al., 2005).

Once assembly of the virus was performed, the next stage in production is to purify the viral particles. Purification strategy varies in many laboratories, in some studies they prefer a combination of density gradient ultracentrifugation including caesium chloride (CsCl) or iodixanol gradient and chromatography (an affinity or ion exchange chromatography depending on the serotype of the virus) and in other studies they chose to perform one-step purification, a density gradient or a chromatography. Since iodixanol density gradient was adapted by Zolotukhin et al., it became the preferred method in many laboratories to purify AAV vectors due to its iso-osmotic and inertness properties at all densities Thus, we selected a one-step purification process using

Iodixanol density gradient to purify our recombinant AAV2/5-F4/80 vector (Zolotukhin et al., 1999).

Following AAV particles purification, viral stocks are titered for use in downstream experiments. Commonly used approaches to titer purified AAV vector particles include Western blot analysis (Zolotukhin et al., 2002; McClure et al., 2011), SDS-PAGE electrophoresis, viral genome quantification by dot blot or qPCR, and AAV infectivity assay. In one viral genome assay (QuickTiter™ AAV Quantitation kit), an anti-AAV2 capsid monoclonal antibody is used to identify AAV particles of serotype 2. Although this antibody was shown to recognise AAV1 and AAV5 capsid proteins as well (Wobus et al., 2000), it is not applicable to all serotypes. SDS-PAGE electrophoresis detects the three AAV capsids VP1, VP2 and VP3 and can assess the purity of the stocks; however, titering AAV vector stocks via capsids proteins only is not accurate as empty capsids might be included in the titer. This assay is commonly used in conjunction with viral genome copies quantification as described above or by Dot-blot assay or qPCR (Iwata et al., 2013; Grieger and Samulski, 2005; Gonga et al., 2004; Paterna et al., 2000). To investigate AAV particles cells tropism and assess their ability to infect cells, an AAV infectivity assay is performed such as single-cell fluorescence assay (SCFA) to determine AAV vector infectious titer (Zolotukhin et al., 2002; McClure et al., 2011).

In order to titer our AAV2/5 viral stocks, we elected to perform an SDS-PAGE electrophoresis followed by quantification of viral genome copies using QuickTiter™ AAV Quantitation kit and a single-cell fluorescent assay. These assays were selected as they provide complementary information about the viral genome copy number, viral proteins, infectivity and cellular tropism. Therefore, using the approach outlined in Figure 4.1, we aimed to generate macrophage/microglia-specific, packaged AAV2/5 to use for further experiments.

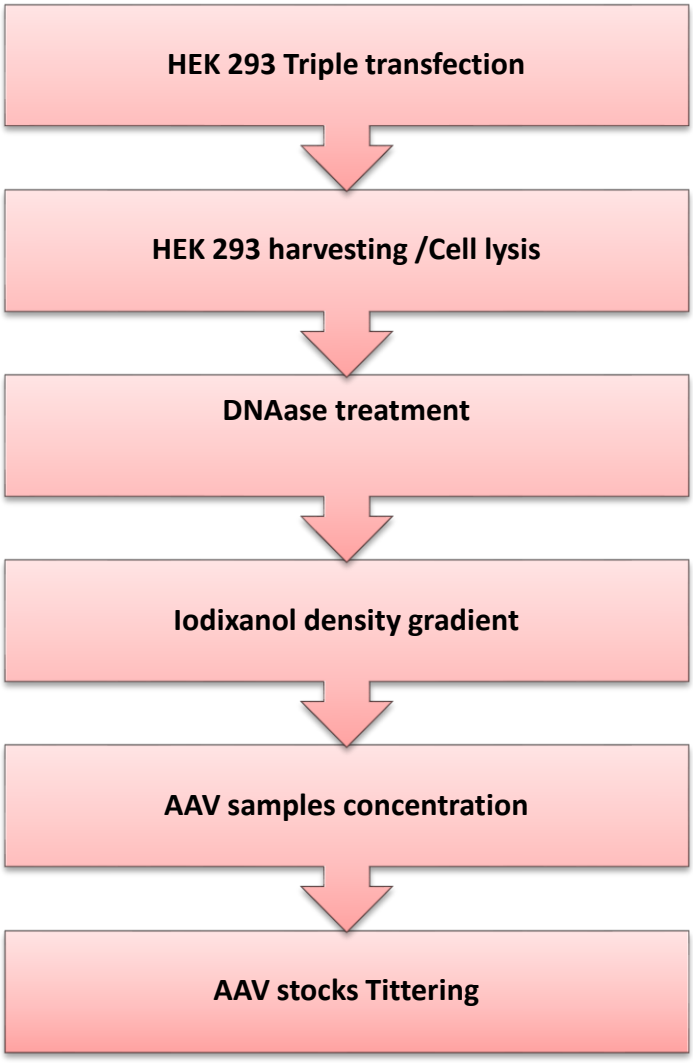

Figure 4.1. ***Recombinant Adeno-Associated virus vector production flow chart***

4.2 Results

4.2.1 AAV2/5-F4/80 packaging via HEK 293 transient transfection

The starting point for generating our AAV-F4/80 pseudotype 2/5 was the calcium phosphate-mediated transient transfection of HEK 293 cells. The following three plasmids were used: the AAV-F4/80 shuttle plasmid, the pAd helper plasmid and the Rep2/Cap5 plasmid. The three plasmids were combined at a 1:2:1 molar ratio respectively. Since F4/80 promoter is not active in HEK 293 cells, we used our AAV-CAG-eGFP vector control to monitor transfection efficiency by tracking eGFP expression as well as AAV production. However, using that control alone was not enough to troubleshoot our experiment because we were not able to detect it in downstream processes; therefore we decided to use another AAV vector control, AAV-CAG-yfp vector serotype 2, which has been successfully produced by others using the same protocol. This second control vector was a kind gift from Associate Professor Bronwen Connor, University of Auckland.

To assess the level of transfection, the cells were examined under the fluorescence microscope. Twenty-four hours post-transfection, both control constructs, AAV-CAG-yfp and AAV-CAG-eGFP, were expressing equivalent amounts of yfp and eGFP, respectively, but the fluorescence levels did not reach 50% (Figure 4.2C and E). In contrast, a very low number of fluorescent cells appeared in cells transfected with AAV-F4/80 vector, which was expected as the promoter activity has been shown to be very low in these cells (Chapter 3, Figure 3.7). In an effort to improve the efficiency of transfection, we monitored the pH of all transfection reagents, added them in the order recommended by the protocol, and used a low passage of HEK 293 cells. However, these adjustments did not improve the transfection efficiency of either AAV vector control.

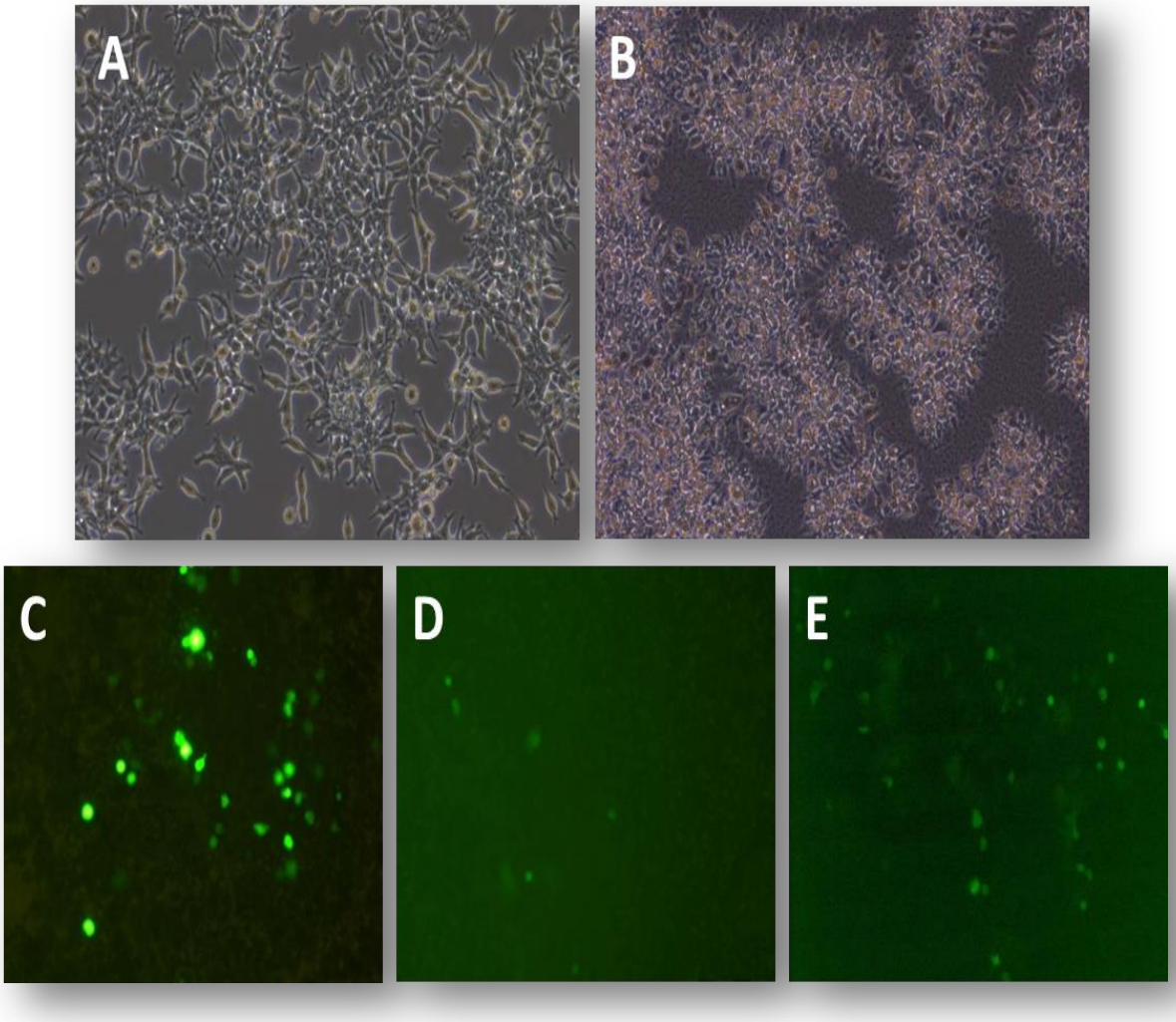

Figure 4.2. HEK 293 cells transient transfection. **A)** A representative image of HEK 293 before transfection (10X magnification). Cells were plated out at 5 x 10^6 cells/T150 flask and were cultured until they reached 80-90% confluency. Three h prior to transfection, complete DMEM media was changed and replaced with IMDM media that is high in glucose and suitable for high density cell cultures. . **B)** A representative image of HEK 293 after triple transfection. Briefly, 12.5 µg of AAV backbone plasmid, 25 µg of of pAd helper plasmid and 12 µg of pRep/Cap plasmid were added with the $CaPO_4$ mixture to each flask. Sixteen hours post-triple transfection, the medium was changed and replaced by complete EMDM with 10% FCS. **C-E)** Representative images at 24h post-triple-transfection of AAV-CAG-yfp **(C)**, AAV-F4/80 **(D)** and AAV-CAG-eGFP **(E)**. Scale bar: 200µM, magnification 10x.

4.2.2 Purification and Titering of AAVs Virions

The next step in the production process of the AAVs consisted of extracting and purifying the AAVs from transiently transfected HEK 293 cells at 92 hours post-transfection. As with the previous step, AAV-CAG-yfp was used to monitor the efficiency of our purification protocol. The transfected HEK 293 cells were harvested from T150 flasks, and after centrifugation at 600 x g for 35 min at 4°C, cell pellets were resuspended in Tris-NaCl lysis buffer (50 mM Tris, 150 mM NaCl at pH 8.4). In order to release as many virions as possible from the cells, samples underwent a vigorous pipetting followed by three freeze and thaw cycles. To determine if the AAV2/5 virions were released into medium (H. Vandenberghe et al., 2010), culture medium of the AAV2/5-F4/80 flask was also centrifuged at 600 x g for 35 min at 4°C. The AAV-CAG-yfp vector control that is a serotype 2 was purified from cell lysates only (H. Vandenberghe et al., 2010).

Both cell lysate and culture medium samples were then treated with benzonase endonuclease to eliminate any extraneous DNA at a final concentration of 50 U/mL and incubated at 37°C for 30 min in a water bath. Cell debris from the cell lysate was removed by centrifugation at 3000 x g for 15 min at 4°C and this supernatant as well as the culture medium containing any released AAV virions were stored at 4°C for downstream processing.

The vector-containing supernatant of each virus type was divided between four Iodixanol gradients in ultracentrifuge tubes (Figure 4.3). After an ultracentrifugation at 48,000 x g for 130 min at 18°C, 3-4 mL of virus were collected at 3-5 mm below the interface between the 60% and 40% Iodixanol layers (shown by an arrow in Figure 2.3B, section 2.5.2.2, chapter 2).

4.2.2.1 Purified AAV stocks contained high amounts of nucleic acid

Prior to titering, samples were concentrated to a smaller volume using a Vivaspin® 4 centrifugal concentrator. We began titering our AAVs stocks by measuring the genome total copies in each sample using QuickTiter AAV quantification protocol (Chapter 2, section 2.5.3.1). In this method, AAV particles were captured by beads via their capsid and heated at 75°C for one hour to denature capsid proteins and release viral DNA. A non-heated sample was used as a control. AAV2 viral DNA standards were used in the assay to obtain a standard curve in order to get AAVs DNA concentration in ng/µL (Figure 4.4).

The relative fluorescence unit (RFU) was calculated for each sample using Enspire 2300 fluorescence at 480/520 nm filter set. The result shown in Table 4.1 indicated that the RFU of all samples controls (non-heated samples) was higher than that of heated samples. This result suggested that the high amount of DNA found in the non-heated sample purified from culture medium might correspond to the DNA derived from packaging plasmids that have not been taken up by HEK cells. The host DNA may be also present in the medium-derived AAV stock as well. Whereas, in the samples purified from cell lysate, the high RFU of their controls might be due to a high amount of cellular DNA and non-packaged viral DNA. This result clearly indicated that benzonase treatment of samples before purification was not sufficient to eliminate extraneous DNA. Therefore, another treatment must be performed at the post-purification step to completely remove unwanted nucleic acids. Because net RFU was negative, we were not able to calculate the titre of AAV vector stocks using this method.

AAVs	Standards (ng/µl)												AAV2 control		AAV2/5-F4/80			
Samples	10	5	2.5	1.25	0.625	0.313	0.156	0.078	0.038	0.02	0.01	0	Control	Cell lysate	Control	Cell lysate	Control	Culture medium
Average RFU (250nm)	14028	7510	3948	1996	1074	575.5	288	152	76.5	41	7	0	3222	3102	3867	2024	4922	3803

Table 4.1. ***Control RFU is higher than the sample RFU*****.** Purified samples (cell lysates and culture medium) were prepared as per manufacturer instructions. Briefly, AAV DNA standards were used to create a standard curve (Figure 4.3). 13.5 µL of each purified AAV sample was added to 1.5 µL of 10X QuickTiter™ Solution C containing beads that capture the virus. Samples were incubated one hour at 75°C to denature the capsid and release viral DNA. A non-heated reaction of each sample was used as a control. Standards, samples and controls were transferred to a 96-well plate in duplicates. 90 µL of freshly prepared 1X CyQuant® GR Dye which labels nucleic acid was added to each well. To calculate the net RFU we use the following formula: net RFU = (RFU of viral sample) – (RFU of non-heated control sample).

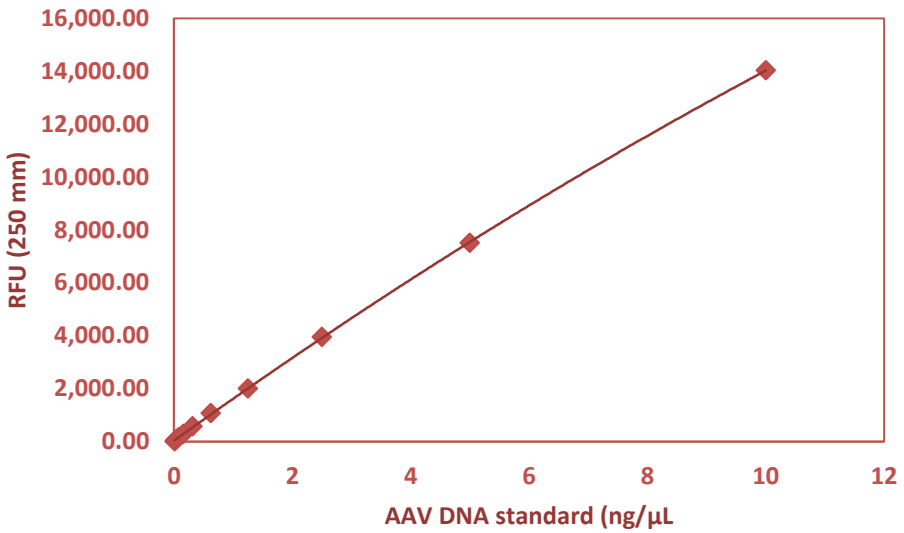

Figure 4.3. ***AAV2 DNA Standard Curve***

4.2.2.2 The three capsid proteins of AAV2/5 virus were not detectable in SDS-PAGE

SDS-PAGE was performed to analyse the AAV stock purity and to detect the three VP proteins of AAV virions capsid: VP1 (82 kDa), VP2 (72 kDa), VP3 (62 kDa). These proteins are present in a 1:1:10 molar ratio, respectively (S. Steinbach et al., 1997). SDS-PAGE gel analysis indicated high cellular protein contamination in both AAV2 control and AAV2/5 stocks purified from cell lysate and culture medium (Figure 4.5). The contamination was much higher in the AAV2/5 stock obtained from culture medium. VP protein capsids were not distinguishable from other proteins in the gel indicating a poor recovery of the vectors. The poor recovery might be due to a low vector production and/or failure in collecting most of the particles from Iodixanol gradient fraction due to a poor performance. Although SDS-PAGE result allowed us to assess the quality, this analysis was not efficient in detecting the few capsid proteins that were present in the stocks. Therefore, a Western blot analysis might be considered when AAV titer is very low.

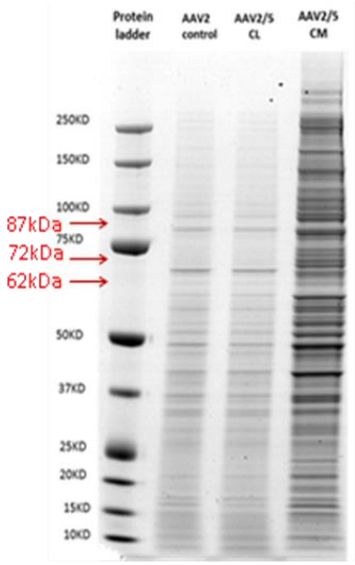

Figure 4.4. ***AAV vector stocks were highly contaminated with cellular material*****.** The protein concentration of each stock was determined by Bradford assay. Five µg of each sample was mixed with 2.5 µL of NuPAGE LDS sample buffer (x4) and 1 µL of NuPAGE sample reducing agent (x10). Samples were heated for 10 min at 70°C. The gel chamber was loaded with 800 mL of 1x MOPS buffer and 500 µL of NuPAGE antioxidant. 1.5 µL of protein size marker was loaded onto the first well and 10 µL of AAV2 vector control cell lysate, AAV2/5 cell lysate (CL) and culture medium (CM) were loaded onto well 2, 3 and 4, respectively. SDS-PAGE gel was run at 200V (400mA) for 45 min and stained with Coomassie Blue to visualize the proteins.

4.2.2.3 Low infectious titer of AAV$_2$ control and AAV$_{2/5}$-F4/80 particles

Performing an infectious titer is crucial to assess the potency of the AAV vector stock that could be affected during construction, purification or storage. The common protocol used for this assay is to transduce HEK 293 or HeLa cells, when the viral vector is driven by a general promoter, with serial dilutions of AAV vector with or without helper adenovirus. Infected cells are visually scored via a fluorescent probe using a fluorescence microscope and the titer is calculated according to the dilution factor (Zolotukhin et al., 1999; McClure et al., 2011). Because the infection process is very slow when AAV vector is transduced without helper adenovirus, transgene expression is assessed commonly from day five. Some laboratories prefer co-infecting cells with helper adenovirus to enhance AAV vector sensitivity (Zolotukhin et al., 1999; Bartlett et al., 2000; Xiao et al., 1998). However, we believe that co-infecting cells with adenovirus is not relevant for this situation since

the purpose of the assay is to test the potency of the viral vector to transduce cells alone and if it does, to determine how long it takes for the cells to express the transgene of interest.

We implemented an infectivity assay as described previously with few changes (Zolotukhin et al., 1999). HEK 293 cells were transduced via AAV-CAG-yfp virus control; however, due to the low activity of F4/80 promoter in HEK 293 cells (Chapter 3, Figure 3.7), we transduced RAW 264.7 cells with the AAV2/5-F4/80 virus purified from cell lysate or from culture medium. Because we were not able to detect any VP proteins in SDS-PAGE gel, we did not infect cells with serial dilutions of stocks as described in the common protocol, instead we infected cells with serial volumes starting from 5 µL to 80 µL to increase chances in detecting any packaged AAV virus. From 24 hours post-infection, fluorescent cells were monitored under the fluorescence microscope and have been scored five days later to determine the infectious titer using the following formula:

$$\textbf{Infectious units/mL} = \frac{\textbf{Number of transduced cells x 1000 µL}}{\textbf{Volume of AAV vector (µL)}}$$

Fluorescence microscope analysis of infected RAW 264.7 cells with our AAV2/5-F4/80 vector, isolated from both culture lysate and culture medium, indicated the presence of fluorescent cells in all wells containing the AAV. This result confirmed the presence of packaged AAV2/5-F4/80 vector in both cell lysate and culture medium stocks. However, the number of infected cells was extremely low and did not exceed 15 units per 40 µL of cell lysate stock (Figure 4.6). Thus the infectious titer was 375 units per mL which was extremely low compared to the reported titers of 6×10^9 IU/mL (McClure et al., 2011) and 1.1×10^{11} IU/mL (Zolotukhin et al., 1999). We checked the plates 10 days and 15 days later to see if the number of infected cells would increase with time since AAV vector has such a slow infection process in absence of helper adenovirus, but the number did not increase.

The low infectious titer of our AAV virus may be due to the low tropism of the capsid 5 for macrophages or to the potency of the vector in infecting cells that has been deteriorated during purification or storage. However, given that we obtained approximately the same infectious titer of the AAV2 vector control in HEK 293 cells (750 IU/mL; Figure 4.6) and the three capsid proteins were undetectable by SDS-PAGE, we believe that the low infectious titer was caused by a poor recovery of AAV virus from the production process.

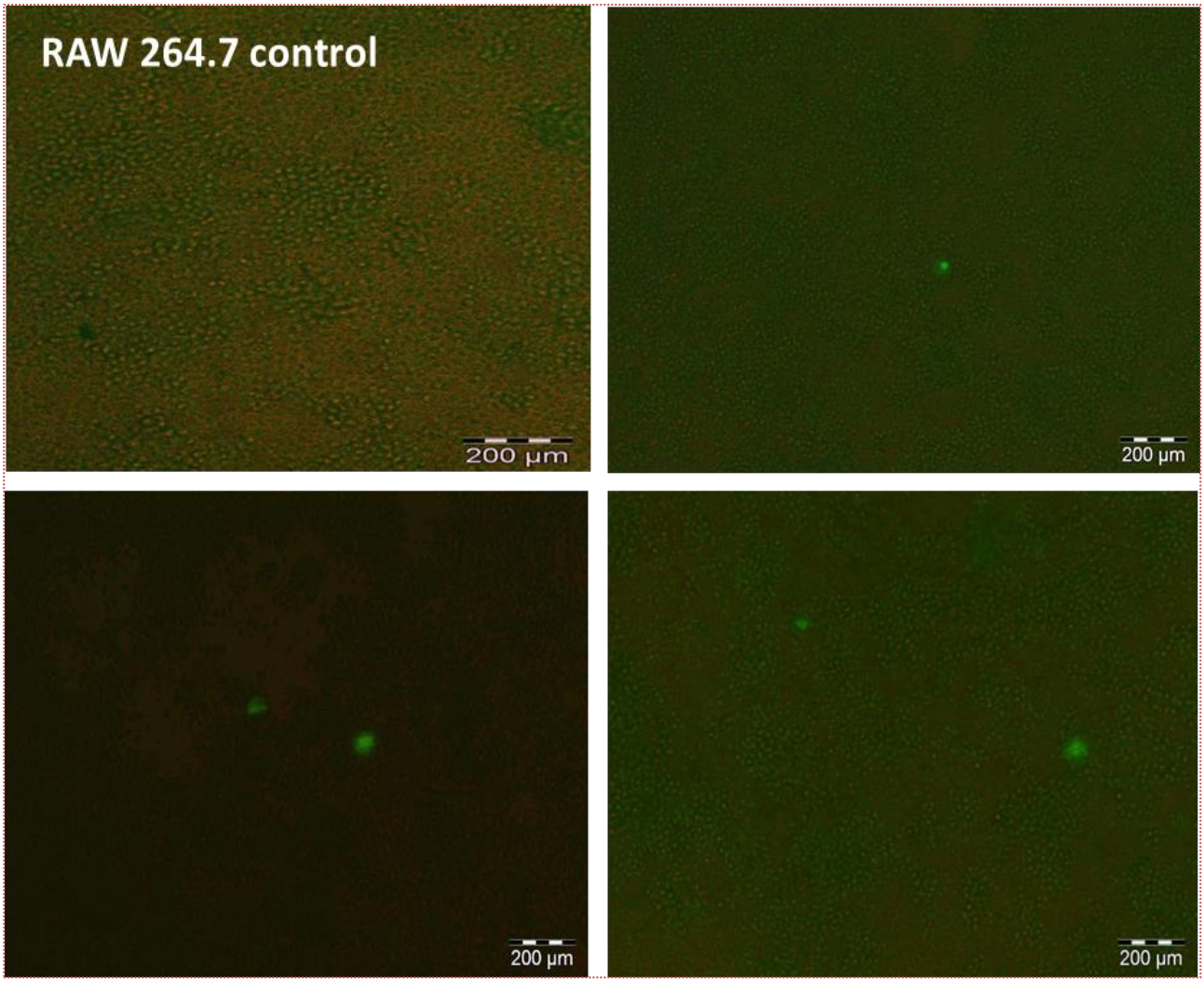

Figure 4.5. ***Few RAW 264.7 cells were infected with the packaged AAV2/5-F4/80 virus***. Images of RAW 264.7 cells infected with purified AAV2/5-F4/80 virus. Non-infected RAW 264.7 cells have been used as a control. Cells have been plated out at 0.6 x 10^5 in a 48 well plate and cultured until they reached 80% confluency after which cells were infected with serial volumes of the AAV vectors: 5 µL, 10 µL, 20 µL, 40 µL, 60 µL, 80 µL without helper adenovirus. Plates were incubated at 37°C in a 5% CO_2 atmosphere, and at 24h post-infection, the presence of infected cells expressing eGFP was observed by fluorescent microscope in all wells containing virus. Scale bar: 200 µm, Magnification 10x.

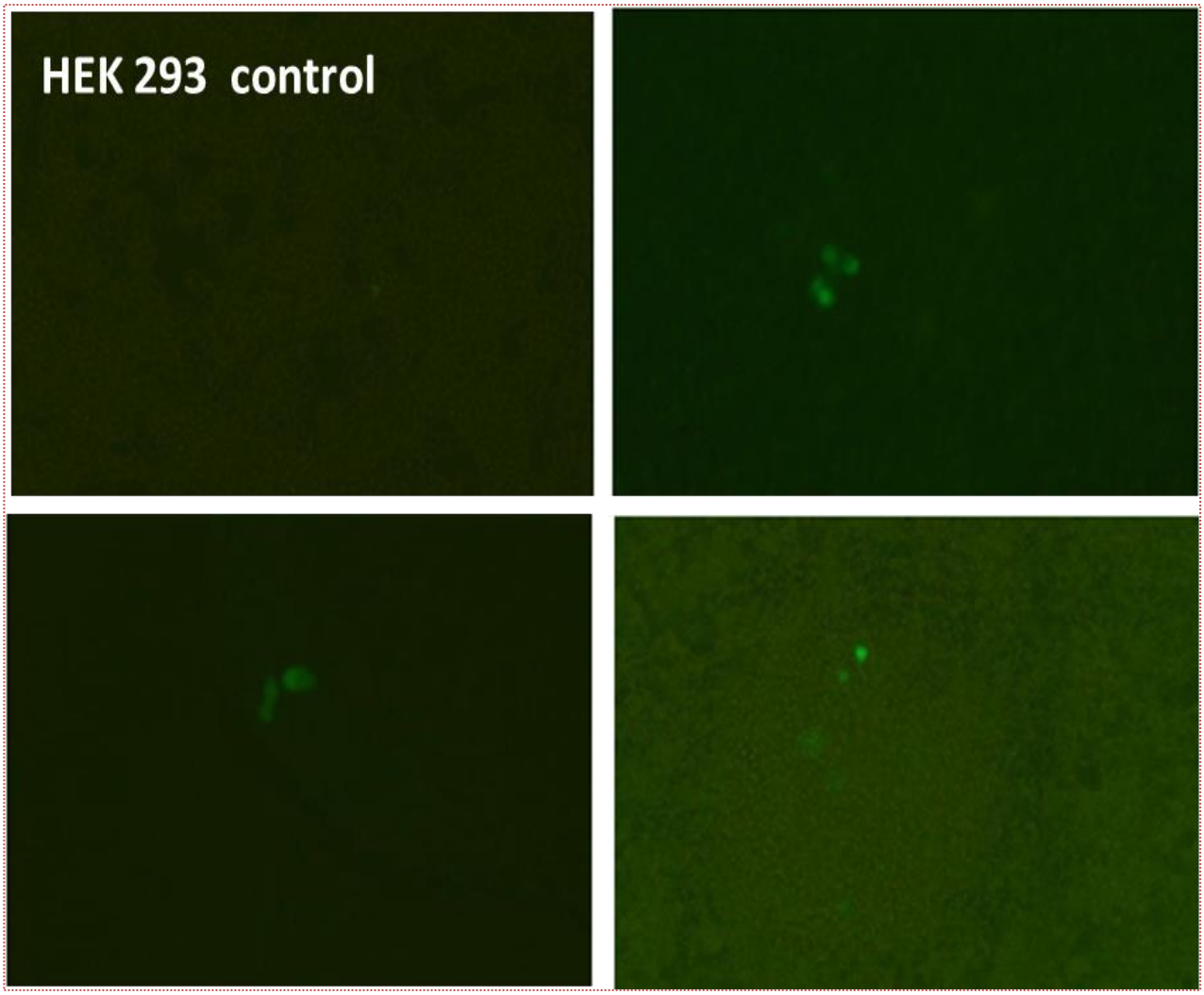

Figure 4.6. ***Few HEK 293 cells were infected by the AAV2 virus control*****.** Fluorescent microscope images of HEK 293 cells infected with the AAV2 vector control using same protocol described in Figure 4.6, which indicated presence of packaged virus in the stock. Scale bar: 200 µm, magnification 10x.

4.3 Discussion

Although AAV vectors have been shown to be very successful candidates in gene delivery into mammalian cells due to their excellent safety profile and long term stability in animal models (Bishop et al., 2008; Kaplit et al., 1994; Fana, 2008), their production is still a challenge and may affect downstream experiments, when recombinant AAV vector generated stock is not consistent in terms of purity and quantity. We aimed in this project to produce our AAV2/5-F4/80 virus to use in our experiments but we failed to produce a sufficient amount that would enable us to test the vector *in vivo* and *in vitro*. In order to troubleshoot our method of production, each step will be discussed in detail and alternative approaches proposed to optimize the protocol for future experiments. Overall, the main production steps that can affect vector yield include: the transient transfection, AAV packaging and AAV purification, and thus it is highly likely that optimization of one or more of these steps in our protocol is required to enable efficient AAV production.

4.3.1 Transient Transfection

Transient transfection of the HEK 293 cell line with the AAV packaging plasmid represents the first challenge in AAV vectors production. While the calcium phosphate method is very efficient when optimized, generating more than 10^5 vector genome per cell (Fraser Wright, 2009), it is still a very sensitive procedure and needs a consistent performance in order to transfect up to 90% of HEK 293 cells. In our experimentation, the HEK 293 transient transfection did not reach 50% according to fluorescent intensity of both AAV controls used AAV-CAG-yfp and AAV-CAG-eGFP (Figure 4.1). This was certainly due to the transfection reagent characteristics as it has been shown earlier that a failure in maintaining transfection reagents at room temperature and at required pH at the time of transfection dramatically affects AAV production (Fraser Wright, 2009). Furthermore, the quality of the HEK 293 cell line affects transfection efficacy and transfection can only be performed at their optimal receptive conditions: maintaining them at their exponential growth, plating them at low passage (lower than 30 passages) the day before transfection and transfecting them when they reach 80% confluency will increase DNA uptake by the cells.

4.3.2 AAV Packaging

Recombinant AAV vector packaging using the triple-transfection protocol is another limitation in the production process. Despite the AAV standard genome size, which does not exceed the limited capacity of the capsid, it was demonstrated previously by Grimm et al. that when the packaging efficacies of both WT AAV and recombinant AAV where compared, the chances in producing empty capsids were very high during the packaging process of recombinant AAV vectors (Grimm et al., 1999). The empty capsids appear when the threshold of assembled capsids that are ready to package recombinant genomes is not reached due to the overexpression of VP proteins (Grimm et al., 1999). Furthermore, Li et al. showed that Rep78/68 protein overexpression affects AAV vector yield as well by decreasing AAV DNA replication efficiency and by lowering capsid proteins synthesis (Li et al., 1997). Thus the amount of *Rep*/*Cap* plasmid supplied in *trans* needs to be optimized for an efficient AAV production. However, in our protocol, the amounts of AAV packaging plasmids have been already optimized previously and generated a good titer (McClure et al., 2011). Another impediment in the AAV vector packaging was the generation of AAV particles that contain DNA sequences other than the vector genome such as pseudo-wild type AAV, residual plasmids and host cell DNA which decreases AAV infectivity and induces unwanted immune responses (Allen et al, 1997; Wang et al., 1998; Chadeuf et al., 2005).

Another major obstacle known to dramatically affect AAV production yield is the timing and process of harvesting the AAV from the transfected HEK 293 cells. The first challenge in this step is to determine the best time to harvest the packaged AAV. Since the time of virions release into the culture medium is unknown, the reported harvesting time varies between 60-120 hours in most laboratories (Vandenberghe et al., 2010). This might affect AAV vector production yield if the cells are harvested after the release of virus into the culture medium since all AAV protocols collect virus from cell fractions only. It has been demonstrated by Vandenberghe et al. that not all serotypes remain in the cell after their production as the AAV2 vector does, and that release of packaged viruses into the culture medium is serotype dependent (Vandenberghe et al., 2010). In their study, while AAV2 and AAV6 were shown to be strongly associated with the cell via the heparin-binding motif after virus production, the AAV5 on the other hand was found mostly in culture medium (Vandenberghe et al., 2010). In order to verify this finding, we collected our AAV2/5 vector from both cell fractions and culture medium; however we found approximately the same infectious titer in both samples (Figure 4.6). Therefore, despite the insignificant titer of

AAV2/5, collection of AAV with capsid of serotype 5 from both sources should be taken into consideration in order to increase vector yield once the production process has been optimized.

Another step that requires optimization is the lysis of the AAV-containing HEK 293 cells to release as many virions as possible. In our previous tests when we were lysing cells using a lysis buffer as described by McClure et al. protocol (McClure et al., 2011); we were unable to detect virions in the crude cell lysates and in purified AAV stocks. However, we found that combination of lysis buffer with thorough pipetting and three freeze/thaw cycles was sufficient to detect packaged viruses using the infectivity assay. Furthermore, formation of aggregates caused by non-specific proteins interactions may decrease the production yield when the virus is not efficiently separated from other proteins. Thus, treatment of the samples with an ionic detergent such as sodium deoxycholate at 0.5% final concentration might be considered to disturb and dissociate proteins interactions and prevent aggregates formation.

4.3.3 AAV Purification

The last step in our AAV production process is Iodixanol density gradient ultracentrifugation followed by virions concentration and filtering. We strongly believe that the majority of the AAV vector that has been packaged was lost during this stage of purification. The SDS-PAGE result (Figure 4.5) indicated that the iodixanol-purified AAV stocks were highly contaminated with cellular proteins and the three AAV capsid proteins (VP1, VP2 and VP3) were undetectable. This result suggested that the collection of AAV fractions from a discontinuous gradient was not accurate and were collected from the interface where most of the cellular proteins migrate and only a low amount of AAV was present (Zolotukhin et al., 1999). To confirm this hypothesis, we compared our finding with those described by Zolotukhin et al. (Zolotukhin et al., 1999), where an AAV vector was similarly purified from crude lysate using an Iodixanol density gradient (Figure 4.8). It was demonstrated, by collection of different fractions of AAV virus from different densities including; 60%-40% interface (lane 5), 40% density (lanes 6 and 7) and 40%-25% interface (data not shown) that fractions 6 and 7 obtained within 40% density were highly contaminated with cellular proteins comparing with fractions obtained from the interface 60%-40%.

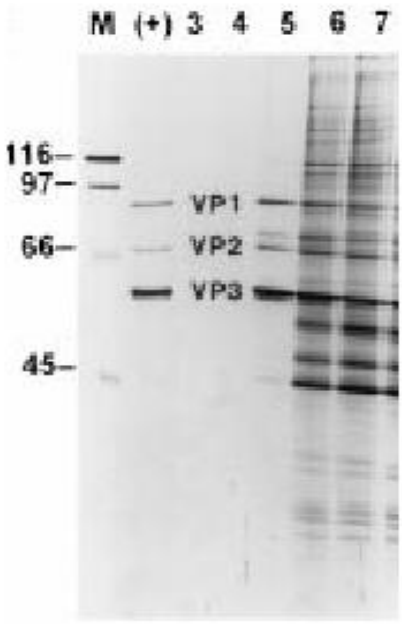

Figure 4.7. ***Zolotukhin et al. (1999) SDS-PAGE result*****.** In Zolotukhin et al. study, AAV was purified from crude lysate and Lanes 5, 6 and 7 are AAV fractions recovered in the Iodixanol density gradient. Lane 5 fraction was collected between 40%-60% interface and fractions 6 and 7 were collected from the 40% density. Lane (+) contains purified AAV virus as a positive control. The lane marked M contains protein standards (Zolotukhin et al., 1999).

Other methods can be used for AAV purification. In particular, before the adaptation of iodixanol gradient, the most used method was caesium chloride (CsCl), and this method is still used in many studies (Iwata et al., 2013). However, the challenge in using this reagent is the large amount of time spent in performing multiple rounds of CsCl gradient to decontaminate AAV stocks from aggregates, this leads to poor AAV recovery and affects AAV infectivity when the stocks are not properly purified (Zolotukhin et al., 1999; Auricchio et al., 2001). Furthermore, the AAV vectors stock must be cesium chloride-free due to the reagent toxicity to cells which must be removed before their transduction.

When comparing the two methods, the non-toxicity of Iodixanol to cells makes AAV purification quicker when AAV infectivity assays are needed to be performed directly on AAV-Iodixanol gradient fractions without further purification (Iwata et al., 2013; Li et al., 2006). In addition, in terms of AAV vector infectivity, Iodixanol gradient was shown to generate the most infective AAV vectors over CsCl (Zolotukhin et al., 1999).The common drawback of both gradients is the limited

loading capacity for AAV samples which can impede large scale production of AAV vectors. However, this was not an issue for us as we wanted to perform a small scale production of AAV vectors to investigate our AAV2/5-F4/80 vector tropism and transgenes function.

Another aspect to consider is that the concentration cycles and filtering of the Iodixanol gradient purified AAV stocks might further decrease the yield. Specifically it is possible that some viruses were attached to the concentrators and filters membrane and were not eluted. Therefore, in order to obtain a good yield of recombinant AAV vectors, every step needs to be carefully optimized to increase production yield of AAV vector to be able to perform downstream experiments.

CHAPTER 5

AAV-MEDIATED MARCH-I EXPRESSION AND FUNCTIONAL TESTING

5.1 Introduction

The major histocompatibility complex class II molecules (MHC-II) are known to be responsible for initiating antigen-specific immune responses through presentation of antigenic peptides to CD4+ T lymphocytes. The immune cells that are known to efficiently express MHC-II include B cells, dendritic cells, and macrophage populations such as microglia in the brain. Together, these cells are considered professional antigen-presenting cells (APCs). Previous studies have reported that in immature or resting dendritic cells (DC), some MHC-II molecules are displayed on the cell surface but most of them are sequestered in the cytoplasm (Shin et al., 2006). Sequestration of MHC-II molecules coincides with the ubiquitination of the cytoplasmic tail of MHC-IIβ chain at the conserved lysine, and this ubiquitination induces MHC-II degradation (Cho and Roche, 2013). However, when cells are stimulated by pro-inflammatory stimuli, MHC-II expression is increased on the cell surface and their ubiquitination is lost (Shin et al., 2006). Once the activation is terminated, MHC-II molecules are re-localized in the cytoplasm and degraded (Shin et al., 2006, Cho and Roche, 2013). The MHC-II ubiquitination process in Interferon gamma (IFN-γ)-stimulated human primary monocytes was recently shown to be directly regulated, by a family member of membrane-associated RING (CH) proteins containing E3 ubiquitin ligase (MARCH-I) when cells were under IL-10 stimulation (Thibodeau et al, 2008). Additionally, Kawasume et al found that this process is necessary for the maintenance of conventional DCs functions in the resting state (Hoshino et al, 2009).

Therefore, to further investigate the potential role of MARCH-I in regulating antigen presentation, we aimed to create an AAV vector that would induce the constitutive expression of MARCH-I in macrophages and microglia. Thus the expression of MHC-II would be reduced and MHC-II antigen presentation would be inhibited. Using our AAV-F4/80-eGFP viral plasmid, we aimed 1) to construct AAV-F4/80-eGFP-MARCH-I vector and 2) to confirm the expression of MARCH-I in RAW 264.7 cells transfected with the AAV-F4/80-eGFP-MARCH-I vector by assessing the expression of MHC-II on the cell surface.

5.2 Results

5.2.1 Construction of AAV vector containing the MARCH-I cDNA

To drive the expression of MARCH-I in our study; we inserted MARCH-I cDNA sequence into the vector AAV-F4/80-eGFP. The MARCH-I sequence and AAV-F4/80-eGFP vector were ligated at a molar ratio of 3:1 respectively using 0.1 units of T4 DNA ligase. The presence of MARCH-I in the vector recipient was confirmed via agarose gel electrophoresis of the colony PCR products (Figure 5.1A). The gel showed an 857 bp band corresponding to MARCH-I fragment in wells 2-4, 6-8 and 10-12 containing PCR products amplified from the AAV-F4/80-MARCH-I clone. The newly constructed AAV-F4/80-MARCH-I-eGFP clone (Figure 5.1C) that is 8884 bp, was purified and its identity verified by agarose gel electrophoresis after restriction digestion using *SpeI*/ *ClaI* (Figure 5.1C). Digestion with these enzymes generated an 8027 bp and an 857 bp fragment corresponding to the vector recipient AAV-F4/80-eGFP and MARCH-I, respectively (Figure 5.1B, well 3).

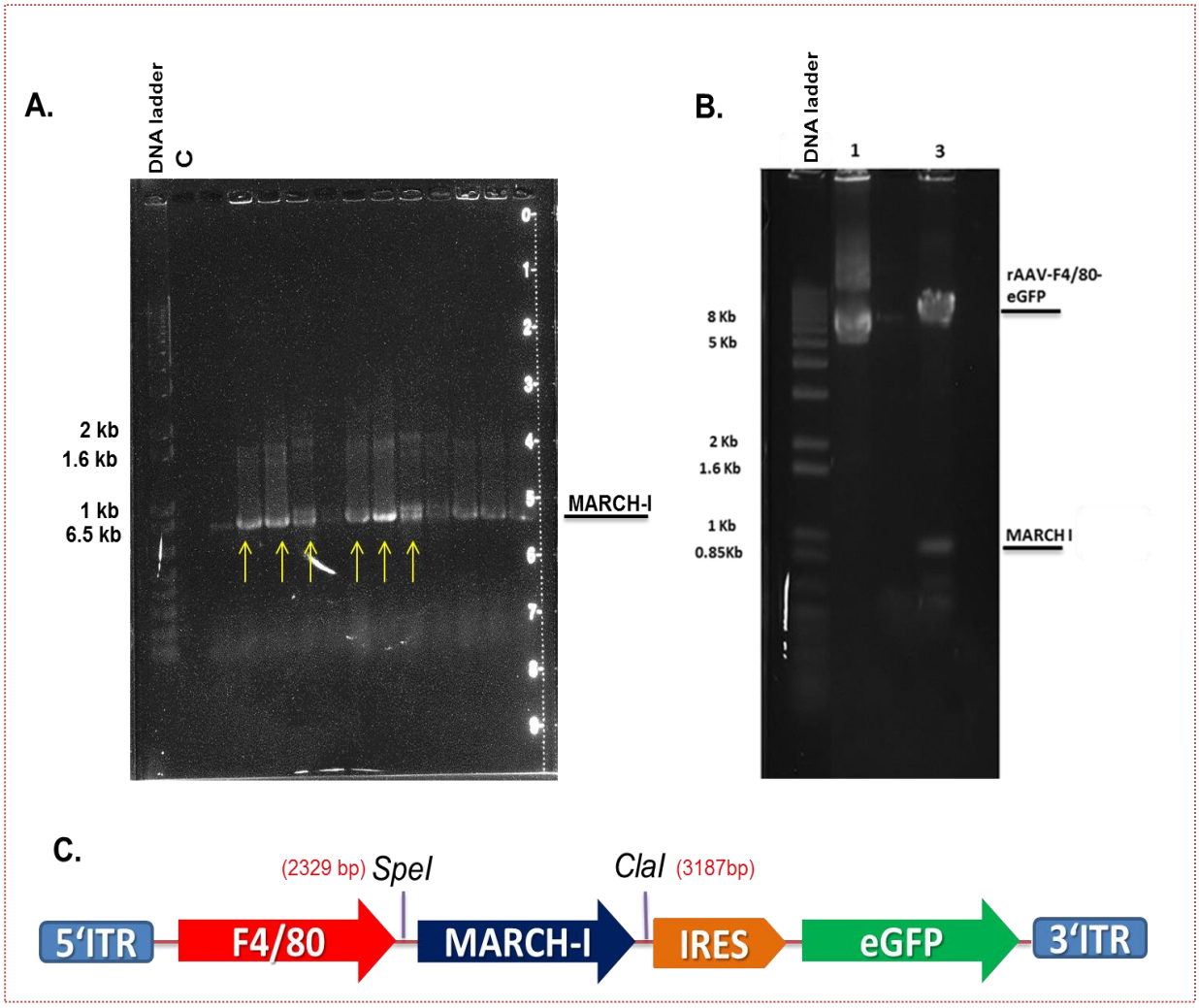

Figure 5.1 ***AAV-F4/80-MARCH-I-eGFP vector construction and confirmation***. **A)** Agarose gel (0.9%) electrophoresis of colony PCR products. In well C, a PCR reaction without ligation product was used as a negative control. The colony PCR was performed using the same protocol as described in chapter 3, figure 3.1A. MARCH-I sequence was amplified using the following customized primers: Forward **5'**CCCCACTAGTATGCCCCTCCACCAGATTTC**3'**, reverse **5'**CCCCATCGATGACTGGTATAACCTCAGGTG**3' B)** Agarose gel of digested AAV-F4/80-MARCH-I-eGFP clone with SpeI/ClaI restriction enzymes. A non-digested clone was used as a control in well 1. **C)** AAV-F4/80-MARCH-I-GFP vector genome organization. The newly constructed AAV-F4/80-MARCH-I-eGFP vector plasmid is 8884 bp containing MARCH-I cDNA that is expressed under control of the macrophage-specific F4/80 promoter. eGFP reporter gene is used to monitor transfection efficiency in cells, and the internal ribosome entry site (IRES) coordinates the expression of MARCH-I and eGFP genes. The transgenes are flanked by two inverted terminal repeats (ITRs) serotype 2.

5.2.2 MHC class II expression on RAW 264.7 cells

To assess whether the AAV-F4/80-MARCH-I-eGFP vector would induce the expression of MARCH-I in transfected cells, we designed a functional assay that would monitor the expression of MHC-II on transfected cells. Because resting macrophages express only low levels of MHC-II, we first needed to induce MHC-II upregulation. Interferon-gamma (IFN-γ) is a pro-inflammatory cytokine that is very effective at up-regulating MHC-II surface expression and is necessary for host's defence to pathogens (Samuel, 2001; Boehm et al., 1997).

To ascertain the appropriate concentration of the monoclonal antibody for staining surface-expressed MHC-II on RAW 264.7 cells, cells were treated with 20 U/mL IFN-γ and stained 24 h later with the rat anti-mouse MHC-II (IA/IE) conjugated to phycoerythrin (PE), using serial dilutions including: 1/100, 1/200, 1/400, 1/800, 1/1600, 1/2000. MHC-II expression was detected better at 1/100 and 1/200 PE-IA/IE dilutions (Figure 5.2B).

To identify the optimal IFN-γ concentration to induce a significant up-regulation in MHC-II surface expression on RAW 264.7cells, we stimulated the cells with 0-100 U/mL IFN-γ and 24 h later, assessed MHC-II expression by flow cytometry. Flow cytometric analysis indicated that the highest expression level of MHC-II was at 100 U/µl (Figure 5.2). However, this level was not significantly different from the other IFN-γ concentrations and even the lowest concentration used, 20 U/mL, was enough to significantly up-regulate MHC-II expression. Therefore, we decided to use 20 U/mL of IFN-γ to induce MHC-II surface expression in RAW 264.7 cells to investigate the functionality of the AAV-encoded MARCHI in transfected RAW 264.7 cells.

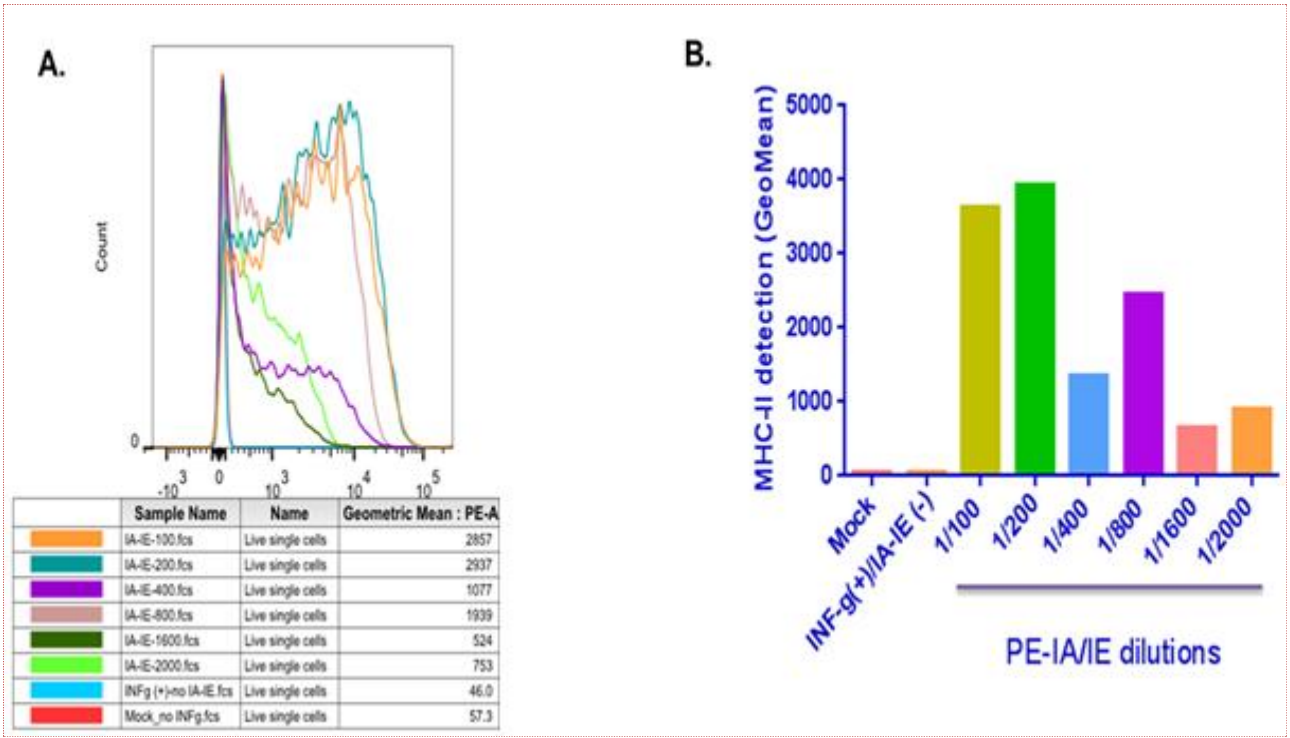

	Sample Name	Name	Geometric Mean : PE-A
	IA-IE-100.fcs	Live single cells	2857
	IA-IE-200.fcs	Live single cells	2937
	IA-IE-400.fcs	Live single cells	1077
	IA-IE-800.fcs	Live single cells	1939
	IA-IE-1600.fcs	Live single cells	524
	IA-IE-2000.fcs	Live single cells	753
	INFg (+)-no IA-IE.fcs	Live single cells	46.0
	Mock_no INFg.fcs	Live single cells	57.3

Figure 5.2 ***MHC-II expression was detected at 1/100 and 1/200 dilutions of PE-IA/IE antibody.*** Prior to staining, RAW 264.7 cells were cultured in complete DMEM in a 24-well plate. At 70% confluency, cells were treated with 20 U/mL IFN-γ and incubated at 37°C, 5% CO_2. RAW 264.7 cells were harvested 24 h later and stained with different dilutions of phycoerythrin (PE)-conjugated rat anti-mouse MHC-II (IA/IE) or with an isotype control antibody, PE-conjugated rat IgG2b (Appendix). **A)** 5000-10,000 live events were collected per assay, and the geometric mean fluorescent intensity (GeoMean) of MHC-II was assessed. **B)** comparison between different PE-IA/IE antibody dilutions. Detection of MHC-II surface expression was greater at 1/100 and 1/200 dilutions.

A.

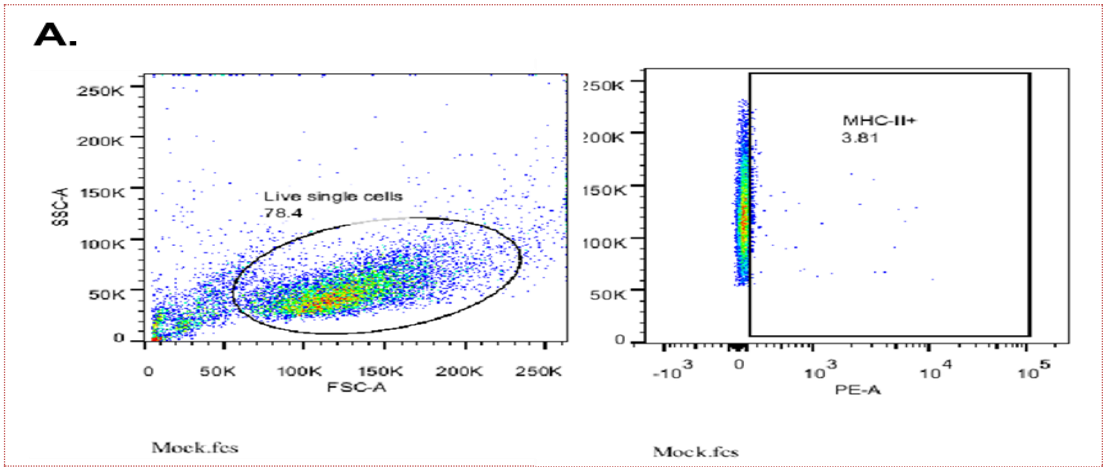

B.

1.

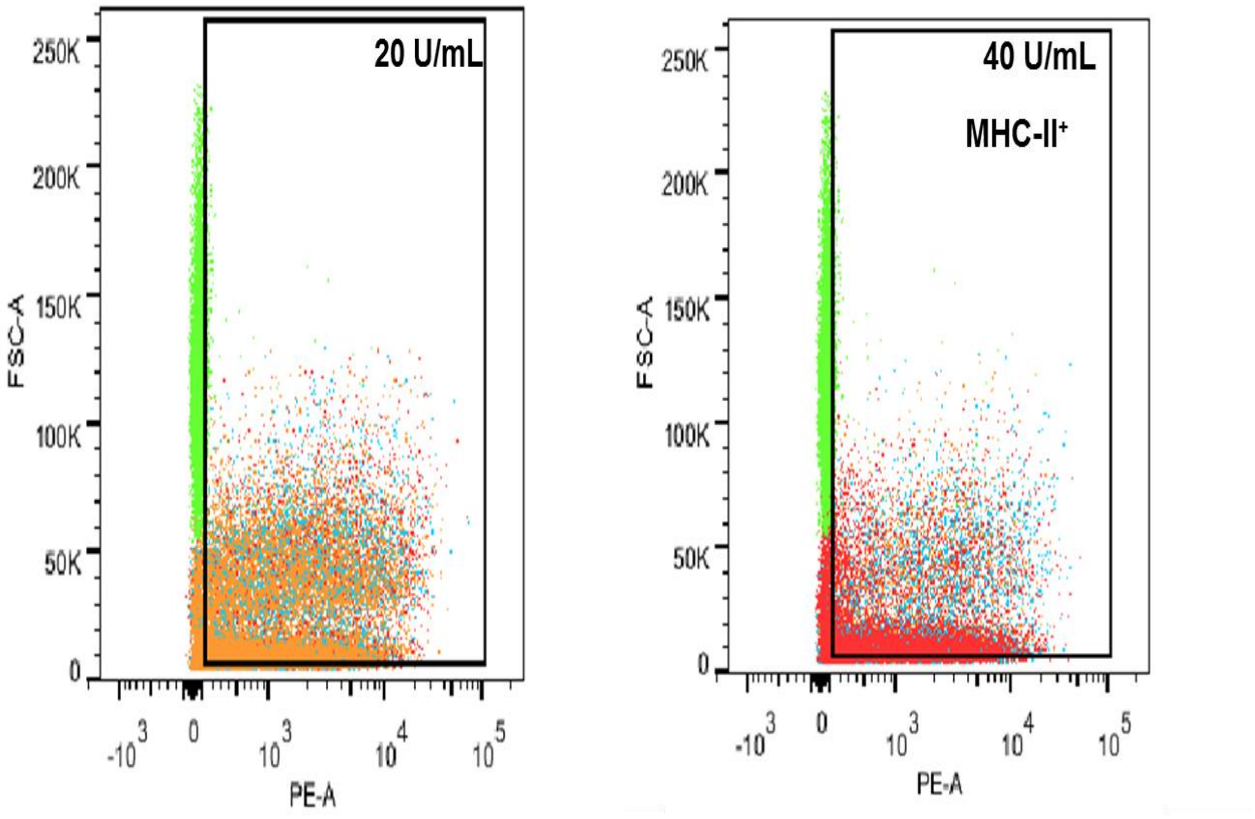

	Sample Name	Name	Geometric Mean : PE-A
	IA,2f,IE-1,2f,200_infg.fcs	Live single cells	51.7
	IA,2f,IE-1,2f,200_20u1-ia-ie.fcs	Live single cells	964
	IA,2f,IE-1,2f,200_20u2-IA,2f,IE.fcs	Live single cells	1015
	IA,2f,IE-1,2f,200_20U3-IA,2f,IE.fcs	Live single cells	1332

	Sample Name	Name	Geometric Mean : PE-A
	IA,2f,IE-1,2f,200_infg.fcs	Live single cells	51.7
	IA,2f,IE-1,2f,200_40-U-1-IA,2f,IE.fcs	Live single cells	851
	IA,2f,IE-1,2f,200_40U2-IA,2f,IE.fcs	Live single cells	1044
	IA,2f,IE-1,2f,200_40U3-IA,2f,IE.fcs	Live single cells	925

2.

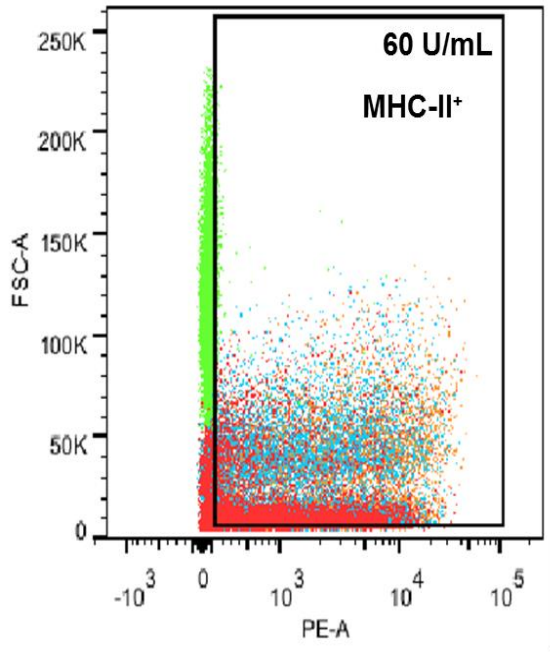

	Sample Name	Name	Geometric Mean : PE-A
	IA,2f,IE-1,2f,200_infg.fcs	Live single cells	51.7
	IA,2f,IE-1,2f,200_60U-1-IA,2f,IE.fcs	Live single cells	909
	IA,2f,IE-1,2f,200_60U-2-IA,2f,IE.fcs	Live single cells	1165
	IA,2f,IE-1,2f,200_60U3-IA,2f,IE.fcs	Live single cells	1837

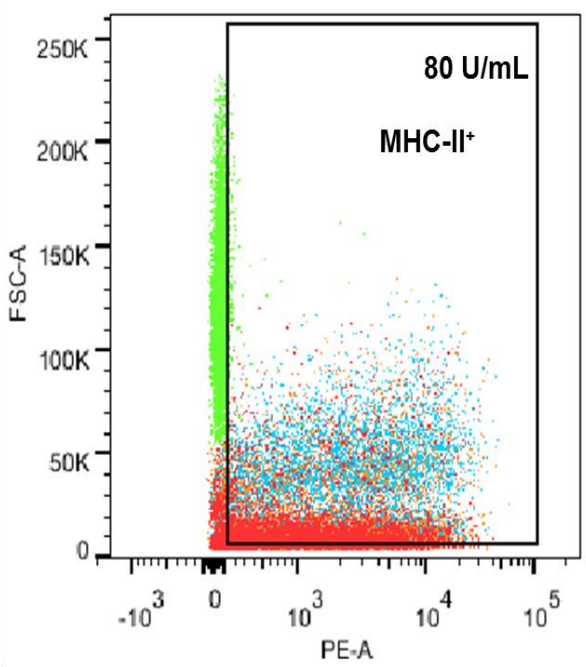

	Sample Name	Name	Geometric Mean : PE-A
	IA,2f,IE-1,2f,200_infg.fcs	Live single cells	51.7
	IA,2f,IE-1,2f,200_80U-1-IA,2f,IE.fcs	Live single cells	1004
	IA,2f,IE-1,2f,200_80U2-IA,2f,IE.fcs	Live single cells	1316
	IA,2f,IE-1,2f,200_80U3-IA,2f,IE.fcs	Live single cells	1592

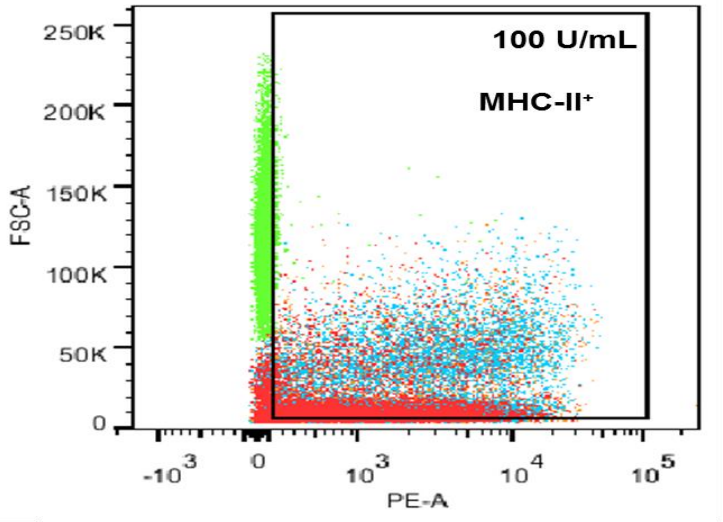

	Sample Name	Name	Geometric Mean : PE-A
	IA,2f,IE-1,2f,200_infg.fcs	Live single cells	51.7
	IA,2f,IE-1,2f,200_100U-1-IA,2f,IE.fcs	Live single cells	910
	IA,2f,IE-1,2f,200_100U2-IA,2f,IE.fcs	Live single cells	1768
	IA,2f,IE-1,2f,200_100U3-IA,2f,IE.fcs	Live single cells	1359

C.

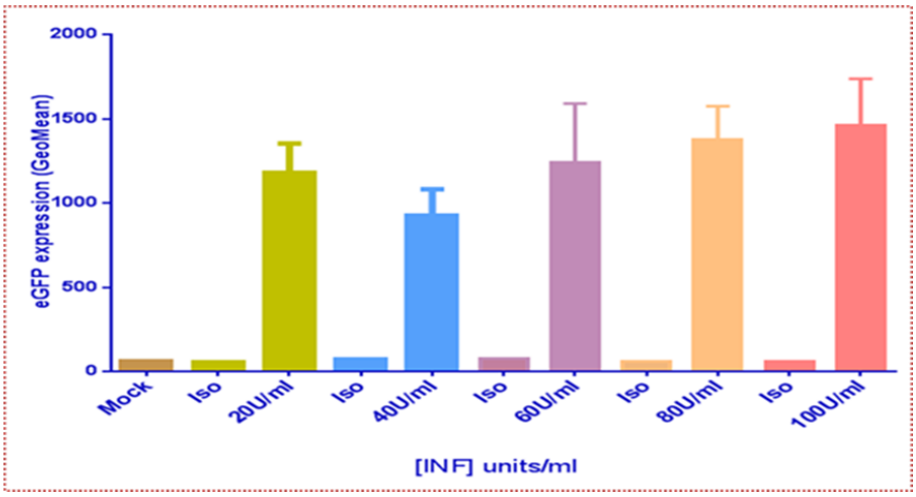

Figure 5.3. ***All concentrations of INF- γ induced significant up-regulation of MHC-II surface expression on RAW 264.7.*** **A)** RAW 264.7 cells treated with IFN-γ and left unstained (Mock) . **B)** Cells were stimulated with serial concentrations of IFN-γ (0-100 U/mL) for 24 h and stained with optimized concentration of PE-IA/IE (1/200) or with an isotype control antibody, PE-conjugated rat IgG2b. 5000-10,000 live events were collected per assay, and the geometric mean fluorescent intensity (GeoMean) of MHC-II was assessed. **C)** Shown are the means and SD of triplicates wells from one representative experiment of three replicates. The significance of MHC-II expression was compared under each concentration of INF-γ using unpaired t test with Weltech's correction of one-way ANOVA test.

5.2.3 Functional AAV-Mediated MARCH-I expression testing in RAW 264.7

To verify the function of MARCH-I in regulating antigen presentation process and to test the usefulness of our AAV-F4/80-MARCH-I-eGFP vector, we began our experiment by forcing the expression of MARCH-I in RAW 264.7 cells by transfecting these cells with AAV-F4/80-MARCH-I-eGFP. We elected to use AAV-CAG-eGFP as a control in this experiment instead of AAV-F4/80-eGFP vector, as the AAV-F4/80-eGFP plasmid quality decreased resulting in low eGFP expression and purifying another plasmid was time consuming; Therefore we decided to use AAV-CAG-eGFP plasmid as an alternative control. Twenty four hours post-transfection, cells were treated with 20 U/mL IFN-γ to prime MHC-II surface expression or left untreated. EGFP and MHC-II expression was assessed simultaneously at day 0 pre-IFN-γ treatment (for eGFP only), day 1, day 2 and day 3 via fluorescence microscopy and flow cytometry.

5.2.3.1 Good expression of eGFP in RAW 264.7 cells before IFN-γ treatment

Prior to stimulating cells with IFN-γ, we visualized eGFP expression 24 h post-transfection using fluorescence microscopy to assess transfection efficacy. Figure 5.4 shows the expression of eGFP from RAW 264.7 cells transfected with either AAV-F4/80-MARCH-I-eGFP or AAV-CAG-eGFP vectors and suggests that eGFP fluorescence was brighter and slightly increased under the F4/80 promoter control compared to the CAG promoter (Figure 5.4B). The level of expression was consistent in all wells containing AAV-F4/80-MARCH-I-eGFP-transfected RAW 264.7 cells and indicated an efficient transfection of RAW 264.7 cells. Additionally, the expression of eGFP is comparable to if not better than our previous experiments (Chapter 2, Figure 3.5). The improved transfection efficacy may be due to the use of early passaged cells (i.e. sixth vs fifteenth passage).

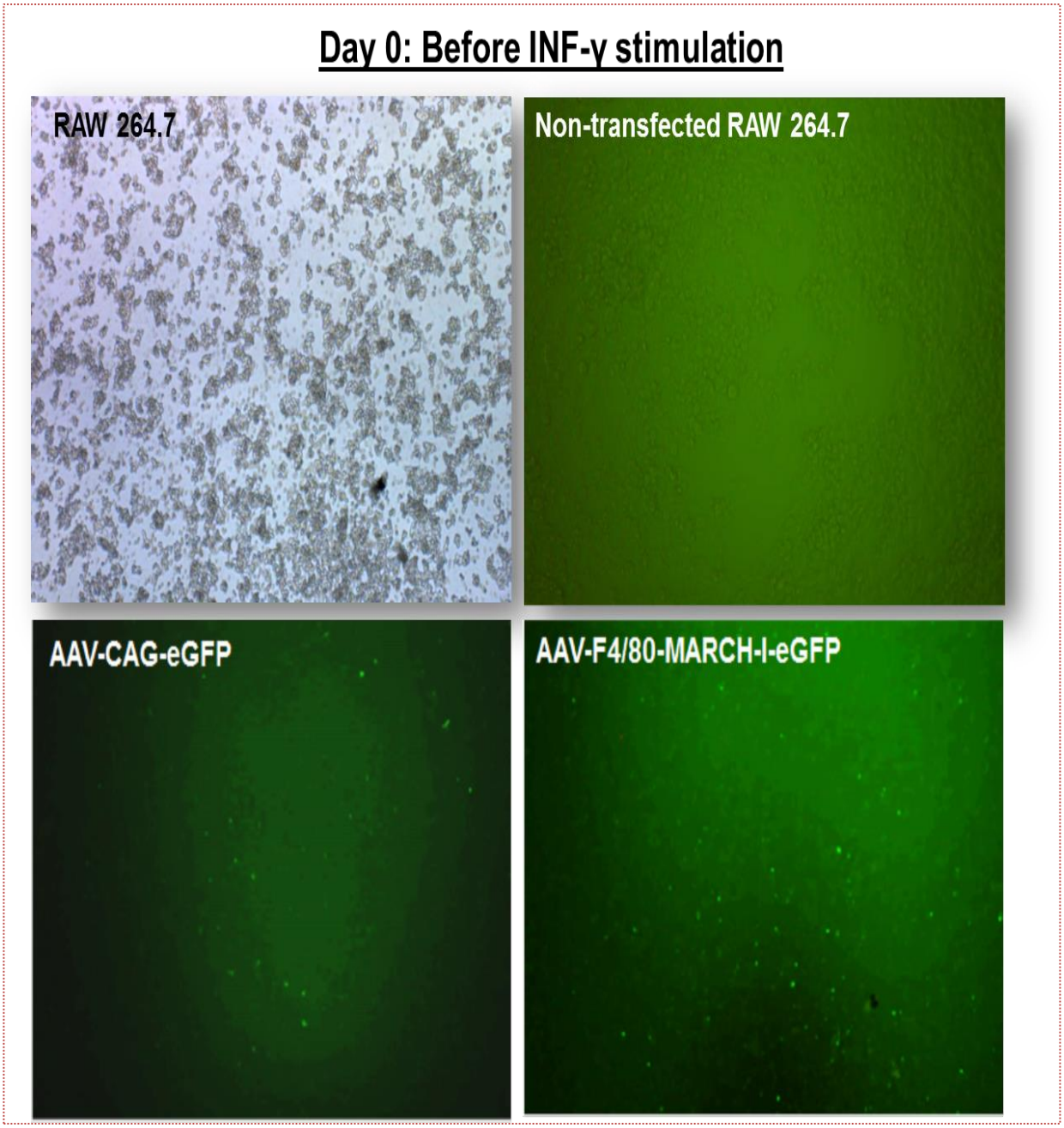

Figure 5.4. Good expression of eGFP under both promoters F4/80 and CAG in RAW 264.7 prior to IFN-γ stimulation. RAW 264.7 cells were maintained in complete DMEM until they became 70% confluent. Cells were transfected in duplicate with the AAV-F4/80-MARCH-I or AAV-CAG plasmid, and plates were incubated at 37°C in 5% CO_2. After 24 h, eGFP fluorescence was assessed by fluorescence microscopy, scale bar: 100 µm.

5.2.3.2 EGFP fluorescence in RAW 264.7 was lost after IFN-γ treatment

Although eGFP was well expressed 24 h post transfection, after stimulating cells with 20 U/mL of IFN-γ for 24 h, we observed a sharp decrease in eGFP expression in cells transfected with the AAV vectors compared to non-IFN-γ treated transfected cells, in which reporter gene expression remained stable through the time course (Figure 5.5B and Figure 5.6 C, D). Using flow cytometry, we quantified the eGFP expression over time and found a significant decrease in eGFP expression when transfected cells were stimulated with IFN-γ, and this decrease was equivalent for both vectors (Figure 5.5). In addition, we observed that cells density in the transfected cells appeared to be much lower than in non-transfected cells (Figures 5.4A and 5.4B). This assay has been repeated several times with the same result verifying the consistency of our findings. Finally, we also attempted to induce MHC-II expression via IFN-γ stimulation prior to the transfection of the RAW 264.7 cells with AAV vectors, but eGFP fluorescent cells were hardly detected the day after their transfection (data not shown).

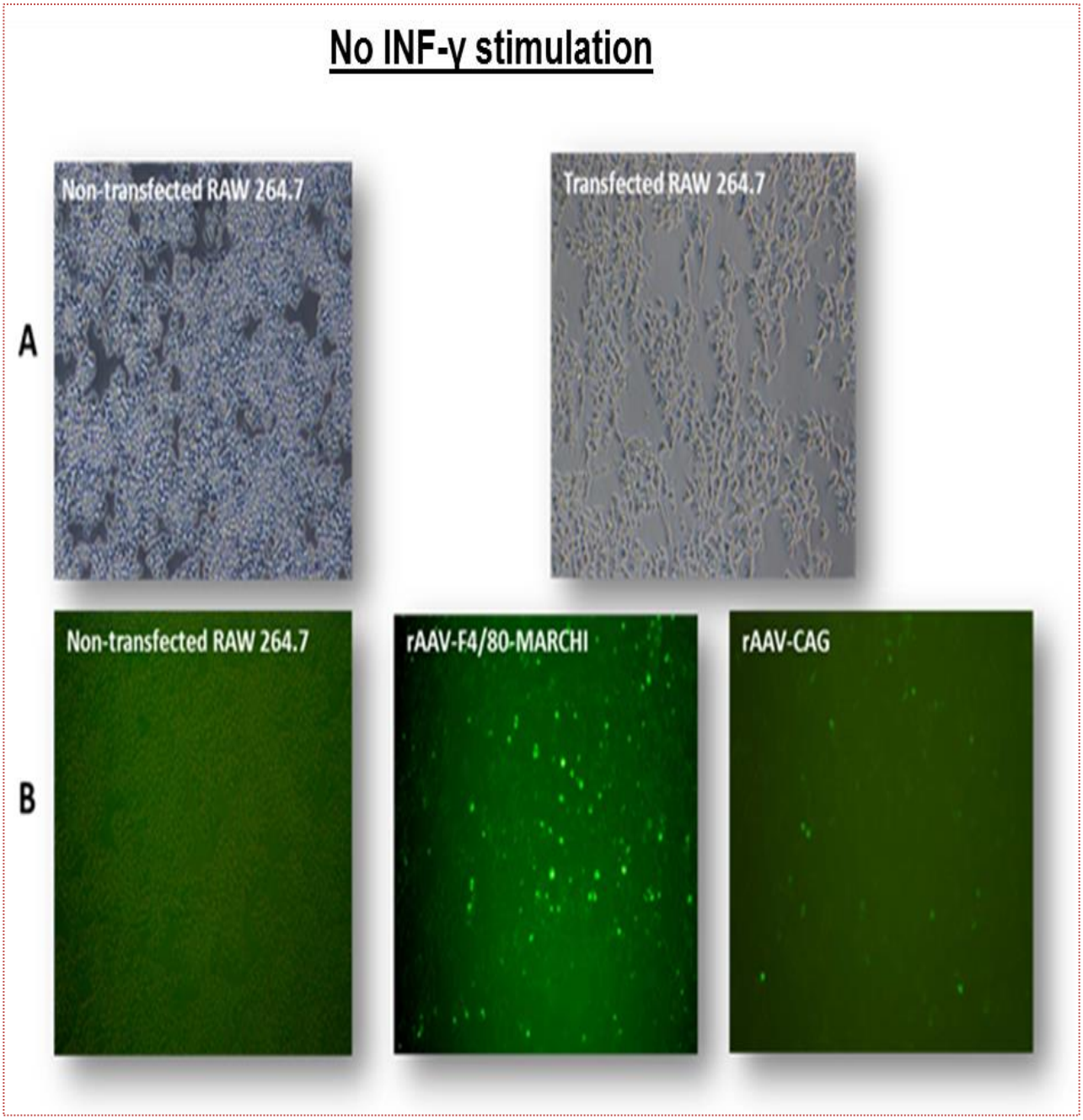

Figure 5.5 ***EGFP expression was stronger under F4/80 promoter than under CAG promoter.*** Prior to transfection, RAW 264.7 cells were maintained in complete DMEM in 24-well plates. At 70% confluency, complete DMEM media was changed and replaced by a reduced serum complete media (2% FCS). Cells were transfected in duplicate with the AAV-F4/80-MARCH-I or AAV-CAG plasmid, and plates were incubated at 37°C in 5% CO_2. After 96 h, eGFP fluorescence was assessed by fluorescence microscopy. **A)** Comparison between AAV-CAG—eGFP- transfected and non-transfected cells under light microscope. **B)** At 96 h post transfection, eGFP is expressed using either vector when no IFN-γ is present. Shown are representative images of non-transfected or transfected (AAV-F4/80-MARCH-I or AAV-CAG-eGFP) cells taken using the fluorescence microscope. Scale bar: 200 µm, magnification 10x.

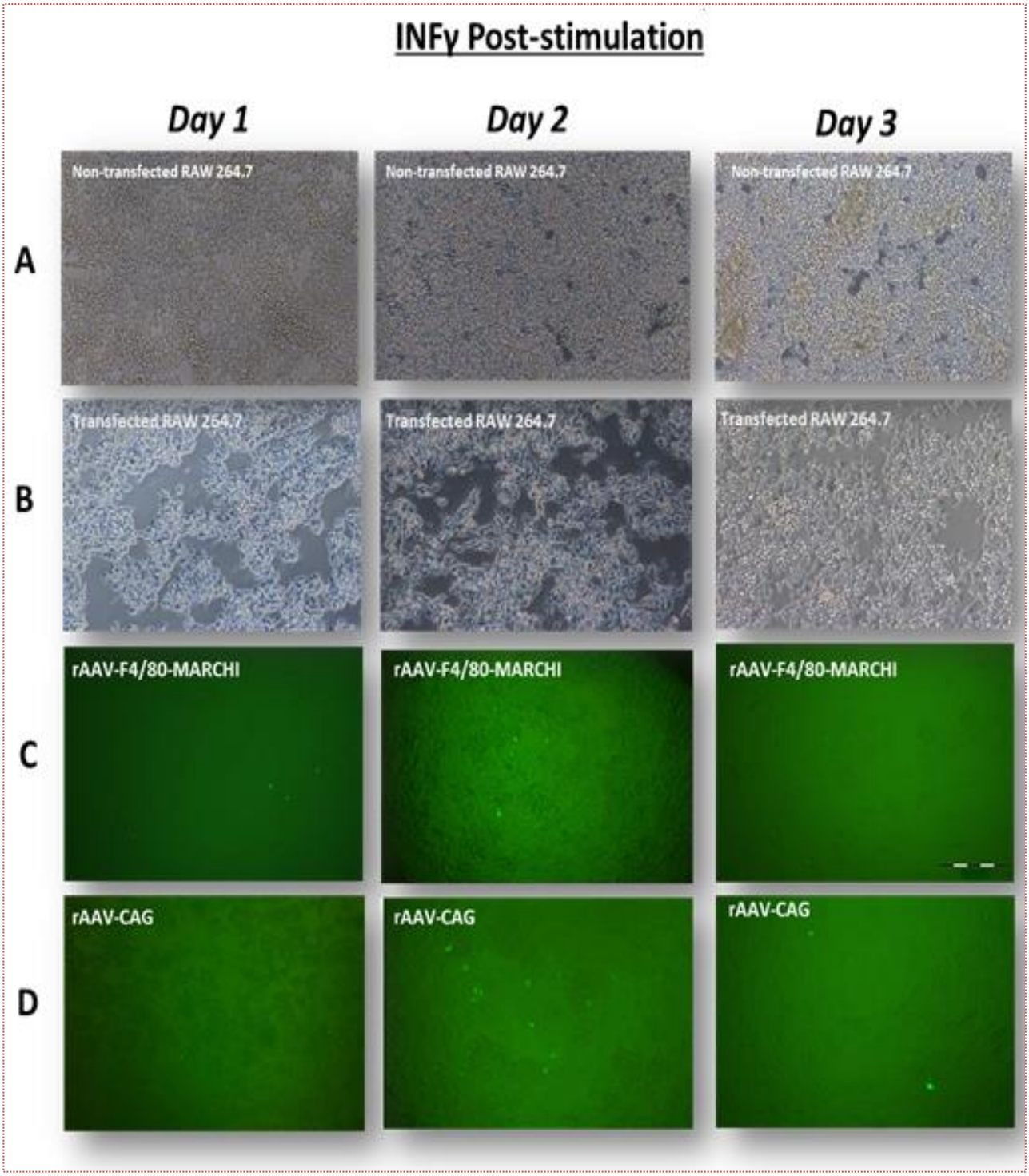

Figure 5.6. ***A sharp decrease of eGFP fluorescence occurred 24 hr after IFN-γ stimulation*****.** RAW 264.7 cells were treated with IFN-γ at 20 U/mL 24 h post-transfection, and the cells were incubated at 37°C, 5% CO_2 for 1-3 days. Panel A and B show RAW 264.7 cell confluency in non-transfected (A) and transfected cells with AAV-CAG-eGFP vector control (B), respectively. EGFP expression from AAV-F4/80-MARCH-I or AAV-CAG –eGFP transfected cells was visualized at each time point using fluorescence microscopy (C, D respectively). Scale bar: 200 µm, magnification 10x.

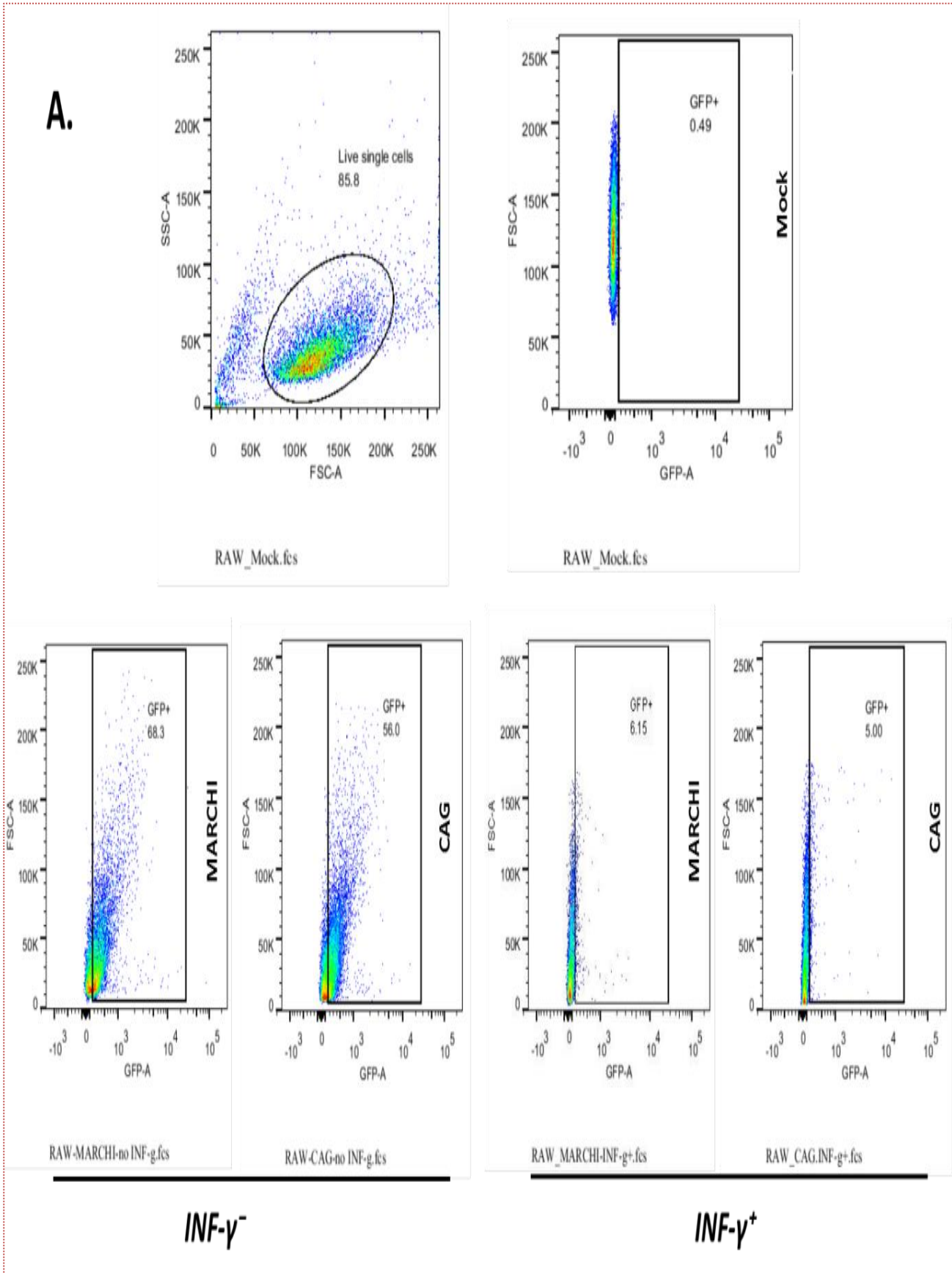
A.
Live single cells
85.8
SSC-A
FSC-A
RAW_Mock.fcs
GFP+
0.49
Mock
GFP-A
RAW_Mock.fcs
GFP+
68.3
MARCHI
RAW-MARCHI-no INF-g.fcs
GFP+
56.0
CAG
RAW-CAG-no INF-g.fcs
GFP+
6.15
MARCHI
RAW_MARCHI-INF-g+.fcs
GFP+
5.00
CAG
RAW_CAG.INF-g+.fcs
INF-γ⁻
INF-γ⁺

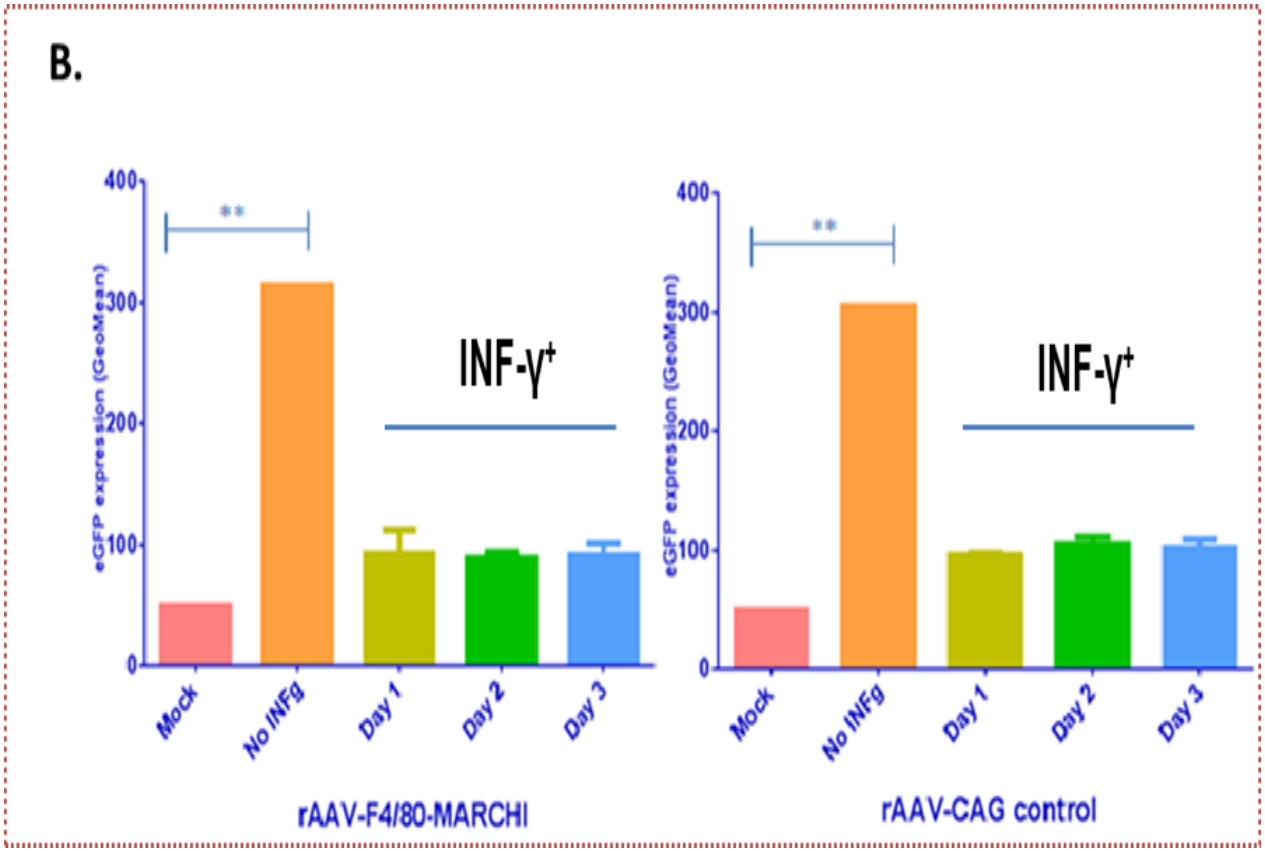

Figure 5.7. ***EGFP*** **expressions** ***in transfected cells decreased after RAW 264.7 IFN-γ stimulation compared to non-IFN-γ stimulated cells.*** **A)** Less eGFP+ cells are detected at day 3 post IFN-γ treatment, when transfected cells are cultured in the presence of IFN-γ. RAW 264.7 AAV-transfected cells that were not treated with IFN-γ were harvested at day three. eGFP expression was quantified in each sample by flow cytometry and shown are representative flow plots. **B)** EGFP expression was reduced in IFN-γ-treated cells at all time points compared to non-IFN-γ-treated AAV-transfected cells. Shown are the means and SD of duplicate wells from one representative experiment of 3 independent replicates. EGFP expression in IFN-γ-treated and non-treated AAV-transfected cells was compared against a mock using one way ANOVA with Sidak's post hoc multiple comparison test. **P < 0.01.

5.2.3.3 IFN-γ-induced MHC-II expression was impaired in AAV-transfected RAW 264.7

We examined MHC-II expression after transfection with the AAV-F4/80-MARCH-I-eGFP vector as a method to assess if a functional MARCH-I was expressed by transfected cells. Although eGFP expression was dramatically decreased after treatment with IFN-γ, eGFP+ cells were still present at day one post transfection. MHC-II surface expression was analysed on IFN-γ-stimulated, non-transfected or transfected cells by flow cytometry in presence and absence of MARCH-I (i.e. IFN-γ with AAV-F4/80-MARCH-I-eGFP or the AAV-CAG-eGFP vector control). We observed a significant expression of MHC-II in non-transfected RAW 264.7 cells which peaked at day 2, indicating that 20 U/mL of IFN-γ treatment efficiently primed the induction of MHC-II in these cells (Figure 5.8B). In contrast, MHC-II expression was very low not only in AAV-F4/80-MARCH-I-eGFP transfected cells but also in cells transfected with AAV-CAG-eGFP control, which was not expected (Figure 5.8A, B). However, MHC-II expression was 2-fold lower in AAV-F4/80-MARCH-I-eGFP-transfected cells at day 3 compared with that in AAV-CAG-eGFP-transfected cells (Figure 5.8B), suggesting that MHC-II expression may be further reduced by the presence of MARCH-I.

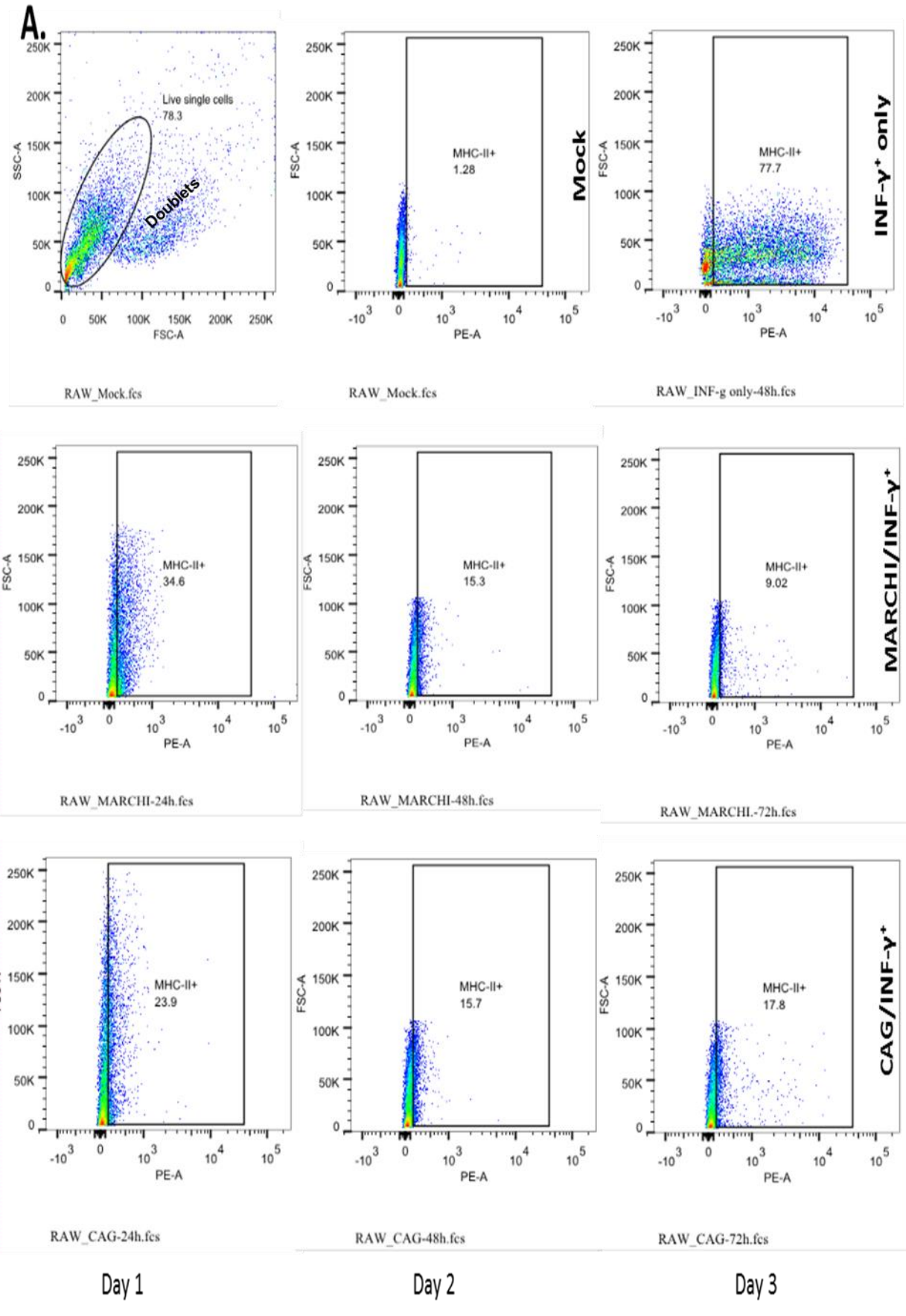
A.
Live single cells
78.3
Doublets
SSC-A
FSC-A
RAW_Mock.fcs
MHC-II+
1.28
Mock
RAW_Mock.fcs
MHC-II+
77.7
INF-γ+ only
RAW_INF-g only-48h.fcs
MHC-II+
34.6
RAW_MARCHI-24h.fcs
MHC-II+
15.3
RAW_MARCHI-48h.fcs
MHC-II+
9.02
MARCHI/INF-γ+
RAW_MARCHI.-72h.fcs
MHC-II+
23.9
RAW_CAG-24h.fcs
MHC-II+
15.7
RAW_CAG-48h.fcs
MHC-II+
17.8
CAG/INF-γ+
RAW_CAG-72h.fcs
Day 1
Day 2
Day 3

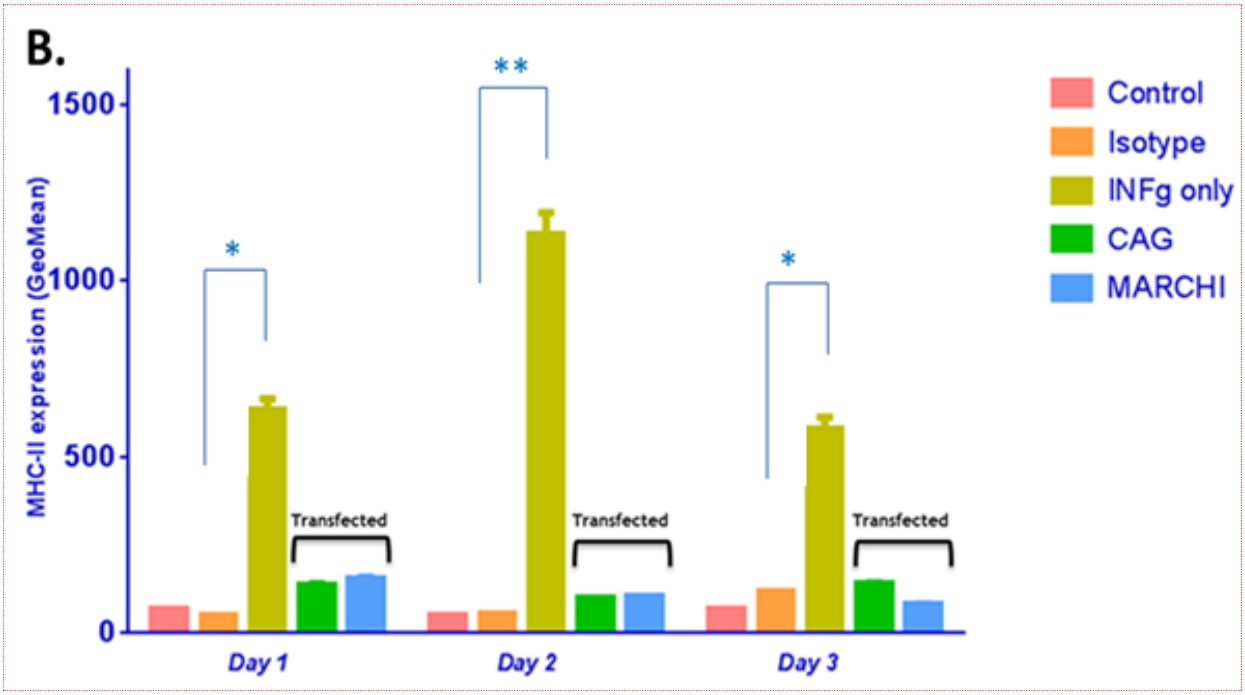

Figure 5.8. ***MHC-II expression was impaired on the surface of AAV-transfected RAW 264.7 cells after IFN-γ treatment***. **A)** RAW 264.7 cells were analysed by flow cytometry for MHC-II surface expression at day 1, day 2 and day 3. Surface expression of MHC-II was measured by flow cytometry with PE-labeled rat anti-mouse MHC-II (IA/IE) antibodies. 5000-10,000 live events were collected per assay. Shown are representative flow plots from one of three experiments. **B)** Comparison of MHC-II expression between AAV-transfected and non-AAV transfected cells over time. Shown are the means and SD of duplicate wells from one representative experiment of three replicates and are expressed as the geometric mean (GeoMean) of the fluorescent intensity. Test for significance was performed using one way ANOVA with Sidak's post hoc multiple comparison test. *P < 0.05, **P < 0.01.

5.2.3.4 Identification of eGFP positive cell population that did not express MHC-II after AAV-F4/80-MARCH-I-eGFP transfection

Although the previous results suggested that a functional MARCH-I may be expressed in the AAV-F4/80-MARCH-I-eGFP transfected cells; the expression of both eGFP and MHC-II that was reduced on all AAV-transfected cells following IFN-γ treatment weakened this conclusion considerably. Thus we attempted to verify at a cellular level whether the few cells that were expressing eGFP expressed MHC-II, in order to confirm that if MARCH-I proteins were expressed in a cell, MHC-II expression would be reduced. At day 1, we observed that the cells that were highly expressing eGFP were not expressing MHC-II in MARCH-I-containing cells, and this $eGFP^+$ population was still present at day 2 but not day 3 (Figure 5.7), consistent with eGFP fluorescence attenuation (Figure 5.4 C). In contrast, the CAG-containing cells expressed both eGFP and MHC-II ($eGFP^+/MHC\text{-}II^+$), and we did not observe the same $eGFP^+/MCH\text{-}II^-$ population as seen in the MARCH-I-containing cells. This finding suggests that in MARCH-I-containing cells, MHC-II surface expression was impaired and provides evidence that the AAV-F4/80-MARCH-I-eGFP vector induces the expression of a functional MARCH-I protein.

A.

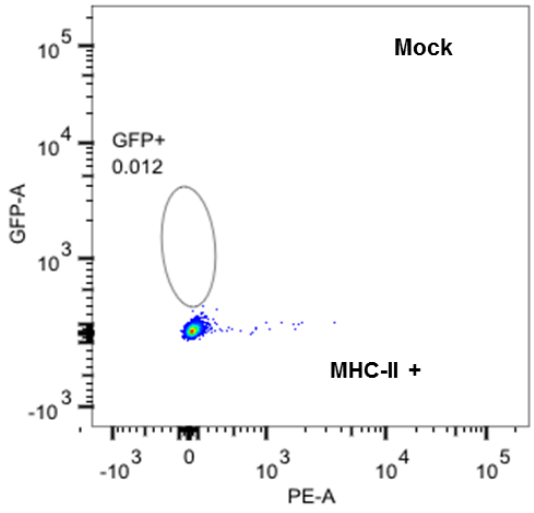

RAW_Mock.fcs

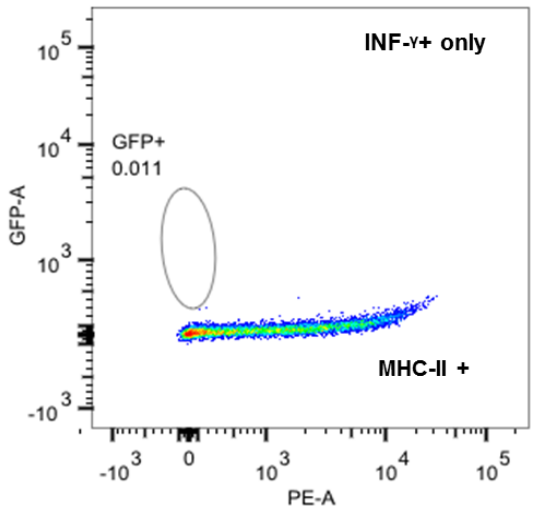

RAW_INF-g+ only.fcs

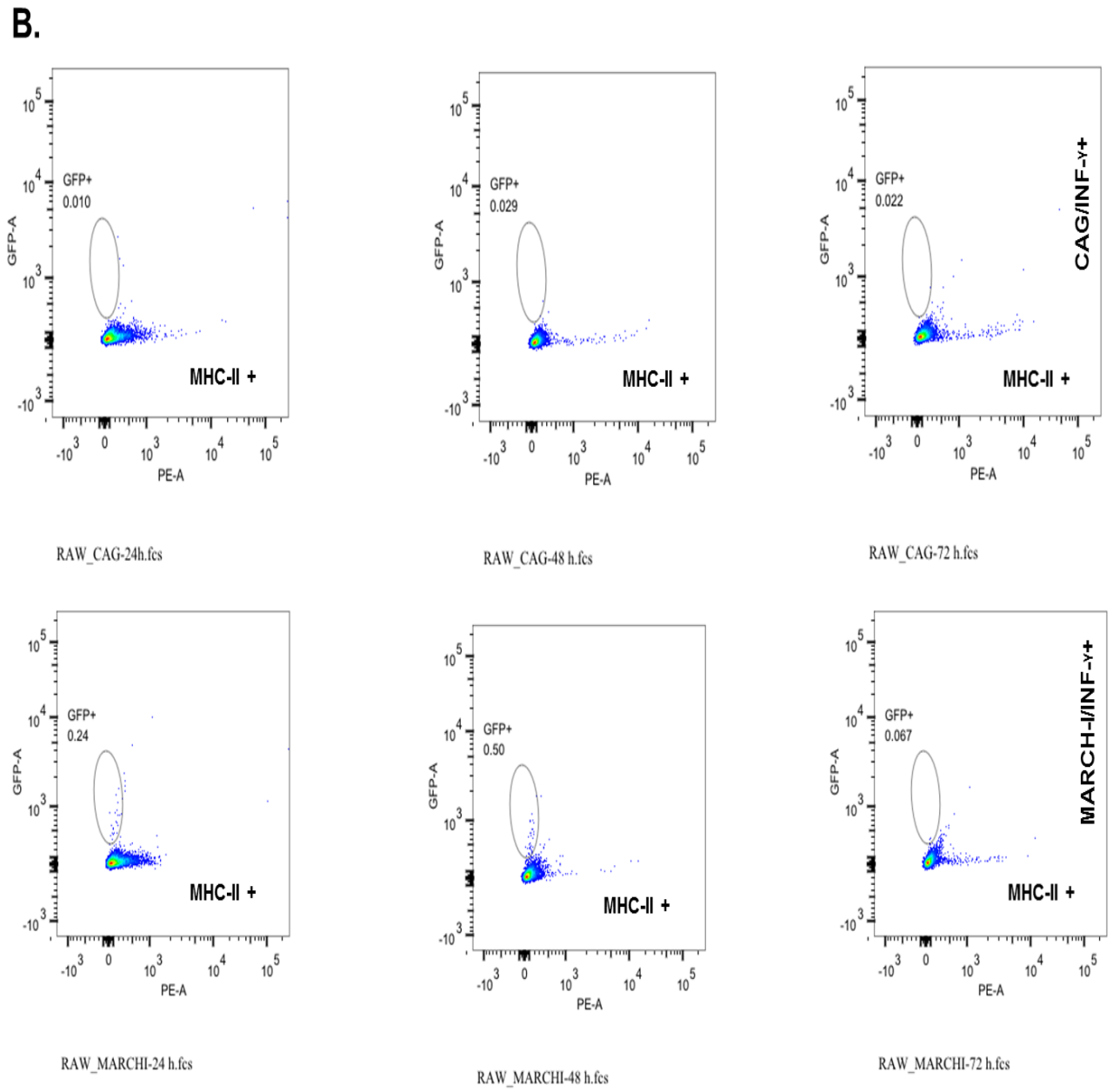

Figure 5.9. ***EGFP⁺/MHC-II⁻ population was identified in MARCH-I-containing cells but not in CAG-containing cells*.** **A)** Transfected and non-transfected RAW 264.7 cells were treated with IFN-γ at 20 U/mL or left untreated. **B)** Cells were harvested at day 1, day 2 and day 3. Prior to FACS analysis, cells were stained with PE-conjugated rat anti-mouse MHC-II (IA/IE), washed, and collected in FACS buffer. Upper panel shows eGFP⁺ cells and lower panel represents the surface level of MHC-II in the live single cells. The GFP⁺/MHC-II⁻ population is indicated in each circle in the upper left corner of each plot.

5.3 Discussion

Previous studies have demonstrated that the expression of the major histocompatibility complexes MHC-I or MHC- II is regulated by ubiquitination through the human ubiquitin ligase MARCH proteins (Bartee et al, 2004, Grimm et al., 2003). These proteins were shown to be structurally and functionally related to the viral K3 family that helps virus evasion from host immune response, by inducing a rapid internalization of their target substrates from the cell surface (Bartee et al, 2004). In Bartee et al. for instance, transient expression of MARCH-IV and MARCH-IX was found to down regulate MHC-I surface expression in transfected HeLa cells. Similarly, ubiquitination of surface expressed-MHC-II was found to be induced by MARCH-I in mouse B cells (Matsuki et al., 2007), in dendritic cells (Cho and Roche, 2013) and in human primary monocytes (Thibodeau et al, 2008). In the latter study, five members of the MARCH family were tested to identify the mediator of IL-10 that is directly involved in inhibiting the MHC-II antigen-presentation process. Although MARCH-I and MARCH-VIII were found to be the most potent family members to down-regulate MHC-II surface expression, a high level of MARCH I mRNA expression was found when cells were induced by IL-10 leading to endocytosis of MHC-II via ubiquitination (Thibodeau et al, 2008).

In the hope of finding similar result, we conducted comparable experiment as previously described (Thibodeau et al, 2008), except that MARCH-I expression was mediated via the AAV-F4/80-MARCH-I-eGFP viral vector. RAW 264.7 cells were treated with IFN-γ, a potent inducer of MHC-II expression on macrophages and other cell types (Steimle et al., 1994; Pestka and Langer, 1987). Stimulation of macrophages with IFN-γ activates CIITA, a trans-activator gene that induces MHC-II expression (Steimle et al, 1994). Upon activation, MHC-II molecules bind to peptides generated from exogenous proteins degradation by proteases in an endosome, and the MHC-II-peptide complexes are transported to the cell surface and induce T $CD4^+$ cells activation (Cho and Roche, 2013).

However, in contrast to our expectations, we observed a loss of eGFP fluorescence in IFN-γ treated cells in all AAV-transfected cells including the AAV-CAG-eGFP control vector and the AAV-F4/80-MARCH-I-eGFP vector. This loss of eGFP was combined with a reduction in MHC-II surface expression in the same cells. A possible explanation is that IFN-γ treatment of AAV-transfected macrophages induced an antiviral response stimulating MHC-I expression and according to Takaoka et al., IFN-γ treatment of mouse cells might prime the induction of the anti-viral cytokine

INF-β in response to a viral infection (Takaoka et al.2000). In this mechanism, viral proteins are fragmented in the cytosol and the fragments are loaded on MHC-I molecules and transported to the cell surface to induce T CD8$^+$ cells-mediated immune response (Komatsu et al., 1996; Farra and Schreider, 1993; Costa et al, 2002). This may explain the loss of eGFP fluorescence and low MHC-II surface expression following IFN-γ treatment of AAV-transfected macrophages (Figure 5.4). Furthermore, the apparent inhibition of AAV-infected cell growth that occurred following the treatment may serve to prepare the cells for apoptosis to prevent virus spread (Pestka and Langer, 1987). Thus, the antiviral state that IFN-γs stimulate in infected cells may be interfering with the assay (58). This anti-viral hypothesis is based on many studies that demonstrated the anti-viral activity of IFN-γ (Komatsu et al., 1996; Liu et al, 2001), however, in order to verify it, MHC-I expression needs to be assessed by FACS analysis.

While we were unable to demonstrate a direct effect of MARCH-I on MHC-II surface display using this approach, a more in depth analysis of eGFP positive cells allowed us to detect a difference in MHC-II expression between cell transfected with AAV-CAG-eGFP and AAV-F4/80-MARCH-I-eGFP. The eGFP$^+$ cells that were present after AAV-F4/80-MARCH-I-eGFP transfection were not expressing MHC-II, whereas, the eGFP$^+$ cells in the AAV-CAG-eGFP transfected population were still expressing MHC-II (Figure 5.7). In addition, MHC-II surface expression was 2-fold lower in MARCH-I- containing cells than that in vector control-containing cells. Thus, despite the loss of a high amount of eGFP in transfected cells, we were able to confirm the role of MARCH-I in inducing MHC-II sequestration in the cytoplasm in the remaining eGFP positive cell population in transfected cells.

However, this result needs further investigation in order to confirm it, including MARCH-I mRNA quantification via qPCR before and after cells treatment with IFN-γ. Furthermore, in order to appreciate the effect of MARCH-I on MHC-II sequestration before losing eGFP, analysing the cells at 16 hours post-IFN-γ treatment might give us a consistent result, or considering other stimuli that would prime MHC-II surface expression in AAV-transfected cells while maintaining the viral plasmids. Lipopolysaccharide (LPS) might be a good candidate to consider as a replacement of IFN-γ to prime MHC-II expression. It was shown in Gassart et al study that upon stimulation of APCs with LPS, MHC-II surface expression is increased in the surface, leading to an increase of antigen presentation while MARCH-I mRNA expression is decreased (Gassard et al, 2008). Therefore, if we prime MHC-II expression in RAW 264.7 cells with LPS and 24 h later we force MARCH-I expression

by transfecting cells with AAV-F4/80-MARCH-I-eGFP or with a vector control, we may have a more sensitive way to assess the effect of MARCH-I on MHC-II surface expression and sequestration.

CHAPTER 6

GENERAL DISCUSSION

AAV has been extensively used as a viral vector in gene therapy in pre-clinical studies and clinical trials, due to its lack of toxicity and non-pathogenicity to humans and the long-term expression of the transgene. It has been extensively used to investigate and treat CNS disorders such as neurodegenerative diseases, in particular Alzheimer and Parkinson's diseases (Mueller and Flotte, 2008). Although microglia have been shown to play a critical role in neurodegeneration by initiating and perpetuating a chronic inflammation (Rogove et al., 2002; Frederik Vilhardt. 2004), most of the AAV vectors employed to study or attempt to cure these conditions target neurons (Iwata et al., 2013; Bishop et al., 2008; Lim et , 2009). Moreover, the potential of AAV vectors to dissect neuroinflammatory disorders such as multiple sclerosis has not been fully utilized yet. Therefore, the ultimate goal of this thesis was to create an AAV-based viral tool that would target microglia specifically and deliver a gene of interest, in order to investigate the role of these CNS resident immune cells in neuronal degeneration in MS, and other neurodegenerative disorders. We began our investigation by constructing an AAV-based viral tool that is driven by the human macrophage marker element F4/80 (EMR1). We then demonstrated the specificity of the vector for macrophages by comparing its activity in human cell lines with macrophage cell line RAW cells. Producing packaged AAV-F4/80 vector was very challenging and the low titer of AAV-F4/80 virions obtained prevented us from pursuing this line of investigation. Despite the antiviral action of IFN-γ that induced AAV-F4/80-MARCH-I vector attenuation in RAW cells, we were able to see the effect of MARCHI on class II MHC surface expression at the cellular level via flow cytometry.

6.1 AAV-mediated gene delivery

The use of selective targeting in gene therapy to control therapeutic gene expression is advantageous, and can only be achieved by the utilisation of a tissue-specific promoter. Among the several advantages of using a specific promoter in an AAV vector is the stable and prolonged transgene expression. For instance, it was documented previously that the neuron-specific enolase (NSE) promoter generated a strong, stable and widespread GFP expression in neurons lasting more

than 19 months in the rat substancia nigra with no apparent attenuation (Peel and Klein, 2000). While in During et al., primate neurons were transfected *in vivo* via an AAV expression cassette containing human tyrosine hydroxylase and aromatic amino acid decarboxylase driven by the CMV promoter, the expression of the vector did not last longer than 2.5 months (Peel and Klein, 2000). Although CMV hybrid promoters, which are a combination of CMV early enhancer element and a mammalian element, such as CMV/human β-globin promoter or CMV/chicken β-actin (CAG) promoter, have shown to achieve a long-term and robust transgene expression (Peel and Klein, 2000; Mandel et al., 1998), these promoters are still not specific and the off-target expression effect is very high (Chen et al., 1999.).

Additionally, Toscano et al. indicated that non-controlled transgene expression generates cytotoxicity induced by an unwanted transgene expression in non-target cells and with the use of tissue-specific promoter this side effect is reduced completely (Toscano et al., 2011).

Therefore, to prevent the previously described side effects and control the expression of the viral tool, we elected to use an element specific to microglia in the CNS (i.e. F4/80) to drive the expression of the AAV vector exclusively in these cells *in vivo*. Although F4/80 is also expressed on other cells of the myeloid lineage outside of the CNS, RFP-labelled AAV vector driven by the murine F4/80 marker element was shown in a study conducted by Cucchiarini et al. to be the most discriminating for microglia compared with CD11b and CD68, when rat primary microglia and neuronal cultures were transduced *in vitro* and *in vivo* (Cucchiarini et al, 2003). In addition, the physiological level of F4/80 expression was reported to be dependent on the biological status of the cells (Siamon Gordon, 2010); its expression is relatively low in blood monocytes and highly expressed in resident macrophages (McKnight and Gordon, 1998; Francke et al. 2011). Nevertheless, despite its heterogeneous expression, F4/80 is present constitutively on the cell surface which is beneficial in viral vector-based gene therapy as its expression is constant, compared with CD11b for instance that was shown to be highly up-regulated in activated monocytes while in resting monocytes, CD11b is down-regulated (Minghetti et al. 2005).

Since F4/80 promoter activity in other types of cells has never been investigated, we transfected different human cell lines *in vitro,* including HEK 293, HepG2 and 1A9 cells and macrophage-like RAW cells via our newly constructed AAV-F4/80 vector and compared F4/80 promoter activity in these cells against a widely expressed promoter CAG. Although it was evident from Cucchiarini et al. that F4/80 is the best currently available promoter to use for driving transgene expression to

microglia (Cucchiarini et al, 2003), we anticipate that our viral tool driven by F4/80 will be expressed in other tissue macrophages (peritoneal cavity, lung, skin epidermis, spleen, thymus and liver) *in vivo* (Gordon et al. 2011). Nonetheless, this depends on the vector delivery method, as stereotaxic injection of AAV virus was shown previously to be adjacent and distal to the injection tract (During et al., 1998; Fan et al., 2008), therefore limiting vector expression to microglia and infiltrating macrophages in the site of inflammation (Wolfgang Bruck, 2005). Tissue specific promoters have been shown to express transgenes very efficiently compared with general promoters (Peel and Klein, 2000; Shevtsova et al., 2004). However, in our study, eGFP expression under F4/80 promoter control in RAW cells was not as high as we anticipated. This might be due to the low transfection efficiency of these cells compared to HEK cells or, because RAW cells are different from primary macrophages since it is a transformed cell line. Hence, we suggest that a higher transgene expression may be achieved *in vivo* (Hartley et al, 2008). Moreover, the human origin of the F4/80 promoter cDNA (EMR1) may explain the low expression of eGFP in murine macrophage-like RAW cells due to species differences (Appendix 2B); it would be interesting to see if the reporter gene expression is higher in human macrophages under human EMR1 element.

In AAV-mediated gene therapy and in particular CNS studies, AAV serotype 2 has been used extensively in preclinical investigations and clinical trials due to the high tropism of this serotype to neurons, astrocytes and microglia (Mueller and Flotte. 2008; Gonga et al., 2004). However, despite the success use of AAV 2 in animal studies, this serotype was shown previously to induce humoral and cellular immune responses in some clinical trials (Herzog, 2010; Mingozzi et al., 2007). In Manno et al. study for instance, AAV2-mediated delivery of human factor IX to seven patients with severe haemophilia, generated a $CD8^+$ T cell-mediated immunity targeting AAV2 capsid antigens, causing destruction of transduced hepatocytes resulting in a decreased in factor IX expression associated with a transient asymptomatic elevation of liver transaminases (Manno et al.,2006; Mingozzi et al., 2007). In addition, while AAV2 mediated brain therapy resulted in successful long-term therapeutic gene expression, due to the tolerance of the brain to foreign antigens (Wu et al., 2009), in McPhee et al. study, AAV2 intracranial infusion that 10 Canavan disease patients have received, generated humoral immune response in 3 of them, where AAV2-neutralizing antibodies were detected in these patients' serum (McPhee et al., 2006). Nevertheless, despite the absence of neutralizing antibodies in their cerebrospinal fluid (McPhee et al., 2006), a long term monitoring is necessary to confirm the safety of the serotype.

Therefore, in order to evade neutralizing antibodies to AAV2 capsids components, we decided to employ a hybrid construct encoding *rep* from AAV serotype 2 whereas *cap* is derived from serotype 5. The selection of this serotype capsid was based on the study published by Cucchiarini et al., where AAV serotype 5 was shown to display a high tropism for microglia (Cucchiarini et al, 2003). In addition, instead of using the serotype 5 in our studies we elected to choose a pseudotype, since it was shown in previous studies that pseudotyping approach generated a greater gene transfer compared with serotypes (Manuel Goncalves, 2005; Daya and Berns, 2008).

To produce our viral vector, we implemented Zolotukhin et al. method using HEK 293 as packaging cells (Zolotukhin et al., 1999). Despite the successful results that other researchers have achieved in producing AAV using this approach, we found this method very challenging as each production parameter required careful optimization for an optimal production of AAV. The very low titer of the recombinant virus that was obtained in this study was definitely not due to the large size of AAV genome, as it did not exceed the wild type genome size (~3.4 kb). We believe that the first barrier in the production process was the calcium phosphate transfection method, which was not efficient according to the GFP fluorescence images of calcium phosphate-mediated HEK 293 cells transfection (Chapter 4, figure 4.2), since less than 50% of cells were transfected. This might be due to the low quality of HEK cells or failure in maintaining transfection reagents at their optimal conditions (Fraser Wright, 2009). Iodixanol density gradient purification was another major obstacle that we believe affected AAV production. Our SDS PAGE result (Chapter 4, figure 4.5) showed contamination of purified AAV stocks with cellular proteins accompanied with very low titer of VP proteins, suggesting a mis-collection of the virus from the density gradient (Zolotukhin et al., 1999). Therefore, the low titer of the AAV-F4/80 virus precluded further investigation which requires a high titer of virus to validate its specificity for microglia *in vivo*.

6.2 Microglia role in neurodegeneration investigation

Among the acquired functions of activated microglia in the healthy brain include regulation of T cell responses through antigen presentation and secretion of pro-inflammatory cytokines (*e.g* TNF-α, IL-1β), chemokines, and proteases, generation of reactive oxygen (ROS) species and nitrogen intermediates (Francesca Aloisi, 2001). Although microglia function is to protect the CNS and maintain its homeostasis, evidence has accumulated since decades regarding the role of these

resident macrophages in inducing chronic inflammation in neurodegenerative and neuroinflammatory disorders (Minghetti et al. 2005). It remains unclear whether this chronic reaction has a protective or detrimental role, since no direct evidence of the functional role of microglia has been found yet in these disorders. For instance, it was reported in previous studies that activated microglia is directly involved in stimulating inflammatory T cells infiltration in the CNS and this stimulation is perpetuated during the effector phase of EAE model generating encephalomyelitis (Becher et al, 2001; Becher et al, 2003; Cua et al., 2003). In addition, Ulvestad et al. have previously demonstrated *in vitro* that microglia cells are potent APCs (Ulvestad et al., 1994), whereas *in vivo* studies of Ford et al. and Greter et al. showed that infiltrating macrophages population, but not microglia, is the effective APC in presenting antigens to $CD4^+$ T cells in the MS model (Ford et al.,1995; Greter et al., 2005). To address this ambiguity, we aimed in this thesis to examine the antigen-presenting abilities of microglia, by forcing the expression of the anti-inflammatory protein MARCHI in RAW cells using our constructed viral tool that, to our knowledge, has not been used for any macrophages/microglia functional studies.

To make a detailed observation of the regulatory role of MARCHI on MHC-II, we used IFN-γ as an inducer of MHC-II surface expression *in vitro*. This pro-inflammatory cytokine was suggested to be the only efficient inducer of class-II (HLA-DR) MHC molecules compared with INF-α/β, and it has been used extensively in assays involving antigen-presentation function (Ulvestad et al., 1994; Samuel, 2001; Tang et al, 2012). However the usage of this pro-inflammatory cytokine in our assay was very challenging, as IFN-γ stimulation before or after transfecting RAW cells with AAV vectors induced eGFP attenuation, possibly due to the anti-viral activity of IFN-γ since this pro-inflammatory cytokine is known to induce immune response to infected cells (Pestka and Langer. 1987; Stark et al. 1998; Zhang et al., 2009), leading to degradation of both AAV-F4/80-MARCHI and AAV-CAG viral plasmids. This phenomenon did not occur in Thibodeau et al. study, as the loss of eYFP fluorescence was not observed following IFN-γ addition, when primary monocytes were transfected with a non-viral vector (Thibodeau et al, 2008). Another strong evidence supported our hypothesis was, the absence of MHC-II surface expression in the IFN-γ-treated cells transfected with the vector control. Similar result was obtained in AAV-F4/80-MARCHI transfected cells, compared with the treated non-transfected cells, in which MHC-II was highly expressed, suggesting an induced MHC-I surface expression instead of MHC-II. Although it was documented previously that both MHC-I and MHC-II play an important role in immune response to infections

and that their levels are increased during viral infection (Samuel, 2001; Boehm et al. 1997), we did observe a slow increase of MHC-II surface expression during the time course in AAV-CAG transfected cells (Chapter 5, figure 5.6) and no MHC-II increase was observed in AAV-F4/80-MARCHI transfected cells, suggesting a down-regulatory effect of MARCHI. However, MHC-I immunostaining of IFN-γ treated RAW cells as well as MARCHI mRNA quantification need to be performed in order to confirm the antiviral activity of IFN-γ and the effect of MARCHI in blocking MHC-II surface expression.

Despite the loss of a large amount of our viral tool in RAW cells following their IFN-γ treatment, we were able to verify the direct effect of MARCHI on MHC-II surface expression at the cellular level, by analysing the remaining portion of AAV transfected cells before the complete loss of eGFP fluorescence. Our results support previous finding (Thibodeau et al, 2008) whereby the down-regulatory effect of MARCHI on MHC-II surface expression. Nevertheless, an alternative stimulus to IFN-γ such as lipopolysaccharide (LPS) that would induce MHC-II expression and maintain MARCHI expression in the majority of the AAV-transfected cells must be considered in order to appreciate MARCHI function (Gassard et al, 2008).

6.3 Future prospects

Once AAV2/5-F4/80 virus production has been optimized, future studies may involve experiments that will approve the selectivity of our recombinant vector for macrophages and microglia. The first approach consists in mouse splenocytes transduction *in vitro;* this assay will generate insight regarding AAV2/5-F4/80 expression in macrophages *vis-a vis* other cell types such as lymphocytes (T cells and B cells), plasma cells and dendritic cells (Mark Cesta, 2006). The effectiveness of the vector in delivering the transgene to microglia as well as to verify the tropism of AAV2/5-F4/80 vector packaged into the serotype-5 capsid for these cells, as reported in Cucchiarini et al., can be assessed by transduction of adult mouse brain *in vivo* via a stereotaxic injection. In addition, to obtain complete information regarding AAV2/5-F4/80 virus itinerary, a systemic injection (Intraperitoneal or intravascular injection) may be performed. This assay will verify Iwata et al. finding concerning the ability of AAV to penetrate the blood-brain barrier and the possibility to reach microglia via systemic administration (Iwata et al., 2013). The pathway of the recombinant virus will be monitored via eGFP fluorescence.

To obtain a better understanding of MARCHI role in down regulating MHC-II surface expression, in vitro transduction of primary activated microglia via AAV-F4/80-MARCHI may be performed. However, prior to draw any conclusion from in vitro experiments, *in vivo* transduction of the brain EAE animal model must be considered as it will certainly generate greater insight regarding the role of chronic inflammation in inducing neuronal demyelination in MS and other degenerative diseases, since microglia are targeted in the environment where they are normally found.

APPENDICES

Appendix 1: Plasmids maps and sequences

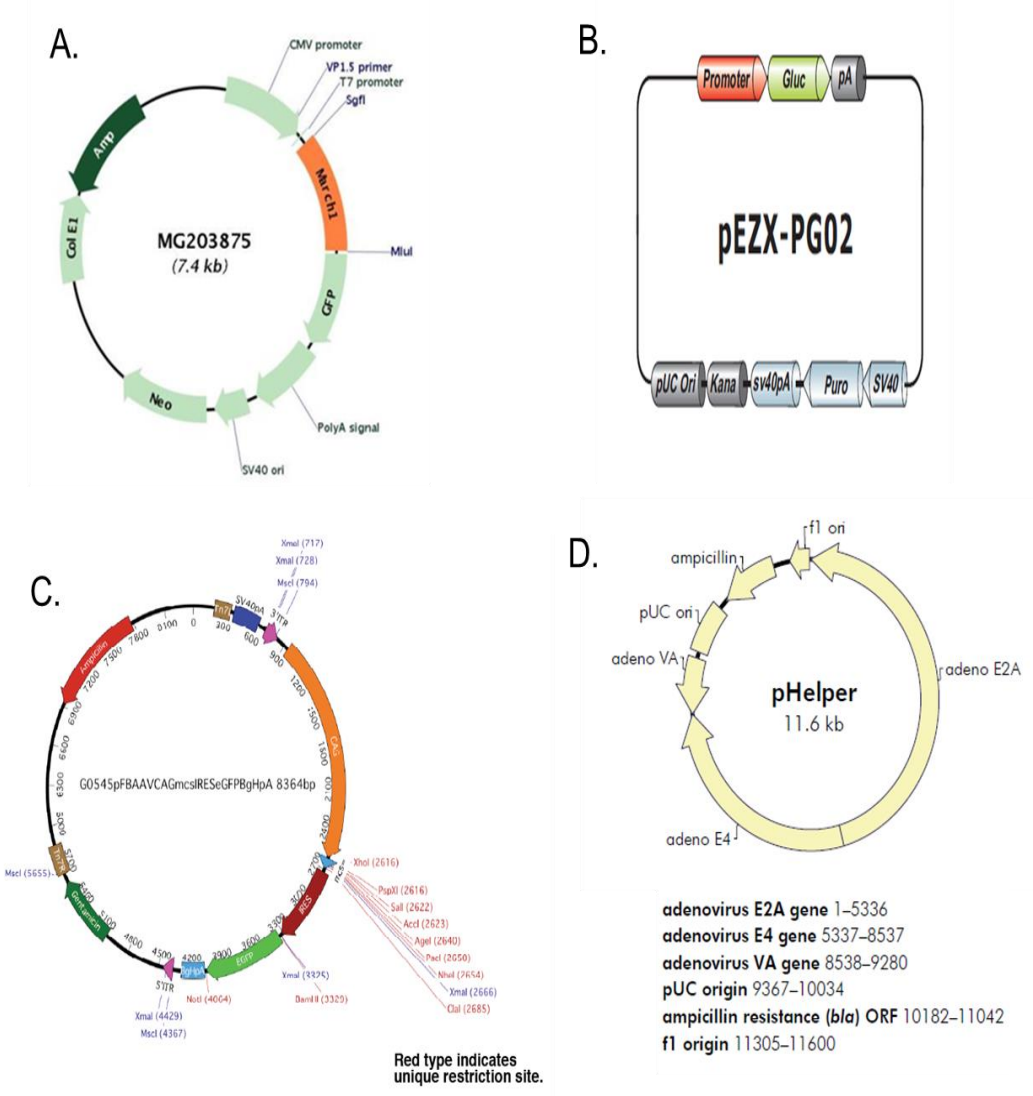

Figure 1A. **Plasmids maps**. **A)** Plasmid donor for mouse MARCH-I cDNA obtained from OriGene. The size of MARCH-I cDNA is 858 bp. **B)** F4/80 promoter plasmid donor obtained fron GeneCopoeia™. The size of the promoter is 1362 bp. **C)** AAV-CAG-eGFP vector plasmid map. The plasmid is obtained from Gene transfer vector core at the university of Iowa. The plasmid size is 8364 bp. D) Helper plasmid map obtained from Gene transfer core. The plasmd contains the three adenovirus genes necessary for AAV packaging (E2A, E4 and VA genes).

Appendix 2: Plasmids sequences

A. AAV-F4/80-MARCH-I-eGFP clone sequence (8894 bp)

CCATTCGCCATTCAGGCTGCAAATAAGCGTTGATATTCAGTCAATTACAAACATTAATAACGAAGAGA
TGACAGAAAAATTTTCATTCTGTGACAGAGAAAAAGTAGCCGAAGATGACGGTTTGTCACATGGAGTT
GGCAGGATGTTTGATTAAAAACATAACAGGAAGAAAAATGCCCCGCTGTGGGCGGACAAAATAGTTG
GGAACTGGGAGGGGTGGAAATGGAGTTTTTAAGGATTATTTAGGGAAGAGTGACAAAATAGATGGGA
ACTGGGTGTAGCGTCGTAAGCTAATACGAAAATTAAAAATGACAAAATAGTTTGGAACTAGATTTCAC
TTATCTGGTTCGGATCTCCTAGGCGATATCAGTGATCAGATCCAGACATGATAAGATACATTGATGAG
TTTGGACAAACCACAACTAGAATGCAGTGAAAAAAATGCTTTATTTGTGAAATTTGTGATGCTATTGCT
TTATTTGTAACCATTATAAGCTGCAATAAACAAGTTAACAACAACAATTGCATTCATTTTATGTTTCAGG
TTCAGGGGGAGGTGTGGGAGGTTTTTTAAAGCAAGTAAAACCTCTACAAATGTGGTATGGCTGATTAT
GATCCTCTAGTACTTCTCGACAAGCTTACATTATTGAAGCATTTATCAGGGTTATTGTCTCAGACCTGC
AGGCAGCTGCGCGCTCGCTCGCTCACTGAGGCCGCCCGGGCAAAGCCCGGGCGTCGGGCGACCTTT
GGTCGCCCGGCCTCAGTGAGCGAGCGAGCGCGCAGAGAGGGAGTGGCCAACTCCATCACTAGGGGT
TCCTTGTAGTTAATGATTAACCCGCCATGCTACTTATCTACGTAGCCATGCTCTAGCGTTTAGTGAACC
GTACTAGAGGTACCGTTTAAACTCGAG**GTCGAC**ATTACAGGTGCCTAACACCATACCACACTGGCTGA
TTTTTTGTATTTTTAGTAAAGACGGGGTTTCCCCATCTTGGCCAGGCTGGTCTTGAACTCCTGACCTCG
TAATCCACCCTCCTCAGTCTCCCAAAGTGCTGAGATTACAGGTGTGAGCCACGGTGCCCGGCCATGT
CTGTATTTTCTATTTCCTTGGTGTGAGGCAATGAACCTCGGGTATTACCCCAGATGGATGACACTGCTT
CAATATCTGCCAGTCACTACACTTTGTTATCAGTGGGATTACATCAACTGGAGCCCATTCTATCTGCTT
GGAGGCCAGGCCTGAAGATTCAAGGGGTTGACACCCTCTAGGAGCAAGCCTCAAGTCAACCCATGA
CTGACAGTAGGTGGGATATAAATACCTCAGCTCCCTCACCCCTCGGTTGGAATAACTGAAGAGTATGT
TCCATGCCGCTCCCCAGTCATCCCTGGGGAGGTTAAGTTCCACTTTCTCACCATGTAACTTATTTGAAG
ACACACCCAGTATTGGCTCTTTGCCTTTCCTGATTCACTTTCTCCTCCCCCAGCTGGTGCTTTCTGGGG
CCACCTTCTTGATAAACTACTTTTGCTAGAATCCTTGTCTGAGGGTCTGCCCTTGTGAGACCCTAAGAT
GTTACCAGAGAGAGTTAGGAAGCTGGGAATGGGGTGGAAGTGTTGCTGTATAATCGTCAGACAGAGT
TGAGATCTGAAGGAAAATAAGATGGTTAAAGCTCTTGACTCTGGAATCAGAGGGTCCTGGGTTCAAAT
CTCAAGTCTGAGAGATCTTGGACAAGTTATAACTCCTCTGCAAGTCTCAGTTTCCATTTTGTTGGTGAA
TAGAGGGAGGGAGGGGAATTCCTACTTTACAAGGTTAACATGATAATGAAATTACACTTTGTTGCCAA
TGTGCCTAGCACACTGCCTGGTACATGATGGTTGTGATGGCTGTCTTTATACGGGAGACTGGGAAGAG
ACCCTAAAGGCTGAGATTTGCTTCACTGGAGGCAGGAAGCGGAAGCTCCTTTATTGGGTGCAATGAA
AGAAGGTGTTGAGAGATGGGAGATAGATGTTGATGGGAAAGAAAAAGGGAGAGACCATGGGAAGGA
GAGAGAGAGAGAATGATATACATTAGGCAGATTAACTTCTCTTTATTGTGAAGAAAGGGGGAAATTAG
GATTTTCTAGGCTGTCTTTTAGTTGCAGCAAGTCAGCAAAAAGGGCTATGATGACCAGGCAGCATTGA
GCAACTCTGACTCCGCCTTCCCCTCTTCGCACACCTTCTGGTTACTGAAAACCCAGCGTTAGTAGAAA
AGTTTCTTTTCTTTGAATGACAGAACTACAGCATA**GCTAGC**GTCGACACGCGTCGGCCGAC**ACTAGT**
ATGCCCCTCCACCAGATTTCTGTAATCCCAGCCCGGGAGACAGCCAGCAATGGGAGAAGTTCAATGG
GCAGAAACAAAGAGAAGAACAAGGAAGTTGAGAATGAAAAGTCCCCAGGGCGATCTGCAAGTCGAT

CAAGTAACATATCAAAAGCAAGCAGCCCAACGACAGGGACAGCTCCCAGGAGCCAGTCAAGGTTGT
CTGTCTGTCCATCTACTCAGGACATCTGCAGGATCTGTCACTGCGAAGGAGATGAAGAGAGCCCACT
CATCACACCCTGTCGCTGCACAGGAACCTTGCGCTTTGTCCACCAGTCCTGCCTCCACCAATGGATCA
AGAGCTCAGACACACGATGCTGTGAGCTCTGCAAGTATGACTTCATAATGGAGACCAAGCTCAAGCC
CCTTCGGAAGTGGGAAAAGCTCCAGATGACCACGAGCGAAAGGAGGAAAATATTCTGCTCTGTCACG
TTCCACGTCATCGCCGTCACCTGTGTGGTGTGGTCCTTGTATGTGTTGATAGATCGGACAGCGGAGGA
AATCAAGCAAGGTAACGACAATGGTGTGCTGGAATGGCCATTTTGGACAAAACTGGTTGTGGTGGCT
ATTGGCTTCACGGGAGGTCTCGTCTTCATGTATGTACAGTGTAAAGTCTACGTCCAACTGTGGCGCCG
GCTGAAGGCCTACAACCGTGTGATCTTTGTGCAGAATTGCCCAGACACTGCCAACAAACTGGAGAAG
AACTTCCCGTGTAATGTGAACACGGAAATCAAGGATGCTGTGGTTGTGCCTGTGCCACAGACAGGTTC
AAATACACTGCCAACTGCAGAGGGAGCCCCACCTGAGGTTATACCAGTC**ATCGAT**CGGTTTAATTAA
GCTAGCGAATTCCCCGGGAAGCTTACTAGTATCGATACGCGTCGAGCATGCATCTAGGGCGGCCAAT
TCCGCCCCTCTCCCCCCCCCCCCTCTCCCTCCCCCCCCCCTAACGTTACTGGCCGAAGCCGCTTGGAA
TAAGGCCGGTGTGCGTTTGTCTATATGTTATTTTCCACCATATTGCCGTCTTTTGGCAATGTGAGGGCC
CGGAAACCTGGCCCTGTCTTCTTGACGAGCATTCCTAGGGGTCTTTCCCCTCTCGCCAAAGGAATGCA
AGGTCTGTTGAATGTCGTGAAGGAAGCAGTTCCTCTGGAAGCTTCTTGAAGACAAACAACGTCTGTAG
CGACCCTTTGCAGGCAGCGGAACCCCCCACCTGGCGACAGGTGCCTCTGCGGCCAAAAGCCACGTG
TATAAGATACACCTGCAAAGGCGGCACAACCCCAGTGCCACGTTGTGAGTTGGATAGTTGTGGAAAG
AGTCAAATGGCTCTCCTCAAGCGTATTCAACAAGGGGCTGAAGGATGCCCAGAAGGTACCCCATTGT
ATGGGATCTGATCTGGGGCCTCGGTGCACATGCTTTACATGTGTTTAGTCGAGGTTAAAAAAACGTCT
AGGCCCCCCGAACCACGGGGACGTGGTTTTCCTTTGAAAAACACGATGATAAGCTTGCCACAACCCG
GGATCCAAGCCACCATGGTGAGCAAGGGCGAGGAGCTGTTCACCGGGGTGGTGCCCATCCTGGTCG
AGCTGGACGGCGACGTAAACGGCCACAAGTTCAGCGTGTCCGGCGAGGGCGAGGGCGATGCCACCT
ACGGCAAGCTGACCCTGAAGTTCATCTGCACCACCGGCAAGCTGCCCGTGCCCTGGCCCACCCTCGT
GACCACCCTGACCTACGGCGTGCAGTGCTTCAGCCGCTACCCCGACCACATGAAGCAGCACGACTTC
TTCAAGTCCGCCATGCCCGAAGGCTACGTCCAGGAGCGCACCATCTTCTTCAAGGACGACGGCAACT
ACAAGACCCGCGCCGAGGTGAAGTTCGAGGGCGACACCCTGGTGAACCGCATCGAGCTGAAGGGCA
TCGACTTCAAGGAGGACGGCAACATCCTGGGGCACAAGCTGGAGTACAACTACAACAGCCACAACG
TCTATATCATGGCCGACAAGCAGAAGAACGGCATCAAGGTGAACTTCAAGATCCGCCACAACATCGA
GGACGGCAGCGTGCAGCTCGCCGACCACTACCAGCAGAACACCCCCATCGGCGACGGCCCCGTGCT
GCTGCCCGACAACCACTACCTGAGCACCCAGTCCGCCCTGAGCAAAGACCCCAACGAGAAGCGCGA
TCACATGGTCCTGCTGGAGTTCGTGACCGCCGCCGGGATCACTCTCGGCATGGACGAGCTGTACAAG
TAAGCGGCCGCACTAGACCTCGACTGTGCCTTCTAGTTGCCAGCCATCTGTTGTTTGCCCCTCCCCCG
TGCCTTCCTTGACCCTGGAAGGTGCCACTCCCACTGTCCTTTCCTAATAAAATGAGGAAATTGCATCG
CATTGTCTGAGTAGGTGTCATTCTATTCTGGGGGGTGGGGTGGGGCAGGACAGCAAGGGGGAGGATT
GGGAAGACAATAGCAGGCATGCTGGGGAACTAGAGCATGGCTACGTAGATAAGTAGCATGGCGGGT
TAATCATTAACTACAAGGAACCCCTAGTGATGGAGTTGGCCACTCCCTCTCTGCGCGCTCGCTCGCTC
ACTGAGGCCGGGCGACCAAAGGTCGCCCGACGCCCGGGCGGCCTCAGTGAGCGAGCGAGCGCGCA
GCTGCCTGCAGGCATGCAAGCTGTAGCCAACCACTAGAACTATAGCTAGAGTCCTGGGCGAACAAAC
GATGCTCGCCTTCCAGAAAACCGAGGATGCGAACCACTTCATCCGGGGTCAGCACCACCGGCAAGC

GCCGCGACGGCCGAGGTCTTCCGATCTCCTGAAGCCAGGGCAGATCCGTGCACAGCACCTTGCCGTA
GAAGAACAGCAAGGCCGCCAATGCCTGACGATGCGTGGAGACCGAAACCTTGCGCTCGTTCGCCAG
CCAGGACAGAAATGCCTCGACTTCGCTGCTGCCCAAGGTTGCCGGGTGACGCACACCGTGGAAACG
GATGAAGGCACGAACCCAGTTGACATAAGCCTGTTCGGTTCGTAAACTGTAATGCAAGTAGCGTATG
CGCTCACGCAACTGGTCCAGAACCTTGACCGAACGCAGCGGTGGTAACGGCGCAGTGGCGGTTTTCA
TGGCTTGTTATGACTGTTTTTTTGTACAGTCTATGCCTCGGGCATCCAAGCAGCAAGCGCGTTACGCC
GTGGGTCGATGTTTGATGTTATGGAGCAGCAACGATGTTACGCAGCAGCAACGATGTTACGCAGCAG
GGCAGTCGCCCTAAAACAAAGTTAGGTGGCTCAAGTATGGGCATCATTCGCACATGTAGGCTCGGCC
CTGACCAAGTCAAATCCATGCGGGCTGCTCTTGATCTTTTCGGTCGTGAGTTCGGAGACGTAGCCACC
TACTCCCAACATCAGCCGGACTCCGATTACCTCGGGAACTTGCTCCGTAGTAAGACATTCATCGCGCT
TGCTGCCTTCGACCAAGAAGCGGTTGTTGGCGCTCTCGCGGCTTACGTTCTGCCCAAGTTTGAGCAGC
CGCGTAGTGAGATCTATATCTATGATCTCGCAGTCTCCGGCGAGCACCGGAGGCAGGGCATTGCCAC
CGCGCTCATCAATCTCCTCAAGCATGAGGCCAACGCGCTTGGTGCTTATGTGATCTACGTGCAAGCAG
ATTACGGTGACGATCCCGCAGTGGCTCTCTATACAAAGTTGGGCATACGGGAAGAAGTGATGCACTTT
GATATCGACCCAAGTACCGCCACCTAACAATTCGTTCAAGCCGAGATCGGCTTCCCGGCCGCGGAGT
TGTTCGGTAAATTGTCACAACGCCGCGAATATAGTCTTTACCATGCCCTTGGCCACGCCCCTCTTTAAT
ACGACGGGCAATTTGCACTTCAGAAAATGAAGAGTTTGCTTTAGCCATAACAAAAGTCCAGTATGCTT
TTTCACAGCATAACTGGACTGATTTCAGTTTACAACTATTCTGTCTAGTTTAAGACTTTATTGTCATAGT
TTAGATCTATTTTGTTCAGTTTAAGACTTTATTGTCCGCCCACACCCGCTTACGCAGGGCATCCATTTAT
TACTCAACCGTAACCGATTTTGCCAGGTTACGCGGCTGGTCTATGCGGTGTGAAATACCGCACAGATG
CGTAAGGAGAAAATACCGCATCAGGCGCTCTTCCGCTTCCTCGCTCACTGACTCGCTGCGCTCGGTC
GTTCGGCTGCGGCGAGCGGTATCAGCTCACTCAAAGGCGGTAATACGGTTATCCACAGAATCAGGGG
ATAACGCAGGAAAGAACATGTGAGCAAAAGGCCAGCAAAAGGCCAGGAACCGTAAAAAGGCCGCGT
TGCTGGCGTTTTTCCATAGGCTCCGCCCCCCTGACGAGCATCACAAAAATCGACGCTCAAGTCAGAG
GTGGCGAAACCCGACAGGACTATAAAGATACCAGGCGTTTCCCCCTGGAAGCTCCCTCGTGCGCTCT
CCTGTTCCGACCCTGCCGCTTACCGGATACCTGTCCGCCTTTCTCCCTTCGGGAAGCGTGGCGCTTTC
TCATAGCTCACGCTGTAGGTATCTCAGTTCGGTGTAGGTCGTTCGCTCCAAGCTGGGCTGTGTGCACG
AACCCCCCGTTCAGCCCGACCGCTGCGCCTTATCCGGTAACTATCGTCTTGAGTCCAACCCGGTAAG
ACACGACTTATCGCCACTGGCAGCAGCCACTGGTAACAGGATTAGCAGAGCGAGGTATGTAGGCGGT
GCTACAGAGTTCTTGAAGTGGTGGCCTAACTACGGCTACACTAGAAGAACAGTATTTGGTATCTGCGC
TCTGCTGAAGCCAGTTACCTTCGGAAAAAGAGTTGGTAGCTCTTGATCCGGCAAACAAACCACCGCT
GGTAGCGGTGGTTTTTTTGTTTGCAAGCAGCAGATTACGCGCAGAAAAAAAGGATCTCAAGAAGATCC
TTTGATCTTTTCTACGGGGTCTGACGCTCAGTGGAACGAAAACTCACGTTAAGGGATtTTGGTCATGAG
ATTATCAAAAAGGATCTTCACCTAGATCCTTTTAAATTAAAAATGAAGTTTTAAATCAATCTAAAGTATA
TATGAGTAAACTTGGTCTGACAGTTACCAATGCTTAATCAGTGAGGCACCTATCTCAGCGATCTGTCTA
TTTCGTTCATCCATAGTTGCCTGACTCCCCGTCGTGTAGATAACTACGATACGGGAGGGCTTACCATC
TGGCCCCAGTGCTGCAATGATACCGCGAGACCCACGCTCACCGGCTCCAGATTTATCAGCAATAAAC
CAGCCAGCCGGAAGGGCCGAGCGCAGAAGTGGTCCTGCAACTTTATCCGCCTCCATCCAGTCTATTA
ATTGTTGCCGGGAAGCTAGAGTAAGTAGTTCGCCAGTTAATAGTTTGCGCAACGTTGTTGCCATTGCT
ACAGGCATCGTGGTGTCACGCTCGTCGTTTGGTATGGCTTCATTCAGCTCCGGTTCCCAACGATCAAG

GCGAGTTACATGATCCCCCATGTTGTGCAAAAAAGCGGTTAGCTCCTTCGGTCCTCCGATCGTTGTCA
GAAGTAAGTTGGCCGCAGTGTTATCACTCATGGTTATGGCAGCACTGCATAATTCTCTTACTGTCATGC
CATCCGTAAGATGCTTTTCTGTGACTGGTGAGTACTCAACCAAGTCATTCTGAGAATAGTGTATGCGG
CGACCGAGTTGCTCTTGCCCGGCGTCAATACGGGATAATACCGCGCCACATAGCAGAACTTTAAAAG
TGCTCATCATTGGAAAACGTTCTTCGGGGCGAAAACTCTCAAGGATCTTACCGCTGTTGAGATCCAGT
TCGATGTAACCCACTCGTGCACCCAACTGATCTTCAGCATCTTTTACTTTCACCAGCGTTTCTGGGTGA
GCAAAAACAGGAAGGCAAAATGCCGCAAAAAAGGGAATAAGGGCGACACGGAAATGTTGAATACTC
ATACTCTTCCTTTTTCAATATTATTGAAGCATTTATCAGGGTTATTGTCTCATGAGCGGATACATATTTG
AATGTATTTAGAAAAATAAACAAATAGGGGTTCCGCGCACATTTCCCCGAAAAGTGCCACCTAAATTG
TAAGCGTTAATATTTTGTTAAAATTCGCGTTAAATTTTTGTTAAATCAGCTCATTTTTTAACCAATAGGC
CGAAATCGGCAAAATCCCTTATAAATCAAAAGAATAGACCGAGATAGGGTTGAGTGTTGTTCCAGTTT
GGAACAAGAGTCCACTATTAAGAACGTGGACTCCAACGTCAAAGGGCGAAAAACCGTCTATCAGGGC
GATGGCCCACTACGTGAACCATCACCCTAATCAAGTTTTTTGGGGTCGAGGTGCCGTAAAGCACTAAA
TCGGAACCCTAAAGGGAGCCCCCGATTTAGAGCTTGACGGGGAAAGCCGGCGAACGTGGCGAGAAA
GGAAGGGAAGAAAGCGAAAGGAGCGGGCGCTAGGGCGCTGGCAAGTGTAGCGGTCACGCTGCGCG
TAACCACCACACCCGCCGCGCTTAATGCGCCGCTACAGGGCGCGTC

N.B: The coloured sequences correspond to F4/80 promoter (red) and MARCH-I cDNA sequence (orange). Restriction enzymes are highlighted in dark green.

B. EMR1 and F4/80 promoters sequences comparison

```
CLUSTAL O(1.2.1) multiple sequence alignment (F4/80 mouse Vs EMR1 human)



EMR1        attacaggtgcctaacaccataccacactggctgatttttgtatttttagtaaagacgg
F4/80       ------------------------------------------------------------



EMR1        ggtttccccatcttggccaggctggtcttgaactcctgacctcgtaatccaccctcctca
F4/80       --------tttctcagcccgtttatcctttgagtagagg----------------------
                       ***  *** *  *   ***  * *   *


EMR1        gtctcccaaagtgctgagattacaggtgtgagccacggtgcccggccatgtctgtatttt
F4/80       ------aaaactactga--------------------------------tt-----tgttt
                   *** * ****                                 *        ***


EMR1        ctatttccttggtgtgaggcaatgaacctcgggtattaccccagatgg---atgacactg
F4/80       gaattaattttatatctagccactaagctgaagttgtttatcagctgtaggagttctctg
              ***   **  * *   ** *  ** **   **  *    *** **    *   * ***


EMR1        cttcaatatctgccagtcactacactttgttatcagtgggattacatcaactggagccca
F4/80       gtggattattttt-------tagggttatttatgtattctaccacatcatctgcaaatag
              *  * *** *         **   **  ****   *   *  ****** *** *


EMR1        ttctatctgcttggaggccaggcctgaagatt-caaggggttgacaccctctaggagcaa
F4/80       tgatatctt---gacttcctcctttctaatttgtatccctttgacctcctttgttgcct
             *  *****    *    **     *  *  **  *     *****  *** * *  **
```

```
EMR1        gcctcaag----tcaacccatgactgac--agtaggtgggatataaatacctcagctccc
F4/80       aattgttctgggtagaactttgagtactatattaaatgataggggaaaag-tggacagcc
               *        *  * *  *** *     * **  **  *    ** *  *   *  **


EMR1        tcacccctc---ggttggaataactgaagagtatgttccatgccgctcc----ccagtca
F4/80       ttgggtgtggtgtgtgtggtatggtgtggtgtgtgtatggtgatgatgcatgtggtgtgt
             *      *     **  *      **  * ** ***    **  * * *       **


EMR1        tccctggggaggttaagttccactttctcaccatgtaacttatttgaagacacacccagt
F4/80       atggtgtggtgtatgtggtgtggtgtgtggtggtggtgata--------atgatgatggt
                ** ** *  *  * *    * * *     **    *         *        **


EMR1        attggctctttgccttt---cctgattcactttctcctccccagctggtgctttctggg
F4/80       ggtctctctgtctctgtctgtctctttctatctctgcctctctctctctgtctctctctg
              *  **** *  ** *    **  ***  * *** *  * *   **    ** ***  *


EMR1        gccaccttcttgataaactacttttgctagaatccttgtctgagggtctgcccttgtgag
F4/80       ccccccctctg--------------------------tctccctctgtctgtctgt--ctg
             ** ***                              * **     ***** *  *    *


EMR1        accctaagatgttaccagagagagttaggaagctgggaatggggtggaagtgttgctgta
F4/80       tctctttggtgtgatgta-------------------tgt--------------ggtgtg
              * **  * *** *                          *             * ***


EMR1        taatcgtcagacagagttgagatctgaaggaaaataagatggt------taaagctcttg
F4/80       tgtgtattctacaaggttgacatgatgacagaatttaattttcttagcagcaagctcatg
            *     *   ***  ***** **    *   ** * *  *           ****** **


EMR1        a-ctctggaatcagagggtcctgggttcaaatctcaagtctgagagatcttggacaagtt
```

```
F4/80      gatcctggtgataaatgcagcatgactttactgaaaaggctttgtgatcttgaagagtgg
                ****    * * *   *  *  *  * *   *** **  * ******* * *


EMR1       a-taactcctctgcaagtctcagtt-----tccattttgttggtgaa-tagagggaggga
F4/80      attgacttcactgtgggcagcacatgcaatctcacttgtttggtgtaatgaaagaagaga
           * * *** * ***   *   **  *       ** **  ****** * *  * * ** **


EMR1       ggggaattcctactttacaaggttaacatgataatgaaattacactttgttgccaatgtg
F4/80      atgagaggt------ggaaggggggatggtaatgttgaaaaaaagaatgg-tacag-----
              *  *            * **  *   * **  *****  *    * * * *


EMR1       cctagcacactgcctggtacatgatggttgtgatggctgtctttatac-gggagactggg
F4/80      ---aggaaactga--ggttggagagagatggggtagatggtaagagatggagaaagaggg
              ** * ****   ***    **  * ** * * * **     * *  * ** *  ***


EMR1       aagagaccctaaaggctgagatttgcttcactggaggcaggaagcggaagctcctttatt
F4/80      aaggaaatggagagaaagacagagagacagagagagacacacagaga---gacacacaga
            ***  *    * **   ** *           *** **   ** *      *    *


EMR1       ggtgcaatgaaagaaggtgttgagagatgggagatagatgttgatgggaaagaaaaagg
F4/80      gacagagaggaagggaaagggaaagagaa---aggaagaggaagaggggagggggaaggg
           *   *  * *** * *   *   *****    **  *** *  ** *** * *  ** **


EMR1       gagagaccatgggaaggagagagagagaatgatatacattaggcagattaacttctct
F4/80      -gaaggggaagggga--agggagagggagaaatgtggacactagccagatt---------
               **   * *** *  ** ***** *****   *  *** *** ******


EMR1       ttattgtgaagaaaggggggaaattagga-ttttctaggctgtc---ttttagttgcagca
F4/80      -----------taagggagaaattagggggttgccagtctgtccacctctgatggtggca
```

```
                      ***** *********   ** * ** *****    * *  * *  ***


EMR1        agtcagcaaaaagggcta--tgatgaccaggcagcattgagcaactctgactccgccttc

F4/80       actcagcagaaagctgctgggctcagtctggctttgttgagcaaccctgactccacc---

             * ****** ****              * ***    ********* ******** **


EMR1        ccctcttcgcacaccttctggttactgaaaacccagcgttagtagaaaagtttcttttct

F4/80       -------------ccttttcttccccacaaagcaagcttttaaagggaaggctttcttca

                        **** *  *  *   *** * *** **   **  ***  * * ***


EMR1        ttgaatgacagaactacagcata

F4/80       ttgaatgactgccacagtacga-

            ********* *    *   *
```

Appendix 3: Transfection optimization in RAW 264.7 and HEK 293 cells

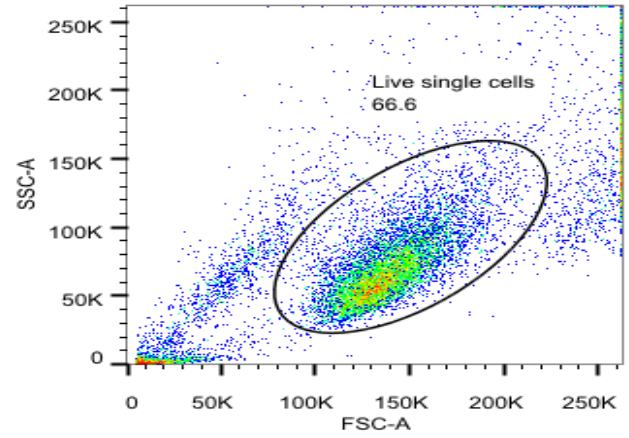

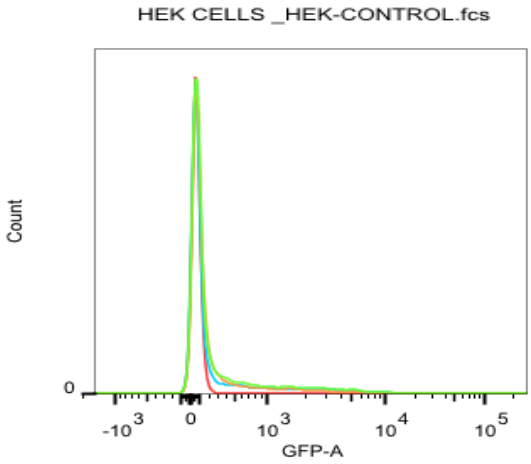

	Sample Name	Name	Geometric Mean : GFP-A
	HEK CELLS _HEK-CAG-075.fcs	Live single cells	331
	HEK CELLS _HEK-CAG-025.fcs	Live single cells	247
	HEK CELLS _HEK-CAG-1.fcs	Live single cells	304
	HEK CELLS _HEK-CONTROL.fcs	Live single cells	63.3

Figure 3A. Transfection optimization in HEK 293 cells. Twenty-four hours prior to transfection, HEK 293 cells were plated out in a 24-well plate at 0.4 x 10^6 cells/well in complete DMEM. At 70% confluency, cells were transfected with serial amount of AAV-CAG-eGFP plasmid: 0.25 µg, 0.75 µg, 1 µg, or left un-transfected. Transfected cells were incubated for 16-24 h at 37°C in 5% CO_2, and eGFP fluorescence in transfected cells was evaluated under fluorescence microscopy and quantified by flow cytometry. Live cells were gated based on forward scatter (FSC-A) and side scatter (SSC-A) of untransfected RAW cells to exclude cell debris and doublets. GFP expression intensity in HEK 923 cells is shown as the geometric mean fluorescence.

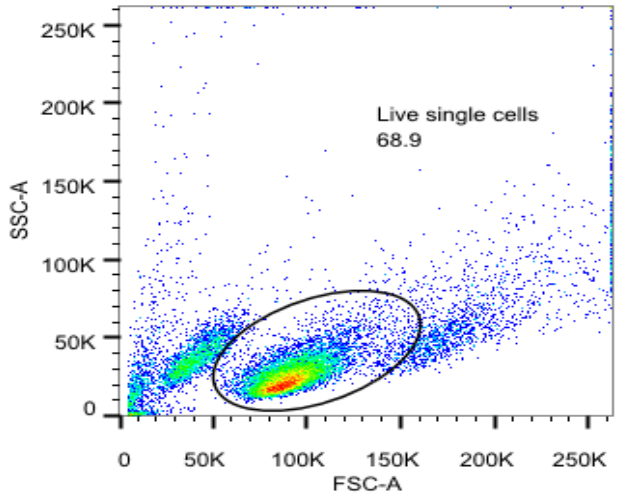

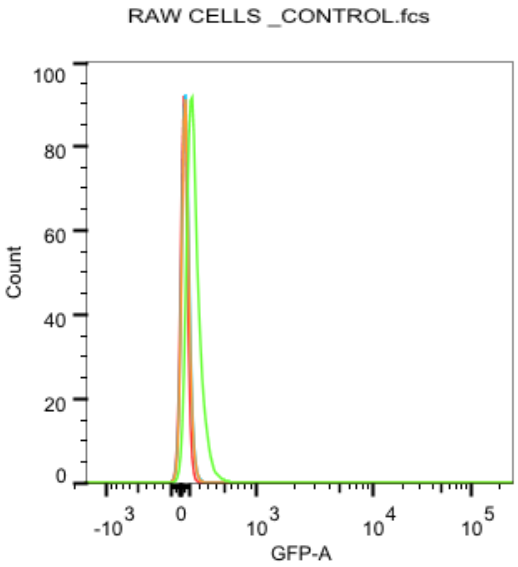

	Sample Name	Name	Geometric Mean : GFP-A
	RAW CELLS-cag_1ug.fcs	Live single cells	154
	RAW CELLS _cag-075.fcs	Live single cells	53.6
	RAW CELLS_cag-025.fcs	Live single cells	52.1
	RAW CELLS _CONTROL.fcs	Live single cells	35.0

Figure 3B. Transfection optimization in RAW 264.7 cells. RAW 264.7 cells were cultured overnight in 24-well plate in comple DMEM with 10% FCS using the same protocol described in figure 3A. cells were transfected at 70% confluency with serial amount of AAV-CAG-eGFP vector plasmid: 0.25 µg, 0.75 µg, 1 µg, or left un-transfected. At 24 h post-transfection, eGFP fluorescence was examined in each well and a FACS analysis was carried out to compare fluorescence intencity in each sample which is shown as the geometric mean fluorescence.

Appendix 4: Recipies

TAE buffer (x50)

For 1 L of 50 x TAE:

242 g Tris-HCl (pH 8.0)

750 mL ddH_2O

57.1 Ml glacial acetic acid

100 mL (0.5 M) EDTA (pH 8.0)

Adjust the solution to final volume of 1L.

0.9 % Agarose gel (200 mL)

1.8 g agarose powder

200 mL 1 x TAE buffer

FACS buffer (For flow cytometry)

0.1% sodium azide

97.9% PBS

2% FCS

Phosphate buffered saline (PBS) (10x)

For 2 L of 10 X PBS:

170 g NaCl (Merck Ltd, Palmerston North, New Zealand)

62.32 g Na2HPO4.12H2O (Merck)

4.04 g NaH2pPO4.2H2O (Merck)

2 L ddH2O

LB liquid media

For 1 L of LB solution:

10 g Tryptone

5 g yeast extra

10 g NaCl

1 L ddH_2O

Agar medium

For 1 L of agar medium:

10 g Tryptone

5 g yeast extra

10 g NaCl

15 g Agar

1 L ddH_2O

REFERENCES

Al-Dosari, Mohammed S., and Xiang Gao. 2009. “Nonviral Gene Delivery: Principle, Limitations, and Recent Progress.” The AAPS Journal 11 (4): 671–81. doi:10.1208/s12248-009-9143-y.

Allen, J. M., D. J. Debelak, T. C. Reynolds, and A. D. Miller. 1997. “Identification and Elimination of Replication-Competent Adeno-Associated Virus (AAV) That Can Arise by Nonhomologous Recombination during AAV Vector Production.” Journal of Virology 71 (9): 6816–22.

Aloisi, F. 2001. “Immune Function of Microglia.” Glia 36 (2): 165–79.

Aravindan, Latha, Katrina A Bicknell, Gavin Brooks, Vitaliy V Khutoryanskiy, and Adrian C Williams. 2009. “Effect of Acyl Chain Length on Transfection Efficiency and Toxicity of Polyethylenimine.” International Journal of Pharmaceutics 378 (1-2): 201–10. doi:10.1016/j.ijpharm.2009.05.052.

Asokan, Aravind, David V Schaffer, and R Jude Samulski. 2012. “The AAV Vector Toolkit: Poised at the Clinical Crossroads.” Molecular Therapy: The Journal of the American Society of Gene Therapy 20 (4): 699–708. doi:10.1038/mt.2011.287.

Atchison, R W, B C Casto, and W M Hammon. 1965. “Adenovirus-Associated Defective Virus Particles.” Science (New York, N.Y.) 149 (3685): 754–56.

Auricchio, A, M Hildinger, E O’Connor, G P Gao, and J M Wilson. 2001. “Isolation of Highly Infectious and Pure Adeno-Associated Virus Type 2 Vectors with a Single-Step Gravity-Flow Column.” Human Gene Therapy 12 (1): 71–76. doi:10.1089/104303401450988.

Austyn, J M, and S Gordon. 1981. “F4/80, a Monoclonal Antibody Directed Specifically against the Mouse Macrophage.” European Journal of Immunology 11 (10): 805–15. doi:10.1002/eji.1830111013.

Balakrishnan, Balaji, Dwaipayan Sen, Sangeetha Hareendran, Vaani Roshini, Sachin David, Alok Srivastava, and Giridhara R Jayandharan. 2013. “Activation of the Cellular Unfolded Protein Response by Recombinant Adeno-Associated Virus Vectors.” PloS One 8 (1): e53845. doi:10.1371/journal.pone.0053845.

Bartee, Eric, Mandana Mansouri, Bianca T Hovey Nerenberg, Kristine Gouveia, and Klaus Früh. 2004. “Downregulation of Major Histocompatibility Complex Class I by Human Ubiquitin Ligases Related to Viral Immune Evasion Proteins.” Journal of Virology 78 (3): 1109–20.

Bartlett, Jeffrey S., Rose Wilcher, and R. Jude Samulski. 2000. “Infectious Entry Pathway of Adeno-Associated Virus and Adeno-Associated Virus Vectors.” Journal of Virology 74 (6): 2777–85. doi:10.1128/JVI.74.6.2777-2785.2000.

Becher, B, B G Durell, A V Miga, W F Hickey, and R J Noelle. 2001. “The Clinical Course of Experimental Autoimmune Encephalomyelitis and Inflammation Is Controlled by the Expression of CD40 within the Central Nervous System.” The Journal of Experimental Medicine 193 (8): 967–74.

Becher, Burkhard, Brigit G Durell, and Randolph J Noelle. 2003. “IL-23 Produced by CNS-Resident Cells Controls T Cell Encephalitogenicity during the Effector Phase of Experimental Autoimmune Encephalomyelitis.” The Journal of Clinical Investigation 112 (8): 1186–91. doi:10.1172/JCI19079.

Bilyk, N, J S Mackenzie, J M Papadimitriou, and P G Holt. 1988. “Functional Studies on Macrophage Populations in the Airways and the Lung Wall of SPF Mice in the Steady-State and during Respiratory Virus Infection.” Immunology 65 (3): 417–25.

Bishop, Kathie M, Eva K Hofer, Arpesh Mehta, Anthony Ramirez, Liangwu Sun, Mark Tuszynski, and Raymond T Bartus. 2008. “Therapeutic Potential of CERE-110 (AAV2-NGF): Targeted, Stable, and Sustained NGF Delivery and Trophic Activity on Rodent Basal Forebrain Cholinergic Neurons.” Experimental Neurology 211 (2): 574–84. doi:10.1016/j.expneurol.2008.03.004.

Blouin, Véronique, Nicole Brument, Estelle Toublanc, Isabelle Raimbaud, Philippe Moullier, and Anna Salvetti. 2004. “Improving rAAV Production and Purification: Towards the Definition of a Scaleable Process.” The Journal of Gene Medicine 6 Suppl 1 (February): S223–228. doi:10.1002/jgm.505.

Boehm, U, T Klamp, M Groot, and J C Howard. 1997. “Cellular Responses to Interferon-Gamma.” Annual Review of Immunology 15: 749–95. doi:10.1146/annurev.immunol.15.1.749.

Brück, Wolfgang. 2005. “The Pathology of Multiple Sclerosis Is the Result of Focal Inflammatory Demyelination with Axonal Damage.” Journal of Neurology 252 Suppl 5 (November): v3–9. doi:10.1007/s00415-005-5002-7.

Cesta, Mark F. 2006. “Normal Structure, Function, and Histology of the Spleen.” Toxicologic Pathology 34 (5): 455–65. doi:10.1080/01926230600867743.

Chadeuf, Gilliane, Carine Ciron, Philippe Moullier, and Anna Salvetti. 2005. “Evidence for Encapsidation of Prokaryotic Sequences during Recombinant Adeno-Associated Virus Production and Their in Vivo Persistence after Vector Delivery.” Molecular Therapy: The Journal of the American Society of Gene Therapy 12 (4): 744–53. doi:10.1016/j.ymthe.2005.06.003.

Chao, H, Y Liu, J Rabinowitz, C Li, R J Samulski, and C E Walsh. 2000. “Several Log Increase in Therapeutic Transgene Delivery by Distinct Adeno-Associated Viral Serotype Vectors.” Molecular Therapy: The Journal of the American Society of Gene Therapy 2 (6): 619–23. doi:10.1006/mthe.2000.0219.

Chen, H, D M McCarty, A T Bruce, K Suzuki, and K Suzuki. 1998. “Gene Transfer and Expression in Oligodendrocytes under the Control of Myelin Basic Protein Transcriptional Control Region Mediated by Adeno-Associated Virus.” Gene Therapy 5 (1): 50–58. doi:10.1038/sj.gt.3300547.

Choi, Vivian W, Douglas M McCarty, and R Jude Samulski. 2005. “AAV Hybrid Serotypes: Improved Vectors for Gene Delivery.” Current Gene Therapy 5 (3): 299–310.

Costa-Pereira, Ana P, Timothy M Williams, Birgit Strobl, Diane Watling, James Briscoe, and Ian M Kerr. 2002. “The Antiviral Response to Gamma Interferon.” Journal of Virology 76 (18): 9060–68.

Cua, Daniel J, Jonathan Sherlock, Yi Chen, Craig A Murphy, Barbara Joyce, Brian Seymour, Linda Lucian, et al. 2003. “Interleukin-23 rather than Interleukin-12 Is the Critical Cytokine for Autoimmune Inflammation of the Brain.” Nature 421 (6924): 744–48. doi:10.1038/nature01355.

Cucchiarini, M, X L Ren, G Perides, and E F Terwilliger. 2003. “Selective Gene Expression in Brain Microglia Mediated via Adeno-Associated Virus Type 2 and Type 5 Vectors.” Gene Therapy 10 (8): 657–67. doi:10.1038/sj.gt.3301925.

Davidson, B L, C S Stein, J A Heth, I Martins, R M Kotin, T A Derksen, J Zabner, A Ghodsi, and J A Chiorini. 2000. “Recombinant Adeno-Associated Virus Type 2, 4, and 5 Vectors: Transduction of Variant Cell Types and Regions in the Mammalian Central Nervous System.” Proceedings of the National Academy of Sciences of the United States of America 97 (7): 3428–32. doi:10.1073/pnas.050581197.

Daya, Shyam, and Kenneth I Berns. 2008. “Gene Therapy Using Adeno-Associated Virus Vectors.” Clinical Microbiology Reviews 21 (4): 583–93. doi:10.1128/CMR.00008-08.

De Felici, M, J Heasman, C C Wylie, and A McLaren. 1986. “Macrophages in the Urogenital Ridge of the Mid-Gestation Mouse Fetus.” Cell Differentiation 18 (2): 119–29.

De Gassart, Aude, Voahirana Camosseto, Jacques Thibodeau, Maurizio Ceppi, Nadia Catalan, Philippe Pierre, and Evelina Gatti. 2008. “MHC Class II Stabilization at the Surface of Human Dendritic Cells Is the Result of Maturation-Dependent MARCH I down-Regulation.” Proceedings of the National Academy of Sciences of the United States of America 105 (9): 3491–96. doi:10.1073/pnas.0708874105.

Di Pasquale, Giovanni, Beverly L Davidson, Colleen S Stein, Inês Martins, Dominic Scudiero, Anne Monks, and John A Chiorini. 2003. “Identification of PDGFR as a Receptor for AAV-5 Transduction.” Nature Medicine 9 (10): 1306–12. doi:10.1038/nm929.

Diemel, L T, C A Copelman, and M L Cuzner. 1998. “Macrophages in CNS Remyelination: Friend or Foe?” Neurochemical Research 23 (3): 341–47.

During, M J, R J Samulski, J D Elsworth, M G Kaplitt, P Leone, X Xiao, J Li, et al. 1998. “In Vivo Expression of Therapeutic Human Genes for Dopamine Production in the Caudates of MPTP-Treated Monkeys Using an AAV Vector.” Gene Therapy 5 (6): 820–27. doi:10.1038/sj.gt.3300650.

Fan, Yongfeng, Wei Zhu, Michael Yang, Yiqian Zhu, Fanxia Shen, Qi Hao, William L. Young, Guo-Yuan Yang, and Yongmei Chen. 2008. “Del-1 Gene Transfer Induces Cerebral Angiogenesis in Mice.” Brain Research 1219 (July): 1–7. doi:10.1016/j.brainres.2008.05.003.

Farrar, M A, and R D Schreiber. 1993. “The Molecular Cell Biology of Interferon-Gamma and Its Receptor.” Annual Review of Immunology 11: 571–611. doi:10.1146/annurev.iy.11.040193.003035.

Ford, A L, A L Goodsall, W F Hickey, and J D Sedgwick. 1995. “Normal Adult Ramified Microglia Separated from Other Central Nervous System Macrophages by Flow Cytometric Sorting. Phenotypic Differences Defined and Direct Ex Vivo Antigen Presentation to Myelin Basic Protein-Reactive CD4+ T Cells Compared.” Journal of Immunology (Baltimore, Md.: 1950) 154 (9): 4309–21.

Francke, Alexander, Joerg Herold, Soenke Weinert, Ruth H Strasser, and Ruediger C Braun-Dullaeus. 2011. “Generation of Mature Murine Monocytes from Heterogeneous Bone Marrow and Description of Their Properties.” The Journal of Histochemistry and Cytochemistry: Official Journal of the Histochemistry Society 59 (9): 813–25. doi:10.1369/0022155411416007.

Gao, Guang-Ping, Mauricio R. Alvira, Lili Wang, Roberto Calcedo, Julie Johnston, and James M. Wilson. 2002. “Novel Adeno-Associated Viruses from Rhesus Monkeys as Vectors for Human Gene Therapy.” Proceedings of the National Academy of Sciences 99 (18): 11854–59. doi:10.1073/pnas.182412299.

Gao, Guangping, Luk H. Vandenberghe, Mauricio R. Alvira, You Lu, Roberto Calcedo, Xiangyang Zhou, and James M. Wilson. 2004. “Clades of Adeno-Associated Viruses Are Widely Disseminated in Human Tissues.” Journal of Virology 78 (12): 6381–88. doi:10.1128/JVI.78.12.6381-6388.2004.

Gehrmann, J, R B Banati, C Wiessner, K A Hossmann, and G W Kreutzberg. 1995. “Reactive Microglia in Cerebral Ischaemia: An Early Mediator of Tissue Damage?” Neuropathology and Applied Neurobiology 21 (4): 277–89.

Glenn, J A, S A Ward, C R Stone, P L Booth, and W E Thomas. 1992. “Characterisation of Ramified Microglial Cells: Detailed Morphology, Morphological Plasticity and Proliferative Capability.” Journal of Anatomy 180 (Pt 1): 109–18.

Gonçalves, Manuel A F V. 2005. “Adeno-Associated Virus: From Defective Virus to Effective Vector.” Virology Journal 2: 43. doi:10.1186/1743-422X-2-43.

Gong, Yan, Shuzhen Chen, Christopher F Sonntag, Colin Sumners, Ronald L Klein, Michael A King, Jeffrey A Hughes, and Edwin M Meyer. 2004. “Recombinant Adeno-Associated Virus Serotype 2 Effectively Transduces Primary Rat Brain Astrocytes and Microglia.” Brain Research. Brain Research Protocols 14 (1): 18–24. doi:10.1016/j.brainresprot.2004.08.001.

Gordon, Siamon, Jörg Hamann, Hsi-Hsien Lin, and Martin Stacey. 2011. “F4/80 and the Related Adhesion-GPCRs.” European Journal of Immunology 41 (9): 2472–76. doi:10.1002/eji.201141715.

Greter, Melanie, Frank L Heppner, Maria P Lemos, Bernhard M Odermatt, Norbert Goebels, Terri Laufer, Randolph J Noelle, and Burkhard Becher. 2005. “Dendritic Cells Permit Immune Invasion of the CNS in an Animal Model of Multiple Sclerosis.” Nature Medicine 11 (3): 328–34. doi:10.1038/nm1197.

Grieger, Joshua C, and Richard J Samulski. 2005. “Packaging Capacity of Adeno-Associated Virus Serotypes: Impact of Larger Genomes on Infectivity and Postentry Steps.” Journal of Virology 79 (15): 9933–44. doi:10.1128/JVI.79.15.9933-9944.2005.

Grimm, D, and M A Kay. 2003. “From Virus Evolution to Vector Revolution: Use of Naturally Occurring Serotypes of Adeno-Associated Virus (AAV) as Novel Vectors for Human Gene Therapy.” Current Gene Therapy 3 (4): 281–304.

Grimm, D, A Kern, M Pawlita, F Ferrari, R Samulski, and J Kleinschmidt. 1999. “Titration of AAV-2 Particles via a Novel Capsid ELISA: Packaging of Genomes Can Limit Production of Recombinant AAV-2.” Gene Therapy 6 (7): 1322–30. doi:10.1038/sj.gt.3300946.

Hansen, J, K Qing, and A Srivastava. 2001. “Infection of Purified Nuclei by Adeno-Associated Virus 2.” Molecular Therapy: The Journal of the American Society of Gene Therapy 4 (4): 289–96. doi:10.1006/mthe.2001.0457.

Hartley, Janet W., Leonard H. Evans, Kim Y. Green, Zohreh Naghashfar, Alfonso R. Macias, Patricia M. Zerfas, and Jerrold M. Ward. 2008. “Expression of Infectious Murine Leukemia Viruses by RAW264.7 Cells, a

Potential Complication for Studies with a Widely Used Mouse Macrophage Cell Line." Retrovirology 5 (1): 1. doi:10.1186/1742-4690-5-1.

Hermonat, P L, and N Muzyczka. 1984. "Use of Adeno-Associated Virus as a Mammalian DNA Cloning Vector: Transduction of Neomycin Resistance into Mammalian Tissue Culture Cells." Proceedings of the National Academy of Sciences of the United States of America 81 (20): 6466–70.

Herzog, Roland W. 2010. "Hepatic AAV Gene Transfer and the Immune System: Friends or Foes?" Molecular Therapy 18 (6): 1063–66. doi:10.1038/mt.2010.96.

Hopkinson-Woolley, J, D Hughes, S Gordon, and P Martin. 1994. "Macrophage Recruitment during Limb Development and Wound Healing in the Embryonic and Foetal Mouse." Journal of Cell Science 107 (Pt 5) (May): 1159–67.

Hunter, A Christy. 2006. "Molecular Hurdles in Polyfectin Design and Mechanistic Background to Polycation Induced Cytotoxicity." Advanced Drug Delivery Reviews 58 (14): 1523–31. doi:10.1016/j.addr.2006.09.008.

Imtiyaz, Hongxia Z., Emily P. Williams, Michele M. Hickey, Shetal A. Patel, Amy C. Durham, Li-Jun Yuan, Rachel Hammond, Phyllis A. Gimotty, Brian Keith, and M. Celeste Simon. 2010. "Hypoxia-Inducible Factor 2? Regulates Macrophage Function in Mouse Models of Acute and Tumor Inflammation." The Journal of Clinical Investigation 120 (8): 2699–2714. doi:10.1172/JCI39506.

Iwata, Nobuhisa, Misaki Sekiguchi, Yoshino Hattori, Akane Takahashi, Masashi Asai, Bin Ji, Makoto Higuchi, Matthias Staufenbiel, Shin-ichi Muramatsu, and Takaomi C. Saido. 2013. "Global Brain Delivery of Neprilysin Gene by Intravascular Administration of AAV Vector in Mice." Scientific Reports 3 (March). doi:10.1038/srep01472. http://www.nature.com/srep/2013/130318/srep01472/full/srep01472.html.

Jacobson, Samuel G, Gregory M Acland, Gustavo D Aguirre, Tomas S Aleman, Sharon B Schwartz, Artur V Cideciyan, Caroline J Zeiss, et al. 2006. "Safety of Recombinant Adeno-Associated Virus Type 2-RPE65 Vector Delivered by Ocular Subretinal Injection." Molecular Therapy: The Journal of the American Society of Gene Therapy 13 (6): 1074–84. doi:10.1016/j.ymthe.2006.03.005.

Kaludov, Nikola, Beverly Handelman, and John A Chiorini. 2002. "Scalable Purification of Adeno-Associated Virus Type 2, 4, or 5 Using Ion-Exchange Chromatography." Human Gene Therapy 13 (10): 1235–43. doi:10.1089/104303402320139014.

Kaplitt, M G, P Leone, R J Samulski, X Xiao, D W Pfaff, K L O'Malley, and M J During. 1994. "Long-Term Gene Expression and Phenotypic Correction Using Adeno-Associated Virus Vectors in the Mammalian Brain." Nature Genetics 8 (2): 148–54. doi:10.1038/ng1094-148.

Kaplitt, Michael G, Andrew Feigin, Chengke Tang, Helen L Fitzsimons, Paul Mattis, Patricia A Lawlor, Ross J Bland, et al. 2007. "Safety and Tolerability of Gene Therapy with an Adeno-Associated Virus (AAV) Borne GAD Gene for Parkinson's Disease: An Open Label, Phase I Trial." Lancet 369 (9579): 2097–2105. doi:10.1016/S0140-6736(07)60982-9.

Kashiwakura, Yuji, Kenji Tamayose, Kazuhisa Iwabuchi, Yukihiko Hirai, Takashi Shimada, Kunio Matsumoto, Toshikazu Nakamura, Masami Watanabe, Kazuo Oshimi, and Hiroyuki Daida. 2005. "Hepatocyte Growth Factor Receptor Is a Coreceptor for Adeno-Associated Virus Type 2 Infection." Journal of Virology 79 (1): 609–14. doi:10.1128/JVI.79.1.609-614.2005.

Kay, M A, J C Glorioso, and L Naldini. 2001. “Viral Vectors for Gene Therapy: The Art of Turning Infectious Agents into Vehicles of Therapeutics.” Nature Medicine 7 (1): 33–40. doi:10.1038/83324.

Kettenmann, Helmut, Uwe-Karsten Hanisch, Mami Noda, and Alexei Verkhratsky. 2011. “Physiology of Microglia.” Physiological Reviews 91 (2): 461–553. doi:10.1152/physrev.00011.2010.

King, J A, R Dubielzig, D Grimm, and J A Kleinschmidt. 2001. “DNA Helicase-Mediated Packaging of Adeno-Associated Virus Type 2 Genomes into Preformed Capsids.” The EMBO Journal 20 (12): 3282–91. doi:10.1093/emboj/20.12.3282.

Klein, R L, E M Meyer, A L Peel, S Zolotukhin, C Meyers, N Muzyczka, and M A King. 1998. “Neuron-Specific Transduction in the Rat Septohippocampal or Nigrostriatal Pathway by Recombinant Adeno-Associated Virus Vectors.” Experimental Neurology 150 (2): 183–94. doi:10.1006/exnr.1997.6736.

Komatsu, T, Z Bi, and C S Reiss. 1996. “Interferon-Gamma Induced Type I Nitric Oxide Synthase Activity Inhibits Viral Replication in Neurons.” Journal of Neuroimmunology 68 (1-2): 101–8.

Kotin, R. M., M. Siniscalco, R. J. Samulski, X. D. Zhu, L. Hunter, C. A. Laughlin, S. McLaughlin, N. Muzyczka, M. Rocchi, and K. I. Berns. 1990. “Site-Specific Integration by Adeno-Associated Virus.” Proceedings of the National Academy of Sciences 87 (6): 2211–15.

Kreutzberg, G W. 1996. “Microglia: A Sensor for Pathological Events in the CNS.” Trends in Neurosciences 19 (8): 312–18.

Kunath, Klaus, Anke von Harpe, Dagmar Fischer, Holger Petersen, Ulrich Bickel, Karlheinz Voigt, and Thomas Kissel. 2003. “Low-Molecular-Weight Polyethylenimine as a Non-Viral Vector for DNA Delivery: Comparison of Physicochemical Properties, Transfection Efficiency and in Vivo Distribution with High-Molecular-Weight Polyethylenimine.” Journal of Controlled Release: Official Journal of the Controlled Release Society 89 (1): 113–25.

Lai, Yi, Yongping Yue, and Dongsheng Duan. 2010. “Evidence for the Failure of Adeno-Associated Virus Serotype 5 to Package a Viral Genome >=8.2 Kb.” Molecular Therapy 18 (1): 75–79. doi:10.1038/mt.2009.256.

Lawson, L J, V H Perry, P Dri, and S Gordon. 1990. “Heterogeneity in the Distribution and Morphology of Microglia in the Normal Adult Mouse Brain.” Neuroscience 39 (1): 151–70.

Levin, M C, U Lidberg, P Jirholt, M Adiels, A Wramstedt, K Gustafsson, D R Greaves, et al. 2012. “Evaluation of Macrophage-Specific Promoters Using Lentiviral Delivery in Mice.” Gene Therapy 19 (11): 1041–47. doi:10.1038/gt.2011.195.

Li, J., R. J. Samulski, and X. Xiao. 1997. “Role for Highly Regulated Rep Gene Expression in Adeno-Associated Virus Vector Production.” Journal of Virology 71 (7): 5236–43.

Li, Xiao-Gang, Takashi Okada, Mika Kodera, Yuko Nara, Naomi Takino, Chieko Muramatsu, Kunihiko Ikeguchi, et al. 2006. “Viral-Mediated Temporally Controlled Dopamine Production in a Rat Model of Parkinson Disease.” Molecular Therapy: The Journal of the American Society of Gene Therapy 13 (1): 160–66. doi:10.1016/j.ymthe.2005.08.009.

Lim, Seung T, Mikko Airavaara, and Brandon K Harvey. 2010. “Viral Vectors for Neurotrophic Factor Delivery: A Gene Therapy Approach for Neurodegenerative Diseases of the CNS.” Pharmacological Research: The Official Journal of the Italian Pharmacological Society 61 (1): 14–26. doi:10.1016/j.phrs.2009.10.002.

Liu, Bin, and Jau-Shyong Hong. 2003. “Role of Microglia in Inflammation-Mediated Neurodegenerative Diseases: Mechanisms and Strategies for Therapeutic Intervention.” Journal of Pharmacology and Experimental Therapeutics 304 (1): 1–7. doi:10.1124/jpet.102.035048.

Liu, J, M L Zhao, C F Brosnan, and S C Lee. 1996. “Expression of Type II Nitric Oxide Synthase in Primary Human Astrocytes and Microglia: Role of IL-1beta and IL-1 Receptor Antagonist.” Journal of Immunology (Baltimore, Md.: 1950) 157 (8): 3569–76.

Liu, T, K M Khanna, B N Carriere, and R L Hendricks. 2001. “Gamma Interferon Can Prevent Herpes Simplex Virus Type 1 Reactivation from Latency in Sensory Neurons.” Journal of Virology 75 (22): 11178–84. doi:10.1128/JVI.75.22.11178-11184.2001.

Liu, Y L, K Wagner, N Robinson, D Sabatino, P Margaritis, W Xiao, and R W Herzog. 2003. “Optimized Production of High-Titer Recombinant Adeno-Associated Virus in Roller Bottles.” BioTechniques 34 (1): 184–89.

Louis, N, C Evelegh, and F L Graham. 1997. “Cloning and Sequencing of the Cellular-Viral Junctions from the Human Adenovirus Type 5 Transformed 293 Cell Line.” Virology 233 (2): 423–29. doi:10.1006/viro.1997.8597.

Lucchinetti, Claudia, Wolfgang Brück, Joseph Parisi, Bernd Scheithauer, Moses Rodriguez, and Hans Lassmann. 1999. “A Quantitative Analysis of Oligodendrocytes in Multiple Sclerosis Lesions A Study of 113 Cases.” Brain 122 (12): 2279–95. doi:10.1093/brain/122.12.2279.

Luo, Xiao-Guang, and Sheng-Di Chen. 2012. “The Changing Phenotype of Microglia from Homeostasis to Disease.” Translational Neurodegeneration 1 (1): 9. doi:10.1186/2047-9158-1-9.

Maheshri, Narendra, James T Koerber, Brian K Kaspar, and David V Schaffer. 2006. “Directed Evolution of Adeno-Associated Virus Yields Enhanced Gene Delivery Vectors.” Nature Biotechnology 24 (2): 198–204. doi:10.1038/nbt1182.

Mandel, R J, K G Rendahl, S K Spratt, R O Snyder, L K Cohen, and S E Leff. 1998. “Characterization of Intrastriatal Recombinant Adeno-Associated Virus-Mediated Gene Transfer of Human Tyrosine Hydroxylase and Human GTP-Cyclohydrolase I in a Rat Model of Parkinson’s Disease.” The Journal of Neuroscience: The Official Journal of the Society for Neuroscience 18 (11): 4271–84.

Manno, Catherine S, Glenn F Pierce, Valder R Arruda, Bertil Glader, Margaret Ragni, John J Rasko, John Rasko, et al. 2006. “Successful Transduction of Liver in Hemophilia by AAV-Factor IX and Limitations Imposed by the Host Immune Response.” Nature Medicine 12 (3): 342–47. doi:10.1038/nm1358.

Manservigi, Roberto, Rafaela Argnani, and Peggy Marconi. 2010. “HSV Recombinant Vectors for Gene Therapy.” The Open Virology Journal 4 (June): 123–56. doi:10.2174/1874357901004030123.

Matsuki, Yohei, Mari Ohmura-Hoshino, Eiji Goto, Masami Aoki, Mari Mito-Yoshida, Mika Uematsu, Takanori Hasegawa, et al. 2007. “Novel Regulation of MHC Class II Function in B Cells.” The EMBO Journal 26 (3): 846–54. doi:10.1038/sj.emboj.7601556.

Matsushita, T, S Elliger, C Elliger, G Podsakoff, L Villarreal, G J Kurtzman, Y Iwaki, and P Colosi. 1998. “Adeno-Associated Virus Vectors Can Be Efficiently Produced without Helper Virus.” Gene Therapy 5 (7): 938–45. doi:10.1038/sj.gt.3300680.

McClure, Christina, Katy L H Cole, Peer Wulff, Matthias Klugmann, and Andrew J Murray. 2011. “Production and Titering of Recombinant Adeno-Associated Viral Vectors.” Journal of Visualized Experiments: JoVE, no. 57: e3348. doi:10.3791/3348.

McKnight, A J, and S Gordon. 1998. “The EGF-TM7 Family: Unusual Structures at the Leukocyte Surface.” Journal of Leukocyte Biology 63 (3): 271–80.

McPhee, S W J, C G Janson, C Li, R J Samulski, A S Camp, J Francis, D Shera, et al. 2006. “Immune Responses to AAV in a Phase I Study for Canavan Disease.” The Journal of Gene Medicine 8 (5): 577–88. doi:10.1002/jgm.885.

Merten, O.-W., C. Gény-Fiamma, and A. M. Douar. 2005. “Current Issues in Adeno-Associated Viral Vector Production.” Gene Therapy 12 (S1): S51–S61. doi:10.1038/sj.gt.3302615.

Mingozzi, Federico, Nicole C Hasbrouck, Etiena Basner-Tschakarjan, Shyrie A Edmonson, Daniel J Hui, Denise E Sabatino, Shangzhen Zhou, et al. 2007. “Modulation of Tolerance to the Transgene Product in a Nonhuman Primate Model of AAV-Mediated Gene Transfer to Liver.” Blood 110 (7): 2334–41. doi:10.1182/blood-2007-03-080093.

Mingozzi, Federico, Marcela V Maus, Daniel J Hui, Denise E Sabatino, Samuel L Murphy, John E J Rasko, Margaret V Ragni, et al. 2007. “CD8(+) T-Cell Responses to Adeno-Associated Virus Capsid in Humans.” Nature Medicine 13 (4): 419–22. doi:10.1038/nm1549.

Mingozzi, Federico, Jorg Schuttrumpf, Valder R. Arruda, Yuhong Liu, Yi-Lin Liu, Katherine A. High, Weidong Xiao, and Roland W. Herzog. 2002. “Improved Hepatic Gene Transfer by Using an Adeno-Associated Virus Serotype 5 Vector.” Journal of Virology 76 (20): 10497–502. doi:10.1128/JVI.76.20.10497-10502.2002.

Moss, D W, and T E Bates. 2001. “Activation of Murine Microglial Cell Lines by Lipopolysaccharide and Interferon-Gamma Causes NO-Mediated Decreases in Mitochondrial and Cellular Function.” The European Journal of Neuroscience 13 (3): 529–38.

Mueller, C, and T R Flotte. 2008. “Clinical Gene Therapy Using Recombinant Adeno-Associated Virus Vectors.” Gene Therapy 15 (11): 858–63. doi:10.1038/gt.2008.68.

Nakai, Hiroyuki, Theresa A. Storm, and Mark A. Kay. 2000. “Recruitment of Single-Stranded Recombinant Adeno-Associated Virus Vector Genomes and Intermolecular Recombination Are Responsible for Stable Transduction of Liver In Vivo.” Journal of Virology 74 (20): 9451–63.

Napoli, I, and H Neumann. 2009. “Microglial Clearance Function in Health and Disease.” Neuroscience 158 (3): 1030–38. doi:10.1016/j.neuroscience.2008.06.046.

Nayak, Ramnath, and David J. Pintel. 2007. “Adeno-Associated Viruses Can Induce Phosphorylation of eIF2α via PKR Activation, Which Can Be Overcome by Helper Adenovirus Type 5 Virus-Associated RNA.” Journal of Virology 81 (21): 11908–16. doi:10.1128/JVI.01132-07.

Nimmerjahn, Axel, Frank Kirchhoff, and Fritjof Helmchen. 2005. “Resting Microglial Cells Are Highly Dynamic Surveillants of Brain Parenchyma in Vivo.” Science 308 (5726): 1314–18. doi:10.1126/science.1110647.

Ohmura-Hoshino, Mari, Eiji Goto, Yohei Matsuki, Masami Aoki, Mari Mito, Mika Uematsu, Hak Hotta, and Satoshi Ishido. 2006. “A Novel Family of Membrane-Bound E3 Ubiquitin Ligases.” Journal of Biochemistry 140 (2): 147–54. doi:10.1093/jb/mvj160.

Ohmura-Hoshino, Mari, Yohei Matsuki, Mari Mito-Yoshida, Eiji Goto, Masami Aoki-Kawasumi, Manabu Nakayama, Osamu Ohara, and Satoshi Ishido. 2009. “Cutting Edge: Requirement of MARCH-I-Mediated MHC II Ubiquitination for the Maintenance of Conventional Dendritic Cells.” Journal of Immunology (Baltimore, Md.: 1950) 183 (11): 6893–97. doi:10.4049/jimmunol.0902178.

Okada, Takashi. 2013. “Efficient AAV Vector Production System: Towards Gene Therapy For Duchenne Muscular Dystrophy.” In Gene Therapy - Tools and Potential Applications, edited by Francisco Martin. InTech. http://www.intechopen.com/books/gene-therapy-tools-and-potential-applications/efficient-aav-vector-production-system-towards-gene-therapy-for-duchenne-muscular-dystrophy.

Paterna, J C, T Moccetti, A Mura, J Feldon, and H Büeler. 2000. “Influence of Promoter and WHV Post-Transcriptional Regulatory Element on AAV-Mediated Transgene Expression in the Rat Brain.” Gene Therapy 7 (15): 1304–11. doi:10.1038/sj.gt.3301221.

Peel, A L, and R L Klein. 2000. “Adeno-Associated Virus Vectors: Activity and Applications in the CNS.” Journal of Neuroscience Methods 98 (2): 95–104.

Pender, M P, and M J Rist. 2001. “Apoptosis of Inflammatory Cells in Immune Control of the Nervous System: Role of Glia.” Glia 36 (2): 137–44.

Pereira, D J, D M McCarty, and N Muzyczka. 1997. “The Adeno-Associated Virus (AAV) Rep Protein Acts as Both a Repressor and an Activator to Regulate AAV Transcription during a Productive Infection.” Journal of Virology 71 (2): 1079–88.

Perry, V. Hugh, and Jessica Teeling. 2013. “Microglia and Macrophages of the Central Nervous System: The Contribution of Microglia Priming and Systemic Inflammation to Chronic Neurodegeneration.” Seminars in Immunopathology 35: 601–12. doi:10.1007/s00281-013-0382-8.

Pintado, Cristina, Elisa Revilla, María L Vizuete, Sebastián Jiménez, Luisa García-Cuervo, Javier Vitorica, Diego Ruano, and Angélica Castaño. 2011. “Regional Difference in Inflammatory Response to LPS-Injection in the Brain: Role of Microglia Cell Density.” Journal of Neuroimmunology 238 (1-2): 44–51. doi:10.1016/j.jneuroim.2011.06.017.

Ponder, KP. 2001. “Vectors of Gene Therapy.” In An Introduction to Molecular Medicine and Gene Therapy, 77–112. Wiley-Liss, Inc.

Prokop, Stefan, Kelly R Miller, and Frank L Heppner. 2013. “Microglia Actions in Alzheimer’s Disease.” Acta Neuropathologica 126 (4): 461–77.

Prösch, S, J Stein, K Staak, C Liebenthal, H D Volk, and D H Krüger. 1996. “Inactivation of the Very Strong HCMV Immediate Early Promoter by DNA CpG Methylation in Vitro.” Biological Chemistry Hoppe-Seyler 377 (3): 195–201.

Qing, K, C Mah, J Hansen, S Zhou, V Dwarki, and A Srivastava. 1999. “Human Fibroblast Growth Factor Receptor 1 Is a Co-Receptor for Infection by Adeno-Associated Virus 2.” Nature Medicine 5 (1): 71–77. doi:10.1038/4758.

Ransohoff, Richard M, and V Hugh Perry. 2009. “Microglial Physiology: Unique Stimuli, Specialized Responses.” Annual Review of Immunology 27: 119–45. doi:10.1146/annurev.immunol.021908.132528.

Reed, Sharon E, Elizabeth M Staley, John P Mayginnes, David J Pintel, and Gregory E Tullis. 2006. “Transfection of Mammalian Cells Using Linear Polyethylenimine Is a Simple and Effective Means of Producing Recombinant Adeno-Associated Virus Vectors.” Journal of Virological Methods 138 (1-2): 85–98. doi:10.1016/j.jviromet.2006.07.024.

Rogove, A D, W Lu, and Stella E Tsirka. 2002. “Microglial Activation and Recruitment, but Not Proliferation, Suffice to Mediate Neurodegeneration.” Cell Death and Differentiation 9 (8): 801–6. doi:10.1038/sj.cdd.4401041.

Rogove, A D, and S E Tsirka. 1998. “Neurotoxic Responses by Microglia Elicited by Excitotoxic Injury in the Mouse Hippocampus.” Current Biology: CB 8 (1): 19–25.

Ryan, J H, S Zolotukhin, and N Muzyczka. 1996. “Sequence Requirements for Binding of Rep68 to the Adeno-Associated Virus Terminal Repeats.” Journal of Virology 70 (3): 1542–53.

Samuel, C E. 2001. “Antiviral Actions of Interferons.” Clinical Microbiology Reviews 14 (4): 778–809, table of contents. doi:10.1128/CMR.14.4.778-809.2001.

Samulski, R J, L S Chang, and T Shenk. 1989. “Helper-Free Stocks of Recombinant Adeno-Associated Viruses: Normal Integration Does Not Require Viral Gene Expression.” Journal of Virology 63 (9): 3822–28.

Schlehofer, J R, M Ehrbar, and H zur Hausen. 1986. “Vaccinia Virus, Herpes Simplex Virus, and Carcinogens Induce DNA Amplification in a Human Cell Line and Support Replication of a Helpervirus Dependent Parvovirus.” Virology 152 (1): 110–17.

Schmidt, Michael, Antonis Voutetakis, Sandra Afione, Changyu Zheng, Danielle Mandikian, and John A Chiorini. 2008. “Adeno-Associated Virus Type 12 (AAV12): A Novel AAV Serotype with Sialic Acid- and Heparan Sulfate Proteoglycan-Independent Transduction Activity.” Journal of Virology 82 (3): 1399–1406. doi:10.1128/JVI.02012-07.

Schwartz, Rachel A, Jose Alejandro Palacios, Geoffrey D Cassell, Sarah Adam, Mauro Giacca, and Matthew D Weitzman. 2007. “The Mre11/Rad50/Nbs1 Complex Limits Adeno-Associated Virus Transduction and Replication.” Journal of Virology 81 (23): 12936–45. doi:10.1128/JVI.01523-07.

Schwarz, E, U K Freese, L Gissmann, W Mayer, B Roggenbuck, A Stremlau, and H zur Hausen. 1985. “Structure and Transcription of Human Papillomavirus Sequences in Cervical Carcinoma Cells.” Nature 314 (6006): 111–14.

Shevtsova, Z, J M I Malik, U Michel, M Bähr, and S Kügler. 2005. “Promoters and Serotypes: Targeting of Adeno-Associated Virus Vectors for Gene Transfer in the Rat Central Nervous System in Vitro and in Vivo.” Experimental Physiology 90 (1): 53–59. doi:10.1113/expphysiol.2004.028159.

Shi, Y, E Seto, L S Chang, and T Shenk. 1991. “Transcriptional Repression by YY1, a Human GLI-Krüppel-Related Protein, and Relief of Repression by Adenovirus E1A Protein.” Cell 67 (2): 377–88.

Shin, Jeoung-Sook, Melanie Ebersold, Marc Pypaert, Lelia Delamarre, Adam Hartley, and Ira Mellman. 2006. “Surface Expression of MHC Class II in Dendritic Cells Is Controlled by Regulated Ubiquitination.” Nature 444 (7115): 115–18. doi:10.1038/nature05261.

Smith, Richard H, Linda Yang, and Robert M Kotin. 2008. “Chromatography-Based Purification of Adeno-Associated Virus.” Methods in Molecular Biology (Clifton, N.J.) 434: 37–54. doi:10.1007/978-1-60327-248-3_4.

Srivastava, A, E W Lusby, and K I Berns. 1983. “Nucleotide Sequence and Organization of the Adeno-Associated Virus 2 Genome.” Journal of Virology 45 (2): 555–64.

Stark, G R, I M Kerr, B R Williams, R H Silverman, and R D Schreiber. 1998. “How Cells Respond to Interferons.” Annual Review of Biochemistry 67: 227–64. doi:10.1146/annurev.biochem.67.1.227.

Steinbach, S., A. Wistuba, T. Bock, and J. A. Kleinschmidt. 1997. “Assembly of Adeno-Associated Virus Type 2 Capsids in Vitro.” Journal of General Virology 78 (6): 1453–62.

Summerford, C, J S Bartlett, and R J Samulski. 1999. “AlphaVbeta5 Integrin: A Co-Receptor for Adeno-Associated Virus Type 2 Infection.” Nature Medicine 5 (1): 78–82. doi:10.1038/4768.

Summerford, C, and R J Samulski. 1998. “Membrane-Associated Heparan Sulfate Proteoglycan Is a Receptor for Adeno-Associated Virus Type 2 Virions.” Journal of Virology 72 (2): 1438–45.

Takahashi, K, F Yamamura, and M Naito. 1989. “Differentiation, Maturation, and Proliferation of Macrophages in the Mouse Yolk Sac: A Light-Microscopic, Enzyme-Cytochemical, Immunohistochemical, and Ultrastructural Study.” Journal of Leukocyte Biology 45 (2): 87–96.

Takaoka, A, Y Mitani, H Suemori, M Sato, T Yokochi, S Noguchi, N Tanaka, and T Taniguchi. 2000. “Cross Talk between Interferon-Gamma and -Alpha/beta Signaling Components in Caveolar Membrane Domains.” Science (New York, N.Y.) 288 (5475): 2357–60.

Tang, Gui-Xia, He-Jun Zhou, Jin-Wei Xu, Jin-Mei Xu, Min-Jun Ji, Hai-Wei Wu, and Guan-Ling Wu. 2012. “Schistosoma Japonicum Soluble Egg Antigens Attenuate IFN-Γ-Induced MHC Class II Expression in RAW 264.7 Macrophages.” PLoS One 7 (11): e49234. doi:10.1371/journal.pone.0049234.

Thibodeau, Jacques, Marie-Claude Bourgeois-Daigneault, Gabrielle Huppé, Jessy Tremblay, Angélique Aumont, Mathieu Houde, Eric Bartee, et al. 2008. “Interleukin-10-Induced MARCH1 Mediates Intracellular

Sequestration of MHC Class II in Monocytes." European Journal of Immunology 38 (5): 1225–30. doi:10.1002/eji.200737902.

Tremblay, Marie-Ève, and Ania K Majewska. 2011. "A Role for Microglia in Synaptic Plasticity?" Communicative & Integrative Biology 4 (2): 220–22. doi:10.4161/cib.4.2.14506.

Tremblay, Marie-Ève, Beth Stevens, Amanda Sierra, Hiroaki Wake, Alain Bessis, and Axel Nimmerjahn. 2011. "The Role of Microglia in the Healthy Brain." The Journal of Neuroscience 31 (45): 16064–69. doi:10.1523/JNEUROSCI.4158-11.2011.

Tsirka, S E, A D Rogove, and S Strickland. 1996. "Neuronal Cell Death and tPA." Nature 384 (6605): 123–24. doi:10.1038/384123b0.

Ulvestad, E, K Williams, R Bjerkvig, K Tiekotter, J Antel, and R Matre. 1994. "Human Microglial Cells Have Phenotypic and Functional Characteristics in Common with Both Macrophages and Dendritic Antigen-Presenting Cells." Journal of Leukocyte Biology 56 (6): 732–40.

Ulvestad, E, K Williams, C Vedeler, J Antel, H Nyland, S Mørk, and R Matre. 1994. "Reactive Microglia in Multiple Sclerosis Lesions Have an Increased Expression of Receptors for the Fc Part of IgG." Journal of the Neurological Sciences 121 (2): 125–31.

Urabe, Masashi, Chuantian Ding, and Robert M Kotin. 2002. "Insect Cells as a Factory to Produce Adeno-Associated Virus Type 2 Vectors." Human Gene Therapy 13 (16): 1935–43. doi:10.1089/10430340260355347.

Urabe, Masashi, Takayo Nakakura, Ke-Qin Xin, Yoko Obara, Hiroaki Mizukami, Akihiro Kume, Robert M. Kotin, and Keiya Ozawa. 2006. "Scalable Generation of High-Titer Recombinant Adeno-Associated Virus Type 5 in Insect Cells." Journal of Virology 80 (4): 1874–85. doi:10.1128/JVI.80.4.1874-1885.2006.

Vandenberghe, Luk H, Ru Xiao, Martin Lock, Jianping Lin, Michael Korn, and James M Wilson. 2010. "Efficient Serotype-Dependent Release of Functional Vector into the Culture Medium during Adeno-Associated Virus Manufacturing." Human Gene Therapy 21 (10): 1251–57. doi:10.1089/hum.2010.107.

Vasileva, Ana, and Rolf Jessberger. 2005. "Precise Hit: Adeno-Associated Virus in Gene Targeting." Nature Reviews. Microbiology 3 (11): 837–47. doi:10.1038/nrmicro1266.

Vilhardt, Frederik. 2005. "Microglia: Phagocyte and Glia Cell." The International Journal of Biochemistry & Cell Biology 37 (1): 17–21. doi:10.1016/j.biocel.2004.06.010.

Vinet, Jonathan, Hilmar RJ van Weering, Annette Heinrich, Roland E. Kälin, Anja Wegner, Nieske Brouwer, Frank L. Heppner, Nico van Rooijen, Hendrikus WGM Boddeke, and Knut Biber. 2012. "Neuroprotective Function for Ramified Microglia in Hippocampal Excitotoxicity." Journal of Neuroinflammation 9 (1): 27. doi:10.1186/1742-2094-9-27.

Virag, Tamas, Sylvain Cecchini, and Robert M Kotin. 2009. "Producing Recombinant Adeno-Associated Virus in Foster Cells: Overcoming Production Limitations Using a Baculovirus-Insect Cell Expression Strategy." Human Gene Therapy 20 (8): 807–17. doi:10.1089/hum.2009.092.

Walseng, Even, Kazuyuki Furuta, Berta Bosch, Karis A Weih, Yohei Matsuki, Oddmund Bakke, Satoshi Ishido, and Paul A Roche. 2010. “Ubiquitination Regulates MHC Class II-Peptide Complex Retention and Degradation in Dendritic Cells.” Proceedings of the National Academy of Sciences of the United States of America 107 (47): 20465–70. doi:10.1073/pnas.1010990107.

Walseng, Even, Kazuyuki Furuta, Romina S Goldszmid, Karis A Weih, Alan Sher, and Paul A Roche. 2010. “Dendritic Cell Activation Prevents MHC Class II Ubiquitination and Promotes MHC Class II Survival regardless of the Activation Stimulus.” The Journal of Biological Chemistry 285 (53): 41749–54. doi:10.1074/jbc.M110.157586.

Walther, W, and U Stein. 2000. “Viral Vectors for Gene Transfer: A Review of Their Use in the Treatment of Human Diseases.” Drugs 60 (2): 249–71.

Wang, Xu-Shan, Benjawan Khuntirat, Keyun Qing, Selvarangan Ponnazhagan, Dagmar M. Kube, Shangzhen Zhou, Varavani J. Dwarki, and Arun Srivastava. 1998. “Characterization of Wild-Type Adeno-Associated Virus Type 2-Like Particles Generated during Recombinant Viral Vector Production and Strategies for Their Elimination.” Journal of Virology 72 (7): 5472–80.

Ward, Peter, Frank B. Dean, Michael E. O’Donnell, and Kenneth I. Berns. 1998. “Role of the Adenovirus DNA-Binding Protein in In Vitro Adeno-Associated Virus DNA Replication.” Journal of Virology 72 (1): 420–27.

Weitzman, Matthew D, and R Michael Linden. 2011. “Adeno-Associated Virus Biology.” Methods in Molecular Biology (Clifton, N.J.) 807: 1–23. doi:10.1007/978-1-61779-370-7_1.

Wobus, C E, B Hügle-Dörr, A Girod, G Petersen, M Hallek, and J A Kleinschmidt. 2000. “Monoclonal Antibodies against the Adeno-Associated Virus Type 2 (AAV-2) Capsid: Epitope Mapping and Identification of Capsid Domains Involved in AAV-2-Cell Interaction and Neutralization of AAV-2 Infection.” Journal of Virology 74 (19): 9281–93.

Wright, J Fraser. 2009. “Transient Transfection Methods for Clinical Adeno-Associated Viral Vector Production.” Human Gene Therapy 20 (7): 698–706. doi:10.1089/hum.2009.064.

Wu, Te-Lang, and Hildegund C J Ertl. 2009. “Immune Barriers to Successful Gene Therapy.” Trends in Molecular Medicine 15 (1): 32–39. doi:10.1016/j.molmed.2008.11.005.

Wu, Zhijian, Aravind Asokan, and R Jude Samulski. 2006. “Adeno-Associated Virus Serotypes: Vector Toolkit for Human Gene Therapy.” Molecular Therapy: The Journal of the American Society of Gene Therapy 14 (3): 316–27. doi:10.1016/j.ymthe.2006.05.009.

Xiao, Weidong, Narendra Chirmule, Scott C. Berta, Beth McCullough, Guangping Gao, and James M. Wilson. 1999. “Gene Therapy Vectors Based on Adeno-Associated Virus Type 1.” Journal of Virology 73 (5): 3994–4003.

Xiao, X, J Li, and R J Samulski. 1998. “Production of High-Titer Recombinant Adeno-Associated Virus Vectors in the Absence of Helper Adenovirus.” Journal of Virology 72 (3): 2224–32.

Yi, Youngsuk, Moon Jong Noh, and Kwan Hee Lee. 2011. “Current Advances in Retroviral Gene Therapy.” Current Gene Therapy 11 (3): 218–28.

Zhang, Shubiao, Yingmei Xu, Bing Wang, Weihong Qiao, Dongliang Liu, and Zongshi Li. 2004. “Cationic Compounds Used in Lipoplexes and Polyplexes for Gene Delivery.” Journal of Controlled Release: Official Journal of the Controlled Release Society 100 (2): 165–80. doi:10.1016/j.jconrel.2004.08.019.

Zolotukhin, S, B J Byrne, E Mason, I Zolotukhin, M Potter, K Chesnut, C Summerford, R J Samulski, and N Muzyczka. 1999. “Recombinant Adeno-Associated Virus Purification Using Novel Methods Improves Infectious Titer and Yield.” Gene Therapy 6 (6): 973–85. doi:10.1038/sj.gt.3300938.